

博 士 論 文

**Development of Conductive Polymer Composites Using
Curable Dopants**

硬化型ドーパントを用いた導電性ポリマー複合材料の開発



PATI SANTWANA

パティ サントワナ

**Department of Aeronautics and Astronautics
Graduate School of Engineering
The University of Tokyo
JAPAN**

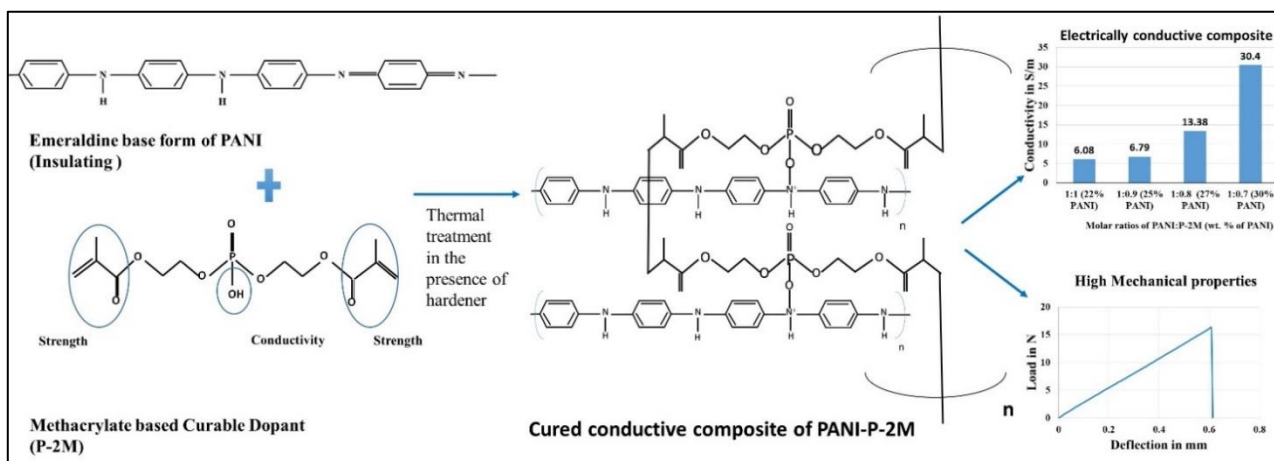
**This dissertation is submitted for the degree of
Doctor of Philosophy**

31ST MAY 2019

Highlights:

- A new concept called curable dopant for polyaniline has been introduced
- The resin properties were studied using Thermal microscopy, DSC, FTIR
- DSC analysis was used to estimate the activation energy and the curing energy for the reactions
- The cured resin showed enhanced mechanical properties as high as 3 ± 0.8 GPa
- CFRPs were fabricated using the technique of long term prepreg storage; first report of a prepreg technology used in a conductive thermoset resin
- Lightning strike test done on the CFRP panels and a mechanical strength enhancer named TMP introduced into the conductive resin
- MD simulations attempted to predict the mechanical properties with variation of the constitution of the resin

Graphical abstract



Dedicated to my Dad Shri T.K.Pati for his constant support

Abstract

CFRPs have revolutionised the aviation industry with many excellent properties like high strength to weight ratio, tailored mechanical properties, corrosion resistance, easy mould ability into complex shapes and low thermal expansion over the conventional aircraft metallic materials like aluminium. Application of composites in aircrafts is the key concept in reduction of fuel emissions, lightweight planes, but for affordability and cost effectiveness the search for new resin is gaining popularity. Conventional CFRPs are fabricated from Carbon fibres impregnated with an insulating resin like epoxy. The conductivity of such panels comes only from the conducting carbon fibres resulting in non-isotropic and non-uniform conductivity as compared to the metallic counterparts. This dielectric nature of the resin results in numerous limitations of the CFRP like limited lightning strike resistance. Lightning strike is a very prominent and frequent danger for the aircrafts. They can not only damage the structural integrity of the plane and hamper the radio system, but also sometimes severe attacks can cause fatal accidents due to fuel vapour ignition[1–4]. Aircrafts companies generally use an efficient and sophisticated Lightning strike protection (LSP) system, which is a multilayer technology to provide metallic conductive path for the lightning current to pass and hence protect the aircraft from damages. However, this strategy does not aid in the goal of a lightweight aircraft plan. This technology not only adds money to the overall cost but also adds weight to the overall aircraft. Researchers have attempted to incorporate conducting nanoparticles like graphene and carbon nanotubes into epoxy, but that comes with its own limitations of agglomerations and percolation threshold .

Conducting polymers are a promising way to accomplish a successful solution to this problem and providing in-built LSP. Polyaniline (PANI) is a hotspot for scientists in various fields owing to its many attractive properties like easy and economical availability , tunable conductivity. Our research team has been working on PANI and developed a PANI/DBSA-DVB based resin that has accomplished to be effective against lightning strike. This resin based CFRP has high conductivity and toughness, however the resin lacks stability and demonstrated compromised mechanical properties. This is due to a lack of connectivity between the three distinct and functionally dissimilar materials which constitute the resin system. Therefore, this thesis attempts to introduce

the new concept of curable dopants. These are the class of dopants which can not only provide conductivity to the resin through PANI, but also cure to form a mechanically strengthened composite. P-2M is a methacrylate containing acid which is predicted to behave like a curable dopant. This thesis efforts to verify that by detailed characterisation by using Thermal microscopy, UV-Vis spectroscopy , FTIR, Differential Scanning Calorimetry (DSC) to confirm the functionality of P-2M as a curable dopant to PANI. After the positive results, a conductive thermoset resin was synthesized after thorough optimisation and analysis of the activation and curing energy . The PANI/P-2M resin was cured to obtain an electrical conductivity of 0.5 S/m in the resin with 20 wt. % of PANI. The flexural modulus didn't show quite a small variation (2.5-3.2 GPa). This can be ascribed to the fact that P-2M is a bi-functional material which is being used for both conductivity and strength, however by two quite different mechanisms and hence employing two different functional groups. The rheological analysis of the resin showed a highly stable steady-state viscosity (1500 mPa.s for the 20 wt. % PANI resin) which is quite favourable for CFRP fabrication.

Further the resin was used to fabricate CFRPs by using the technique of previously impregnated and stored carbon fibres i. e. prepregs. This is the first report of a CFRP fabricated using the prepreg technique for a PANI based conducting thermoset resin. The stability of the prepreg was studied in detail. In the next step, another methacrylate group based material called TMP was introduced into the resin to enhance its mechanical properties. Finally, the lightning strike test was done on the CFRP panels which showed minimum damage in the initial layers caused due to the impact and hence proved effective against the strike.

At the final stage, MD simulations were attempted on the PANI/P-2M resin. This is the first study on the prediction of the mechanical properties of the conducting PANI resin done by using MD simulations. The initial results showed a good agreement with the experimental results.

These results prove that PANI/P-2M conducting thermoset resin has compromised conductivity and strength than its counterpart PANI/DBSA-DVB resin, even though conductivity is better than epoxy, but it has splendid steady state viscosity

which makes it easy to be fabricated using prepregs and extremely convenient to store and transport. This property makes it valuable for small aircrafts accidents and on the spot and sudden repair. This thesis has introduced a wonderful concept of curable dopants for PANI which can be studied for many other applications which require easy to synthesize, conducting thermoset resin that shows good mechanical properties.

Acknowledgements

I would first like to express my sincere gratitude to my respected supervisor Assoc. Professor Tomohiro Yokozeki for accepting me as his PhD student and making me a part of the Aoki-Yokozeki lab which I shall delightfully cherish throughout my life. I am also thankful to Prof. Takahira Aoki for his invaluable research lessons. I am thankful to Dr Teruya Goto and Prof. Tatsuhira Takahashi from the Yamagata University for the key insights about conducting polymers. Indispensable thanks to Assoc. Professor Jun Koyanagi and his students Miss Norie Itano and Mr Shohei Kasahara from the Tokyo University of Sciences for helping me learn the MD simulations using JOCTA software. Further I would like to thank the JSOL corporation for constant technical support. I am also grateful to Asst. Prof. Ryo Higuchi for his feedback and advice and technician Yayoi Kobayashi for her all the time service towards our experimental needs.

I am indebted to the Japanese MEXT and the Indian MHRD for providing me fellowship to complete my doctoral studies. I am also thankful to the GMSI for supporting my international trips for various lectures and workshops. I would like to thank Challenergy Inc. for the valuable internship at the Tokyo head office in the wind turbines international expansion project. My teammates have been a great support and we all learn how research can be fun at the Aoki-Yokozeki lab. Thanks to my tutor Shimizu, Shun Kokubo, Shitanaka, Dobashi, Shiina and Fujioka for showing me the best of Japan. I am lucky to have Sanshiro, Sukanta, Yu and Kumar as my teammates, for PANI has been made fun to work with them.

Apart from all these, I am thankful to my beloved family; my mother for her constant care and prayers, my little brother for always being there, my father for the encouragement and Alok for the optimistic push to go higher in life.

Life in Tokyo was made magical with my dear friends Ashish and Hiya for always being there for me. And Srikanth, Vinod, Akhil, Raja and Arjun for being the best batchmates I could ever have. Japan has been the most beautiful country to learn and it was made so easy with UTISA (University of Tokyo Indian Students Association) and the OCJ (Odia Community Japan).

Content

	Abstract	iv
	Acknowledgements	vii
	Chapters	viii
	List of Figures	x
	List of Tables	xii
	Nomenclature	xiii
Chapter 1	Introduction	1
	1.1.CFRPs and Lightning strike Protection	1
	1.2. Conducting polymer and polyaniline (PANI)	3
	1.3. Outline of the thesis	5
Chapter 2	Literature survey and Motivation for this research	6
Chapter 3	Methodology	10
	3.1. Materials	10
	3.2. Tools and Techniques	10
	3.2.1. Thermal microscopy	10
	3.2.2. UV-Vis spectroscopy	11
	3.2.3. Fourier Transform Infra-Red Spectroscopy (FTIR)	12
	3.2.4. Differential Scanning Calorimetry (DSC)	14
	3.2.5. Viscometer	15
	3.2.6. Electrical Conductivity	16
	3.2.7. Mechanical properties	17
Chapter 4	Introduction of a curable dopant for PANI	20
	4.1. Mechanism of P-2M	20
	4.2. P-2M as a curable dopant	22
	4.2.1. Thermal Microscopy	22
	4.2.2. UV-Vis spectroscopy	23
	4.2.3. FTIR analysis	24
	4.2.4. Differential Scanning Calorimetry	27
	4.3. Optimisation of the PANI/P-2M	28
	4.4. Discussion	30

Chapter 5	Development of PANI/P-2M composites	32
	5.1. Samples preparation	32
	5.2. DSC analysis for chemical kinetics study	32
	5.2.1 Estimation of the activation energy	32
	5.2.2 Estimation of the curing and doping energy	36
	5.3. Rheological analysis of the resin	38
	5.4. Cured composite characterisation	41
	5.5. Discussion	44
Chapter 6	Development of CFRPs using the PANI/P-2M resin	45
	6.1. CFRP fabrication Prepreg technique	46
	6.2. Prepreg study	47
	6.3. Characterisation of the CFRPs	52
	6.4. Morphological studies	57
	6.5. Introducing Trimethylolpropane trimethacrylate (TMP) as a strength enhancer	59
	6.6. Lightning strike test on the CFRP samples	63
	6.7. Discussion	66
Chapter 7	MD simulations on the resin	67
	7.1. Methodology and Models	67
	7.2. Results and discussions	72
	7.3. Discussion	75
Chapter 8	Conclusions	77
	References	80
	Achievements	87

List of Figures:

Fig. 1.1	Conductive fillers into the polymers: Theoretical expectation and practical applications	3
Fig. 1.2	Specimen damage after simulated lightning current tests: a) CF/epoxy –40 kA, b) CF/epoxy –100 kA , c) CF/PANI –40 kA , and d) CF/PANI –100 kA	4
Fig. 1.3	Various forms of PANI according to the position of amines and imines	5
Fig. 2.1	Structure of P-2M	8
Fig. 2.2	Comparison between the PANI-DBSA/DVB system and the new PANI-P-2M resin system	8
Fig. 3.1	Various parts of the thermal microscope	11
Fig. 3.2	Set up of UV-Vis spectrometer	12
Fig. 3.3	UV-Vis spectroscopy general working principle	12
Fig. 3.4	FTIR analyser set up	13
Fig. 3.5	FTIR working principle	13
Fig. 3.6	DSC instrument used in this study. The right-hand side image shows inside of the heating chamber	14
Fig. 3.7	Inside the DSC heating chamber	15
Fig. 3.8	Viscometer used for the rheological analysis	16
Fig. 3.9	LCR tester for Electrical conductivity measurement	17
Fig. 3.10	The UTM for conducting flexural tests on the composites	18
Fig. 4.1	Doping mechanism of polyaniline by P-2M	21
Fig. 4.2	Generation of P-2M based free radicals in the presence of Perbutyl-E	21
Fig. 4.3	Curing mechanism by radical Polymerisation: Cross-linked network formation of the PANI-P-2M complex due to radical polymerisation upon thermal treatment.	22
Fig. 4.4	Thermal microscopy image of PANI-P-2M sample at various temperature and the onset of green colour due to doping at elevated temperature	23
Fig. 4.5	UV-Vis plot of PANI-P-2M sample	24
Fig. 4.6	Comparative FTIR analysis of the various stages in the process of synthesis of PANI-P-2M composite	27
Fig. 4.7	Comparison between cured and uncured resin FTIR	27
Fig. 4.8	Comparison between doping peaks and curing peaks of FTIR	28
Fig. 4.9	DSC analysis of PANI-P-2M samples in periodic thermal treatment for doping estimation	29

Fig. 4.10	Chemical structure of PANI and P-2M	30
Fig. 4.11	Electrical conductivity of uncured PANI-P-2M samples mixed in various molar ratios	31
Fig. 5.1	Dynamic DSC thermographs from Room Temp until 200 °C at different heating rates	33
Fig. 5.2	Kissinger plot to determine the activation energy	34
Fig. 5.3	Plot of $\ln k$ vs $1/T$ for the Barrett's method	35
Fig. 5.4	DSC thermograph for the analysis of doping complex	36
Fig. 5.5	DSC of the uncured resin with 20 wt. % PANI	37
Fig. 5.6	Estimated curing energy for each constitution of the resin	38
Fig. 5.7	Change in viscosity of the resin with shear rate	39
Fig. 5.8	Steady state viscosity for 20 wt. % PANI resin	40
Fig. 5.9	Variation of the viscosity with increasing wt. % of PANI in the resin	41
Fig. 5.10	Flexural modulus with various wt. % of PANI in the resin	42
Fig. 5.11	Maximum stress with various wt. % of PANI in the resin	42
Fig. 5.12	Load displacement curve of a cured composite of PANI-P-2M	43
Fig. 5.13	Electrical conductivity for various wt. % of PANI	43
Fig. 6.1	Sequence of the process for the fabrication of CFRP	46
Fig. 6.2	(a) Prepreg of Carbon fibre impregnated with PANI/P-2M resin (b) Fabricated CFRP using the PANI/P-2M resin	47
Fig. 6.3	Steady-state viscosity of the resin over a period of 80 days and calculated at regular intervals	48
Fig. 6.4	Steady state viscosity day-wise for a span of 80 days	49
Fig. 6.5	The comparative picture showing resin physical appearance for PANI/P-2M and PANI/DBSA	50
Fig. 6.6	Plot of viscosity with increasing temperature for both neat resin as well as 10 wt. % resin	51
Fig. 6.7	Flexural modulus of the CF/P-2M samples with various wt. % of PANI	52
Fig. 6.8	The polisher used for the sample preparation and the samples prepared using clear rings and clear epoxy	54
Fig. 6.9	Load -Displacement Curves for the CFRP samples with various wt. % of PANI in the resin	55
Fig. 6.10	Electrical conductivity in S/cm of the samples with various wt. % of PANI	56
Fig. 6.11	Optical microscope images of the CFRP samples showing the damage sites	58

Fig. 6.12	Magnified view of the sample showing the spot of breakage from the edge	59
Fig. 6.13	Chemical structure of TMP with illustration on the methacrylate functional groups	60
Fig. 6.14	Comparative DSC of the resin with and without TMP	60
Fig. 6.15	Steady state viscosity of the resin with 15 wt. % TMP added	61
Fig. 6.16	Effect of TMP on the maximum stress of the CFRP samples	62
Fig. 6.17	Load displacement curve showing the effect of adding TMP into the resin	62
Fig. 6.18	The optical microscope images for 10 wt. % PANI with (a) and without (b) TMP.	63
Fig. 6.19	Set up for the lightning strike test. Right hand side shows the enlarged view of the specimen holding set up	64
Fig. 6.20	Sample on the specimen holder before and after the strike	65
Fig. 6.21	The sample physical study and the NDI before and after the lightning strike	65
Fig. 7.1	Flow chart showing the execution of the COGNAC	69
Fig. 7.2	Building the MD model for simulation	70
Fig. 7.3	Monomer modelling step wise illustration	70
Fig. 7.4	Structure of the fundamental resin constituents: P-2M (neat resin) and PANI/P-2M (basic resin)	71
Fig. 7.5	Stress strain curves obtained from the MD simulations	72
Fig. 7.6	Illustration of achieving 3 axis rotation in the MD elongation.	73
Fig. 7.7	Improved stress strain curve for the basic model	73
Fig. 7.8	Comparative analysis of the modulus obtained from experiments and MD simulations	75

List of Tables:

Table 2.1. List of a few popular dopants for PANI and their functionality	7
Table 4.1. Different stages of the sample for FTIR analysis	25
Table 6.1. Different heats of reaction for the resin on various days	51
Table 6.2. Summary of the volume fraction obtained	55
Table 7.1. Models with the respective PANI constitution	71
Table 7.2. Summary of the results obtained	74

Nomenclature:

- PANI: Polyaniline
- P-2M: 2-Methacryloyloxyethyl acid phosphate
- TMP: Trimethylolpropane trimethacrylate
- DSC: Differential scanning Calorimetry
- FTIR spectroscopy: Fourier Transform Infra Red Spectroscopy
- CFRP: Carbon Fibre reinforced plastic
- MD: Molecular Dynamics

Chapter-1

Introduction:

The world is developing towards making the planet a better place with more and more convenience evolving day by day. Such transformations with continuous upgradation of technology is inevitable in every field of engineering. Similarly, Aerospace engineering needs constant upgradation through continuous research and multidisciplinary development. This research work is such an example in which the author tried to apply the emerging field of conducting polymers into the fabrication of CFRP panels for application in aircraft industries. This chapter briefly introduces the concept of the thesis explaining the various terminologies involved in this research.

1.1. CFRPs and Lightning Strike Protection:

CFRP with its high strength and low weight is one of the most critical material for the 21st century. Owing to the high mechanical strength, low weight CFRP has made its way into various sectors like aerospace, automobiles, space vehicles, etc. Additionally, CFRPs also provide exceptional durability and low thermal expansion. This makes it an attractive material for shipbuilding and other externally exposed materials.

Among all these areas of applications, CFRPs have attained a considerable role in revolutionizing the Aviation industries. Since the 1970s aircraft manufacturers have started shifting towards CFRPs from Aluminium based aircrafts. CFRPs have reduced the aircraft weight by a significant amount which has led to lesser fuel requirements. Consequently, that has reduced the price of the airfare and led to lesser CO₂ emission. Finally, we have achieved an interconnected world with air travel being a easier and more convenient source of travel.

The final property of the CFRP depends on the resin material that is used to bind the carbon fibres intact together. Currently, epoxy is one of the most widely used resin for the aircrafts, as well as other applications of CFRPs requiring high structural and mechanical strength . Epoxy has many desirable properties like high mechanical strength, chemical resistance, thermal stability. Additionally, epoxy provides excellent adhesion to the surface and is quite economical. Subsequently, epoxy has set itself a benchmark in being a resin material for CFRP fabrication. However, at the same time, it faces a few limitations. Epoxy being a dielectric material has no resistance towards high electrical discharges thereby no electromagnetic shielding effectiveness. It is also not resistant to fire and the aircrafts repair after a mishap occurs is quite expensive.

Among all these, the major limitation that this report works on is the Lightning strike problem in aircrafts due to the dielectric nature of epoxy.

Lightning strike is a major problem for aircrafts and critical structures like wind turbines made up of Epoxy based CFRPs. Lightning strikes can affect airline operations and cause expensive delays. Strikes to aircrafts are relatively common but the damages are mostly insignificant due to the effective lightning strike protection. The strikes can damage the structural integrity of the plane. A strike of high intensity can damage components such as electrically controlled fuel valves, generators, power feeders. Sometimes fatal accidents are also caused during unexpected intense strikes. Lightning strike damages are mostly visible as pits, burn marks or small holes. Direct effects of the damages caused by lightning strikes to the airplane structure are melt through, burn indications around fasteners and sometimes missing parts. Another severe effect on the structure is the damage caused by the shock waves generated by the lightning strike. Airline companies invest a lot of money, technology, maintenance personnel and data analysis teams to prepare for an effective lightning strike protection system. Lightning strike protection includes composite structures expanded foils, wire mesh, aluminium flame spray coating, embedded metallic wires. Aircrafts also implement much more complex and high-end LSPs like Non-woven veil made with nickel or copper-coated-carbon fibres and Nickel Nano-strands dispersed in epoxy. This technology adds a lot of weight to the aircraft and comes with a huge price. In the end this huge addition of weight hinders the main aim of using CFRPs i.e. lightweight materials. Further, this LSP is easily affected by corrosion and hence requires expensive repair.

Researchers have tried to incorporate conductivity into the resin system in order to obtain a conductive CFRP. They have used nanoparticles that are quite efficient in incorporating conductivity into the resin. There are many reports in which conductivity has been significantly enhanced owing to the introduction of nanoparticles like graphene nanoplatelets, silver nanoparticles, carbon nanotubes [5–7] into the CFRPs. Though these nanoparticles have shown to provide conductivity only after a certain weight loading so this necessitates to add a specified amount to ensure high conductivity (over the percolation threshold) [7–9]. Additionally, the conducting fillers need to be well dispersed in the matrix in proper weight loadings otherwise, they tend to form agglomerates owing to the intermolecular Van der Waals forces as illustrated in Fig. 1.3. Therefore undispersed nano fillers may lead to compromised tensile strength, solid like behaviour from a rheological point of view that eventually reduces the process ability of CFRPs [10,11]. These limitations bring the scope for further research to obtain conductive CFRPs implementing conducting polymers instead of epoxy.

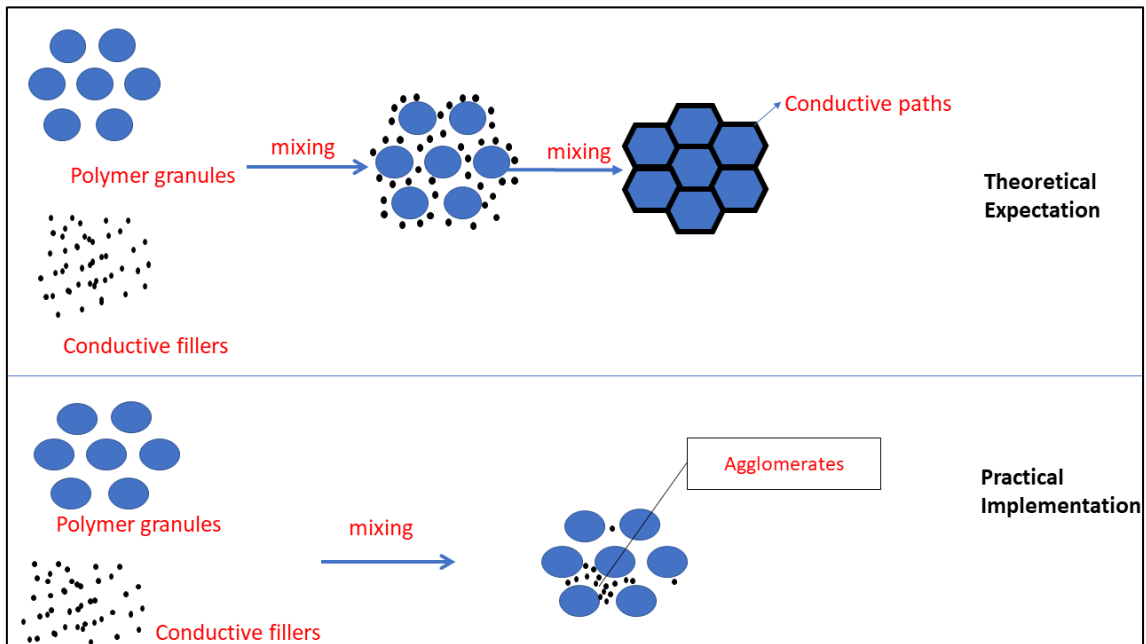


Fig. 1.1. Conductive fillers into the polymers: Theoretical expectation and practical applications

1.2. Conducting Polymers and polyaniline (PANI):

Polymers, with their ease of fabrication and mouldability have replaced metals almost everywhere. They are correctly remarked as: From buckets to rockets. There are numerous polymers gaining grounds in the aerospace industries [12] like PEEK is a popular choice for the aircraft interiors. Similarly, polyphenylsulfone has outperformed its metal counterparts owing to its corrosion resistance and significant weight reduction. Traditionally, all the properties and applications of polymers relied on the fact that they are electrically insulating in nature. However, now researchers are focussing on another class of polymers which have alternate double bonds and hence conjugated π - bonding and are known as intrinsically conducting polymers. There have been several reports on ICPs like Polyacetylene, Polypyrrole, Polythiophene, Polyaniline, PEDOT, etc being applied in various fields. Among all these polymers, Polyaniline has been the emphasis for the scientific community owing to its several advantages [13]. Polyaniline offers easy synthesis routes and is easily available [14,15]. Further the conductivity is tuneable and

the polymer is environmentally friendly. Another major reason for working on PANI is that it has already been proven effective against lightning strike [16] .

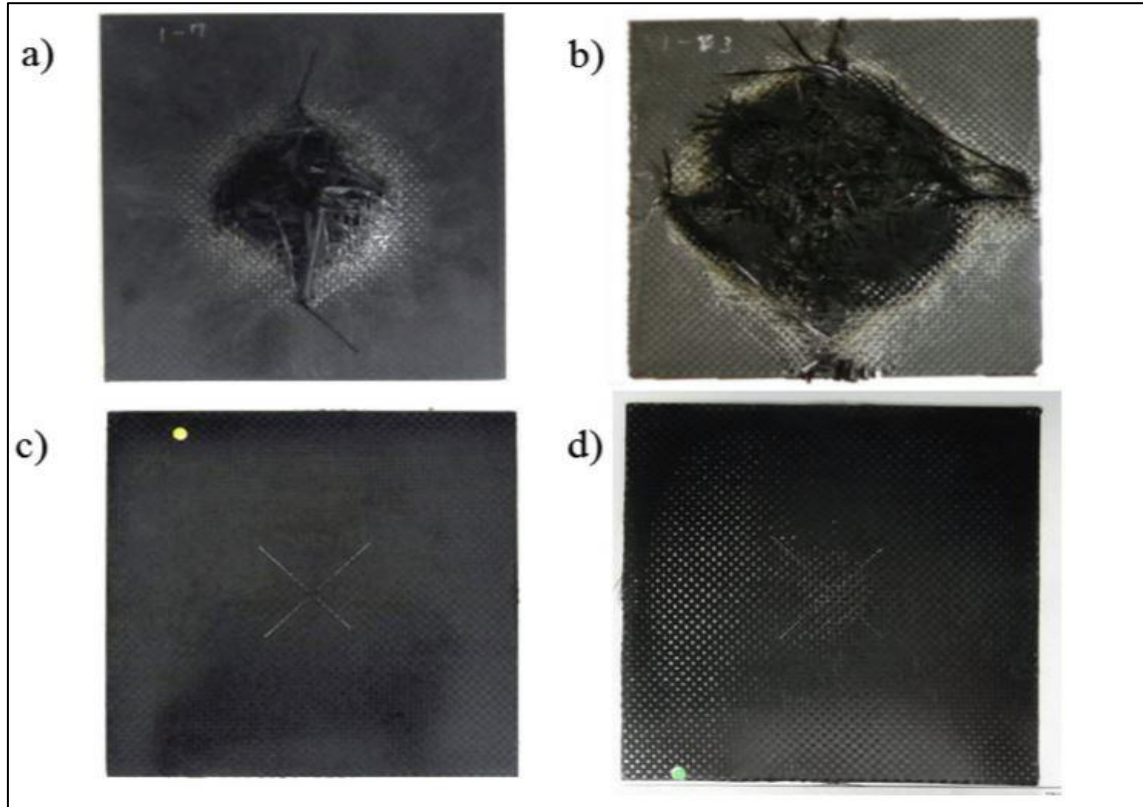


Fig. 1.2. Specimen damage after simulated lightning current tests: a) CF/epoxy –40 kA , b) CF/epoxy –100 kA , c) CF/PANI –40 kA , and d) CF/PANI –100 kA [16] .

PANI has a typical structure with alternating benzene rings and nitrogen atoms. The nitrogen atoms appear in two different hybridization states: amine (sp^3) and imine (sp^2). Depending on the relative positioning of these two different states of the nitrogen atoms , PANI is found in 3 different oxidation states: Emeraldine, Leucoemeraldine, Pernigraniline [17] as shown in the Fig. 1.3.

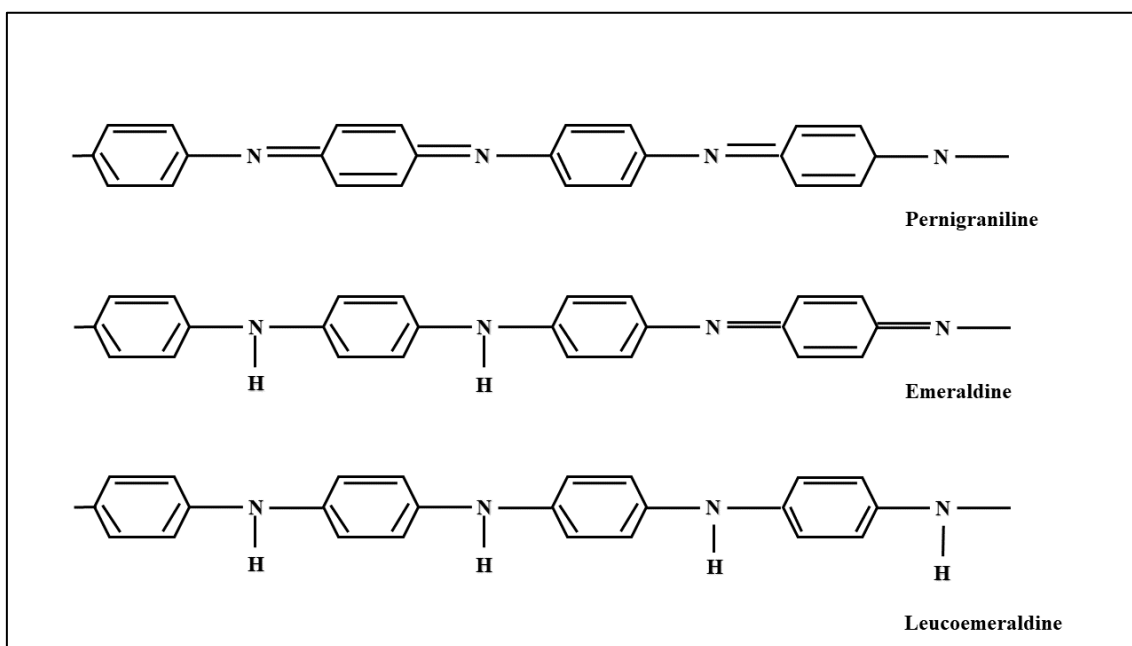


Fig. 1.3. Various forms of PANI according to the position of amines and imines

The emeraldine state of PANI is a base form and electrically insulating in nature. In the presence of an acidic functional group, the emeraldine base form changes into salt form by forming a polar bond with the -OH group of the acid. The acidic group that aids in this process is called a dopant and this concept is called the doping of PANI.

1.3. Outline of the thesis:

In the next chapter we have consolidated the literature survey about the various other classes of dopants that have been used with PANI. It also explains the motivation to develop a new resin system with P-2M. The 3rd chapter then explains the experimental methodology for the synthesis of the composites and the various tools and techniques used for the characterization. Further the functionality of P-2M as a curable dopant with all the characterisation and mechanism is discussed in the chapter 4.

Next, in the 5th chapter we discussed the resin development and characterised it using various techniques and confirmed the estimated properties. 6th chapter shows the consolidated work on the fabrication of CFRPs using this new resin preregs. Next, the lightning strike test results conducted on the CFRP panels were discussed. Additionally, the molecular dynamics simulations on this resin material for the prediction of the mechanical properties done using JOCTA software is presented in the 7th chapter of this thesis work. The 8th chapter discusses the conclusions and comparisons with the various other systems for composites.

Chapter-2

Literature survey and motivation for this research

PANI is generally available in an emeraldine base form which is insulating in nature. This can be changed into a conducting form by two independent doping routes : i) oxidation either electrochemically or chemically; ii) acid base chemistry leading to protonation [18,19]. The second route happens due to an internal redox reaction in which the imine nitrogen sites are protonated by a protonic acid owing to an internal spin unpairing mechanism [19,20]. The second route is a more commonly used method for imparting conductivity to PANI. The protonic acid is in the form of H^+M^- , where the H^+ reacts with the PANI chains and the negatively charged M^- is the counter ion and provides overall neutrality of charge to the whole complex [20,21]. Several protonic acids have been used as dopants such as hydrochloric acid (HCl), nitric acid (HNO_3), sulphuric acid (H_2SO_4) and, perchloric acid ($HClO_4$) [22,23]. However, some of these acids are volatile and thereby are ineffective in full conversion of the emeraldine insulating form to conducting form of PANI. This led the researchers to explore other types of acids like Tartaric acid, salicylic acid, oxalic acid and citric acid for doping of PANI [19,24,25]. The choice of dopant determines the ultimate property of the conducting PANI and hence the application for which it can be used for. Sulphonic acids and its various derivatives have also been studied widely like dodecylbenzenesulphonic acid (DBSA), and p-toluenesulphonic acid (p-TSA) and Camphorsulphonic acid (CSA) [26–28]. All these variants of acids gave various levels of charge mobility and conductivity, which have scope for various applications. Derivatives of phosphoric acid have also been explored as a dopant for PANI with improved processability and optimised conductivity [19,29,30]. Our research team used dodecylbenzene sulfonic acid (DBSA) as the dopant for PANI and then added divinylbenzene (DVB) as a crosslinking polymer which provided mechanical stiffness and hence attained a thermosetting polymer composite with the dopant DBSA providing conductivity and the polymer DVB imparting mechanical strength to the composite [31]. This conducting structural composite can then be used as an aerospace composite with CFRP [16,32]. However, the PANI/DBSA –DVB system involves scope for further research to improve the mechanical properties and process ability. In depth analysis of the developed system of PANI/DBSA –DVB shows that the resin encompasses two entirely different material systems for conductivity (PANI-DBSA dopant system) and strength (DBSA-DVB crosslinking polymer system). The lack of linking between them hampers the maximum strength and conductivity. This motivates the research to work for a new resin that combines both the systems

of strength and conductivity. Table 2.1 summarises a few popularly used dopant for PANI and their conductivity and functionality.

Table 2.1. List of a few popular dopants for PANI and their functionality

Sl. No.	Dopant system	Conductivity in S/cm	Functionality
1.	PANI-HCl	0.16	Cationic doping, provide conductivity only, No structural effect
2.	PANI-PTSA	0.048	
3.	PANI-LA	0.034	
4.	PANI-DBSA	0.026	

In this thesis, we report a new dopant for PANI that also embeds the property of polymerisation using methacrylate functional groups. This bifunctional material, which can be used as a polymerizable dopant with PANI, is called 2-Methacryloyloxyethyl acid phosphate (P-2M). This concept is termed as curable dopant, a dopant which can be cured by itself thereby providing conductivity as well as mechanical strength to the PANI based resin.

P-2M has a methacrylate functional group as well as an acidic functional group that can aid in the doping process. This bifunctional material has a strong protonic group to provide H^+ to dope the PANI and make it conducting and also has acrylic functional groups like Poly(methyl methacrylate) (commonly known as PMMA). This acrylic group helps the P-2M to radically polymerize and hence provides strengthening to the resin system. This curing reaction requires an initiator called perbutyl. Fig. 2.1 shows the structure of P-2M in which part 1 provides conductivity to PANI and part 2 imparts strength for the resin. Hence, a single material works both ways and solves the complications of the previous system. The fig. 2.2 illustrates the difference between the new resin system of PANI/P-2M and the previous resin system PANI/DBSA/DVB.

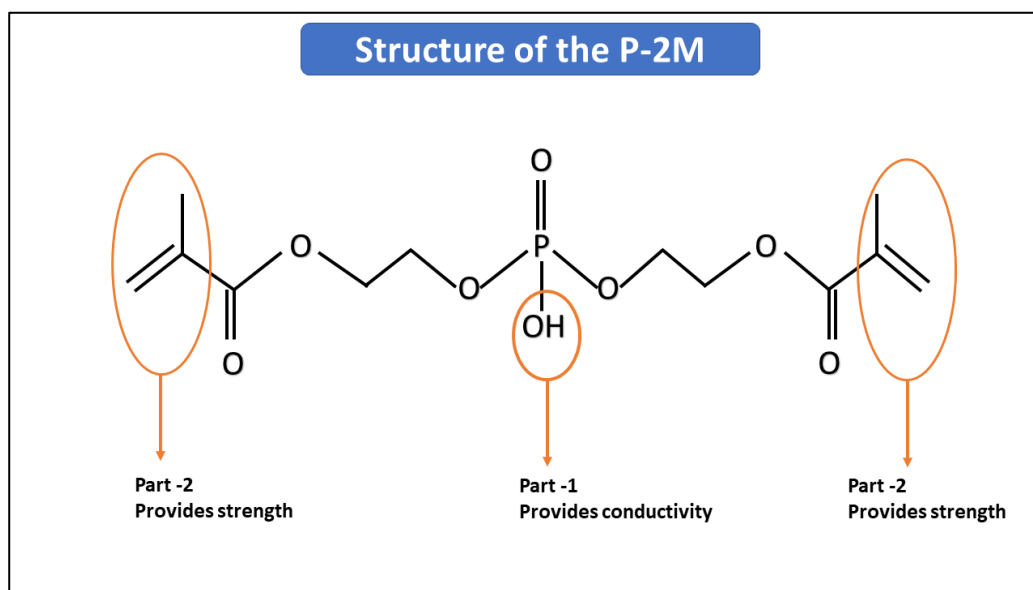


Fig 2.1. Structure of P-2M

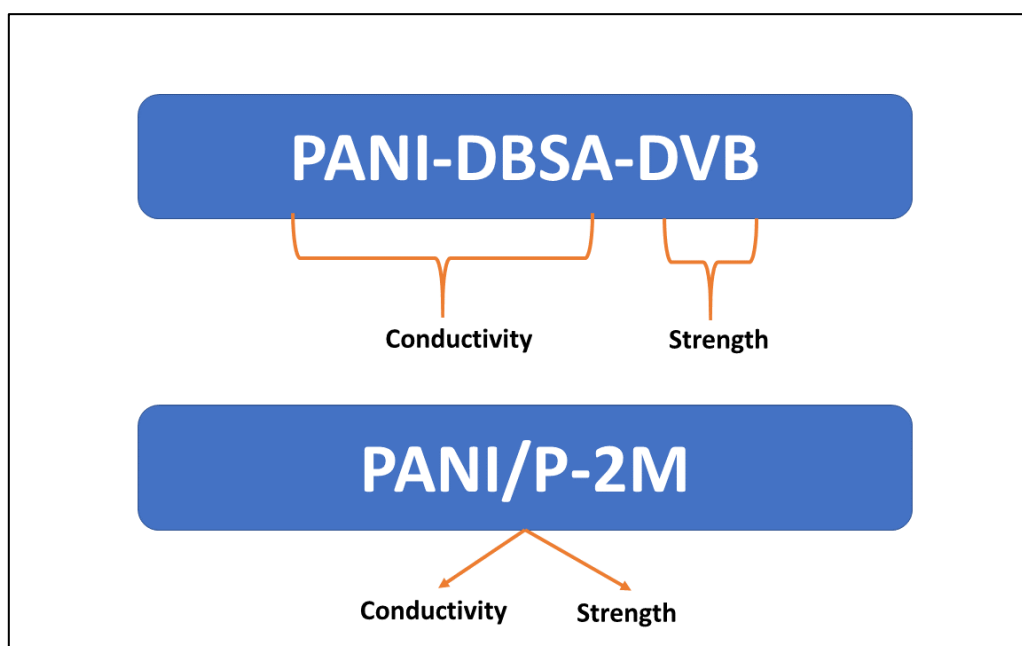


Fig. 2.2. Comparison between the PANI-DBSA/DVB system and the new PANI-P-2M resin system [19]

The major motivation of using P-2M with PANI as a conductive composite is that it is cured by radical polymerisation, and acts as a dopant. Therefore, both the properties are obtained simultaneously. Methacrylate materials have not yet been explored much in this field [19]. There

have been studies on the synthesis of conducting composites of polyaniline/poly(alkyl methacrylate) by emulsion method by Yang et al [33]. Emulsion route involves adding HCl as a dopant and polymerising aniline in the process. Choi et al [34] reported their work on a class of polymerizable dopant using diacetylenes added with sulphonic groups which showed higher thermal stability and conductivity of PANI. Although the dopant was self-polymerized in the process, the curing ability and hence the mechanical properties were not observed. Nevertheless, in our report, PANI is used directly rather than being polymerised in the process. On the other hand, P-2M, the dopant, undergoes radical polymerisation to form a cross-linked network and its curability is well studied for the fabrication of a structural conductive composites with PANI. As per our literature survey, there have been no reports of research on an acidic methacrylate group material like P-2M to make a conductive thermosetting composite with PANI, nor any reports on curable dopant yet. Hence, we developed a new PANI based resin system using a curable dopant named 2-Methacryloyloxyethyl acid phosphate P-2M that can not only provide conductivity but also get radically cured to obtain a conductive cured resin system[7,19]. The chemical structure and the exact mechanism of the bifunctional P-2M as a curable dopant for PANI has been discussed in our articles [19,35] . Moreover, this resin system provides a single step convenient synthesis technique due to a steady state viscosity and we can obtain heightened mechanical properties with optimal conductivity.

Chapter 3

Methodology

3.1. Materials:

PANI in its emeraldine base form was procured from Regulus Co. Ltd., Tokyo, Japan. P-2M was supplied by Kyoeisha chemicals co. ltd. The crosslinking agent : Perbutyl -E was procured from NOF corporation. All the materials used were brought untreated and in raw form. Conductive adhesive silver paste DOTITE used for electrical conductivity measurement was procured from Fujikura Kasei Co. Ltd. TMP was procured from Kyoeisha chemicals co. ltd.

3.2. Tools and techniques:

P-2M is a new material introduced in the field of composites. Therefore, the detailed material characterisation was necessary. We used the various techniques to confirm the doping property, curing analysis, estimated the energy required for curing the composite and the activation energy for the composite synthesis. The various techniques are introduced in this section.

3.2.1. Thermal microscopy:

Thermal microscopy is a simple technique used to analyse the morphology of the material with change in temperature. An optical microscope by Olympus-BX50 connected with a heating plate system and a computer attached to it comprises the set up for the thermal microscope. The sample under study was pressed between glass slides which was then placed in the sample holder slot . The samples were observed from 25°C to 120°C. The images obtained from this instrument was used for the analysis of P-2M as a dopant. The set up is shown in the Fig. 3.1.

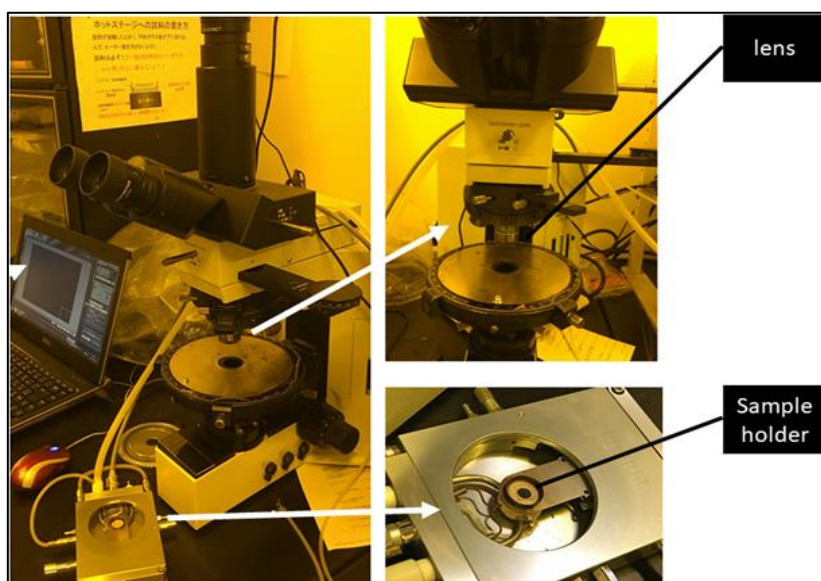


Fig.3.1. Various parts of the thermal microscope

3.2.2. UV-Vis spectroscopy

UV-Vis spectroscopy is a critical technique. It helps in detection of the functional groups as it analyses the transition of electrons within the levels in a molecule. The model used in this study is UV-vis-NIR analyzer (U-4100, Hitachi High Technologies Corporation) as shown in the Fig. 3.2. The basic principle followed here is that the material when placed between the glass slides absorbs the incoming light and undergoes transitions at molecular level. The outgoing light is then studied and the difference between the incoming and the outgoing is a fingerprint of the chemical functional groups in the material. The last image in the Fig 3.2. shows the detailed set up from inside the chamber. The principle is illustrated in the Fig. 3.3.

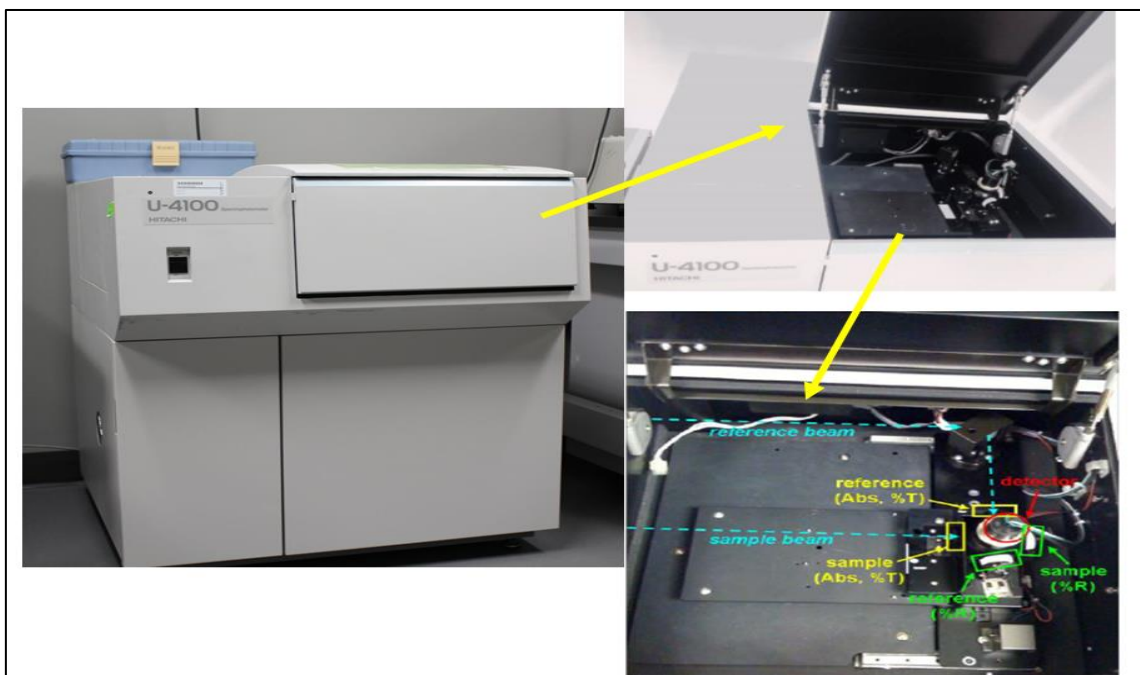


Fig.3.2. Set up of UV-Vis spectrometer

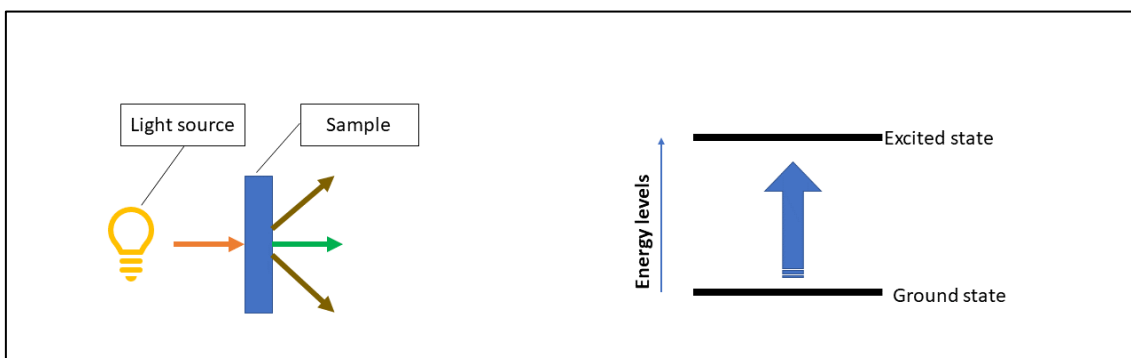


Fig. 3.3. UV-Vis spectroscopy general working principle

3.2.4. Fourier Transform Infra-Red Spectroscopy (FTIR)

FTIR is the most essential characterisation technique for materials analysis. We used it to check the various bond formations due to doping and curing. It works on the simple principle that molecules absorb light in the infra-red region which corresponds to the molecular bonds in the material and its vibrations. The model used for this work is IRAffinity-1S by Shimadzu corporation. The FTIR analyser and the sample platform is

shown in the Fig 3.4. The simple general working principle for the FTIR analyser is illustrated in the Fig. 3.5.

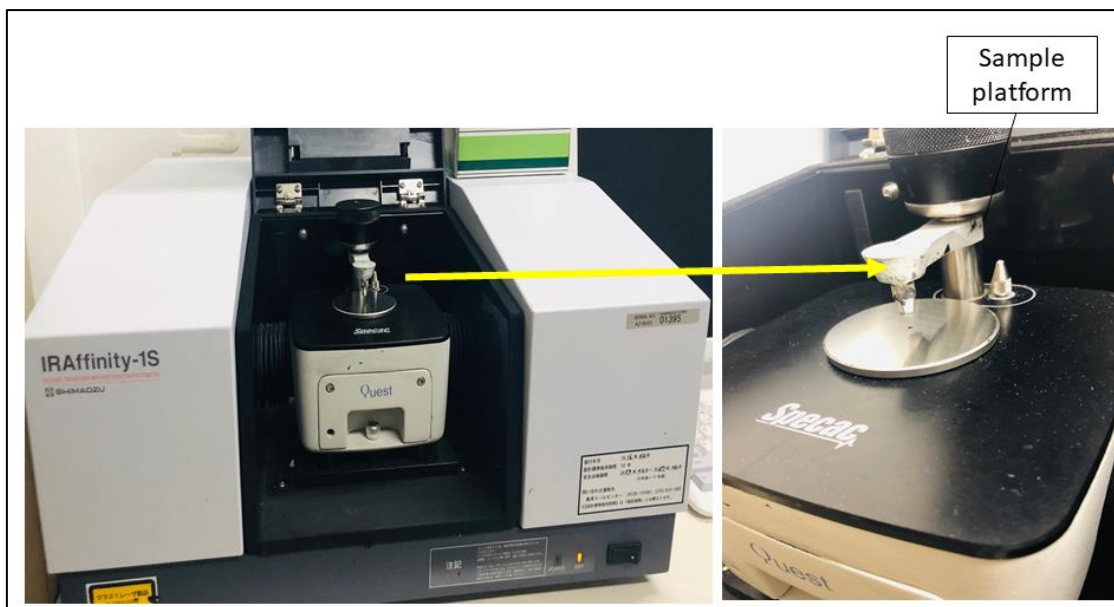


Fig. 3.4. FTIR analyser set up

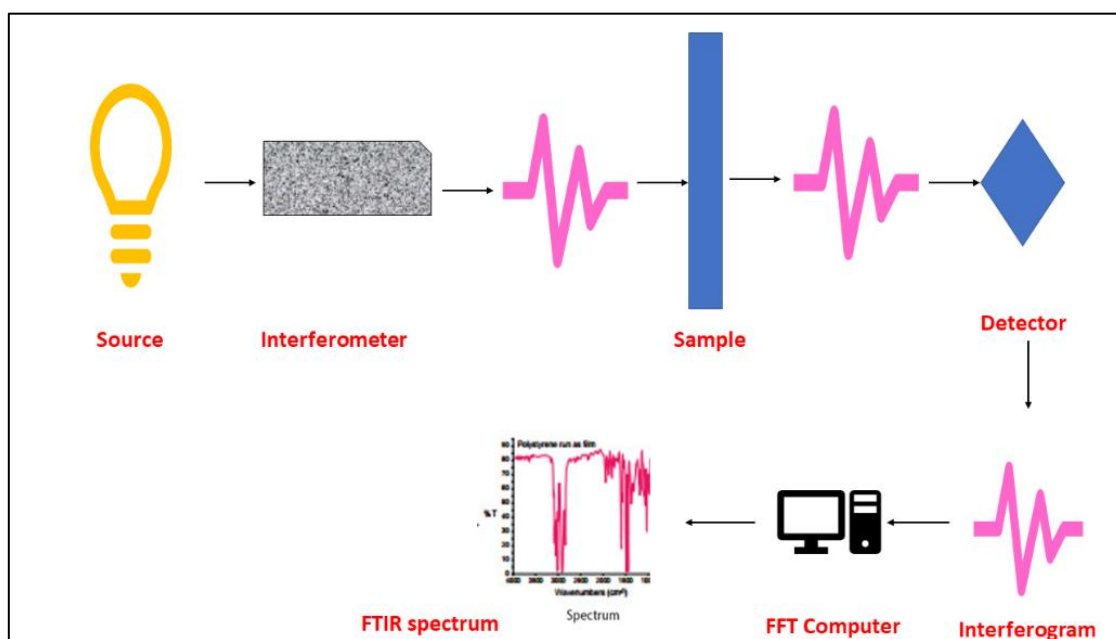


Fig. 3.5. FTIR working principle

3.2.5 Differential Scanning Calorimetry (DSC):

DSC is a thermo-analytical technique and the most essential step for this study. It helped us estimate the amount of energy for each reaction (Doping and curing). We also estimated the activation energy for the reactions between PANI and P-2M by studying the reaction kinetics. Further after each composite synthesis, the degree of cure was estimated, and the further experiments were done accordingly. The DSC instrument used in this study is DSC-60Plus by Shimadzu Corporation. The basic working principle is that the heat of reaction is studied with time and temperature. Two separate pans are implemented, one with the sample and the other with reference, and the difference in the heat flux is plotted against time and temperature. The plot is then used for the thermal transition study of the thermosets and polymers. The Fig. 3.6 shows the image of the instrument used in this study and Fig. 3.7 illustrates the schematic of the working principle.

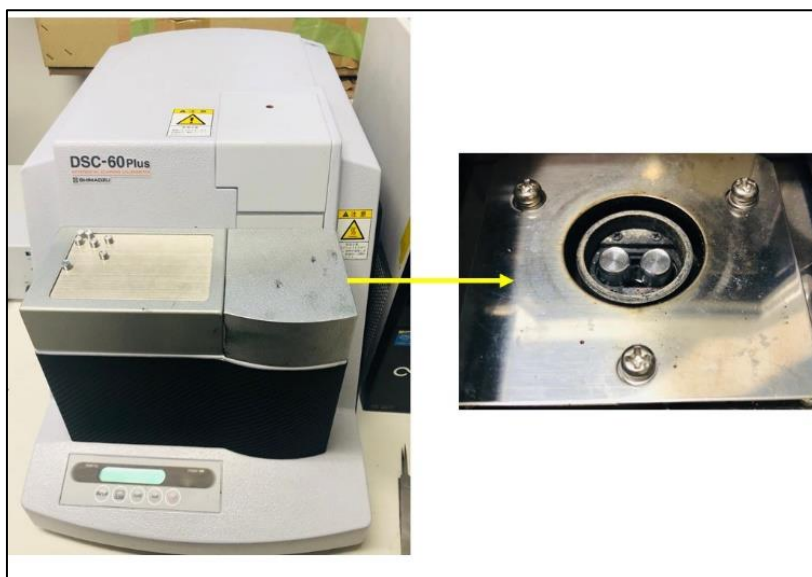


Fig. 3.6. DSC instrument used in this study. The right-hand side image shows inside of the heating chamber.

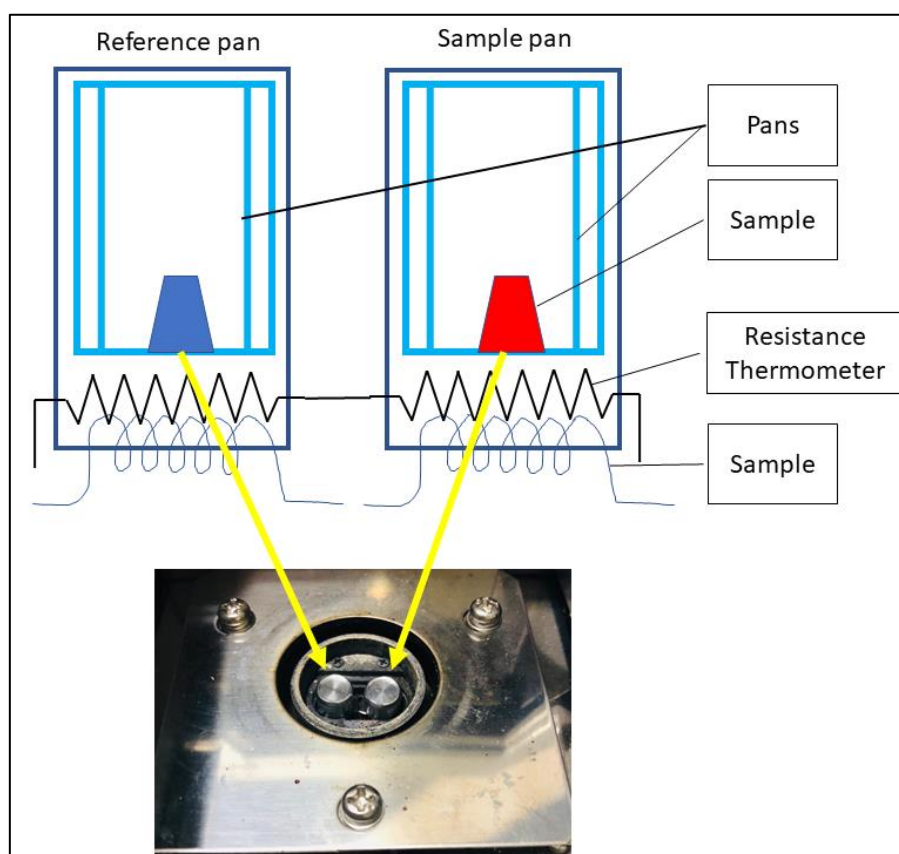


Fig. 3.7. Inside the DSC heating chamber

3.2.6. Viscometer:

Viscosity is an inevitable property for resin analysis. CFRPs fabrication is completely reliable on the viscosity of the resin. TV-25 H type model by Toki Sangyo Co. Ltd was used for conducting this study. The resin material under analysis is put in a chamber and the rotor set is immersed in it. Various kinds of analysis were done by varying the shear rate, Temperature and speed of the rotor. The detailed parametric studies done are elaborated in the further chapters. The Fig. 3.8. shows the instrument used for this study



Fig. 3.8. Viscometer used for the rheological analysis

3.2.7. Electrical Conductivity:

DC electrical conductivity was measured using the LCR meter (3522-50 LCR HiTESTER, Hioki E.E. Corporation) by four probe method. The Fig. 3.9. shows the picture of the LCR tester. The samples are cut in the dimension of $50 \text{ mm} \times 12 \text{ mm} \times 1.5 \text{ mm}$ for cured resin and $25 \text{ mm} \times 25 \text{ mm} \times 1.5 \text{ mm}$ for CFRPs. The samples are thoroughly cleaned before applying the DOTITE conducting paste on both the faces of the sample. (In the case of CFRPs, the faces depend on which conductivity is being measured: Through thickness or through plane). Then conducting tapes are attached on both the surfaces. Then the samples are dried (overnight at Room Temperature or 15mins at 45 degrees) in order to ensure the proper connection. Thereafter the probes are attached to the tapes and the value of resistance is obtained. This resistance is further converted to conductivity with the value of the dimensions of the sample.

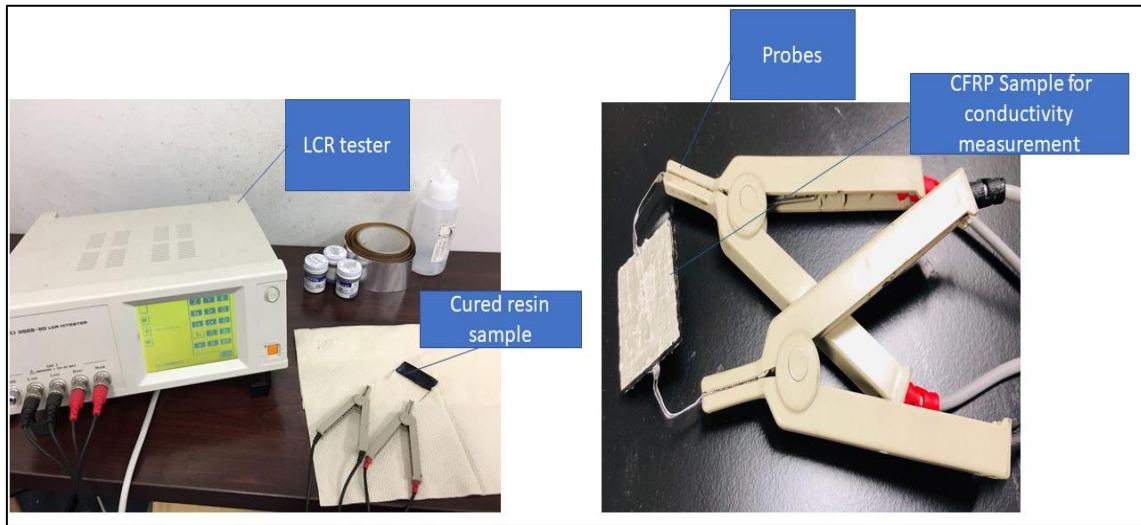


Fig. 3.9. LCR tester for Electrical conductivity measurement

3.2.8. Mechanical properties:

The primary characterisation of a composite for aerospace applications is its mechanical properties. Flexural properties were measured for the composites using the Universal Testing machine (Intron 5582) by using the three-point bending method. Fig. 3.10. shows the image of the test machine used for the technique. The sample dimensions for cured composite are 50 mm in length, 12.5 mm in width and 2 mm in thickness. The standard ASTM D790-02 was followed for the test. The load cell of 5kN was used and the crosshead speed was maintained at 1mm/min. The ratio of the thickness to span was maintained at 1:16 for unreinforced samples and 1:32 for CFRPs. Five samples were measured for each measurement to get an average of the property. The flexural modulus in GPa, the maximum stress in MPa and the maximum load in Newtons was obtained from the test along with a load-displacement curve for each measurement.



Fig. 3.10: The UTM for conducting flexural tests on the composites.

3.3. Experimental Procedure:

PANI tends to absorb unnecessary moisture from the environment due to storage and this can affect the curing profile of the resin. Thus, before the beginning of the sample preparation PANI was kept in an oven set at 60°C for almost 24hrs to eliminate this moisture effect. Dried PANI was mixed with P-2M in the weight ratio of PANI (30 wt. %) and P-2M (70 wt. %) and then mixed using a centrifugal mixture at 2000 rpm for a few minutes to prepare a homogenous mixture. This complex is then heated at 80°C for 2 hours and is named as Doping complex and the thermal treatment stage can be further termed as semi doping process. Semi doping process enhances the conductivity of the sample [7]. Next, the doping complex was mixed with more amount of P-2M to get the specific wt. % of PANI in the resin. Different batches of the resin were synthesized with PANI as the following; 0 wt. %, 5 wt. %, 10 wt. %, 15 wt. %, 20 wt. % to conduct the parametric study.

This sample was then added with the crosslinking agent perbutyl-E (10 wt. %) to get the final resin . The mixture was then poured into a flexible teflon sheet mold (dimensions: 50 mm × 15 mm × 2 mm), and thereafter pressed using a hot press at 120°C for 2 hours to obtain a cured composite. The cured composite was then post-cured at 100°C for a few hours, depending upon the composition, to release the internal stress due to pressurized curing and obtaining a completely

cured composite. Finally the cured sample was tested using non isothermal DSC test to check if any residual heat of reaction is left. If not, the sample is then used for the characterization of the electrical and the mechanical properties.

3.4. Discussions:

We have introduced P-2M as a curable dopant for polyaniline. Therefore, the characterisation was essential to confirm and understand the working of P-2M. The various characterisation techniques are discussed along with their working principle in brief. The significance of each technique is also mentioned. This chapter also explains the methodology to prepare the matrix, the resin, the cured composite. Further sections explain and analyse the results obtained through these characterisations.

Chapter -4

Introduction of a curable dopant for PANI

The functionality of P-2M has been discussed in the previous chapters. This Chapter comprises of all the study done to analyse P-2M as a curable dopant for PANI. This includes the confirmation of the doping, curing, optimisation of the amount of dopant through a series of experiments.

4.1. Mechanism of P-2M

P-2M has two functional groups: The -OH acidic group is utilized for the doping of PANI and the methacrylate group is used for curing by radical polymerisation. The main function of a dopant is to provide H^+ from its protonic functional group. The doping takes place at an elevated temperature which provides energy through the heat [25,35]. The exact mechanism of doping is illustrated in the Fig. 4.1. The H^+ ion from the acidic functional group of P-2M helps in the doping of the PANI chains. The doping process is quite similar to that of any other protonic dopant [10,15]. After the doping of PANI, it changes its state from an insulating emeraldine base form to a conducting emeraldine salt form. P-2M is a curable dopant for PANI and hence can be polymerized as well. P-2M is crosslinked by radical polymerisation to form a network of PANI attached P-2M which has high mechanical strength and this mechanism is named curing. In order to initiate the radical polymerisation [26] of P-2M, a curing initiator named Perbutyl-E is added in the amount of 10 wt.% of the total material weight. The plausible mechanism of the reaction is shown in Fig. 4.2. The Fig. 4.2 illustrates how the $C=C$ bond breaks in the presence of perbutyl-E and forms free radicals from the structure of P-2M. These free radicals initiate the radical polymerisation [19]. The applied thermal energy helps in the crosslinking between the P-2M molecules. These P-2M molecules are attached to the PANI chains in turn, hence curing the whole PANI-P-2M chains and synthesis of PANI-P-2M cured composite, which has both, mechanical strength and electrical conductivity [19]. Fig. 4.3 illustrates the route of radical polymerisation of P-2M.

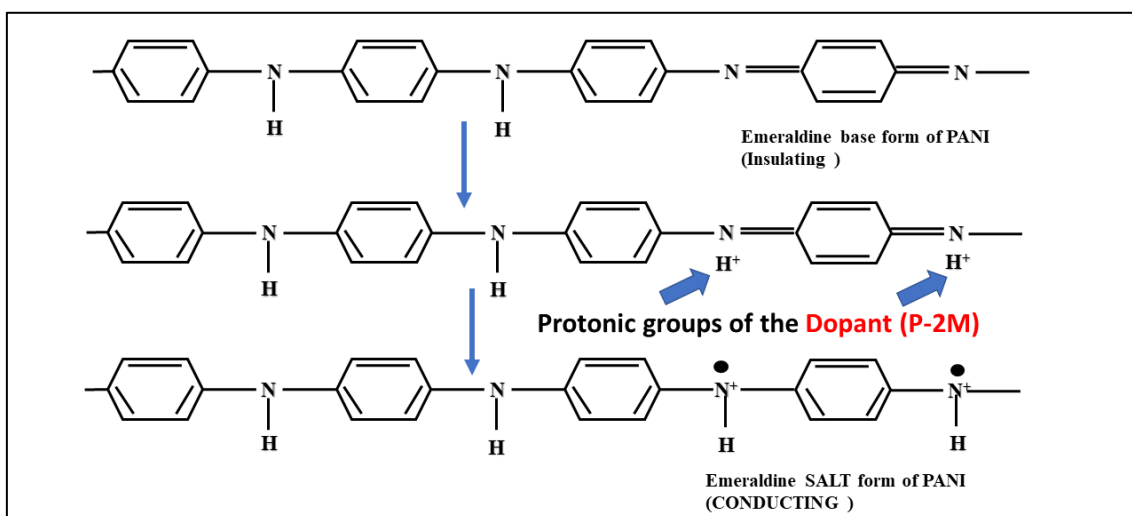


Fig. 4.1. Doping mechanism of polyaniline by P-2M [19]

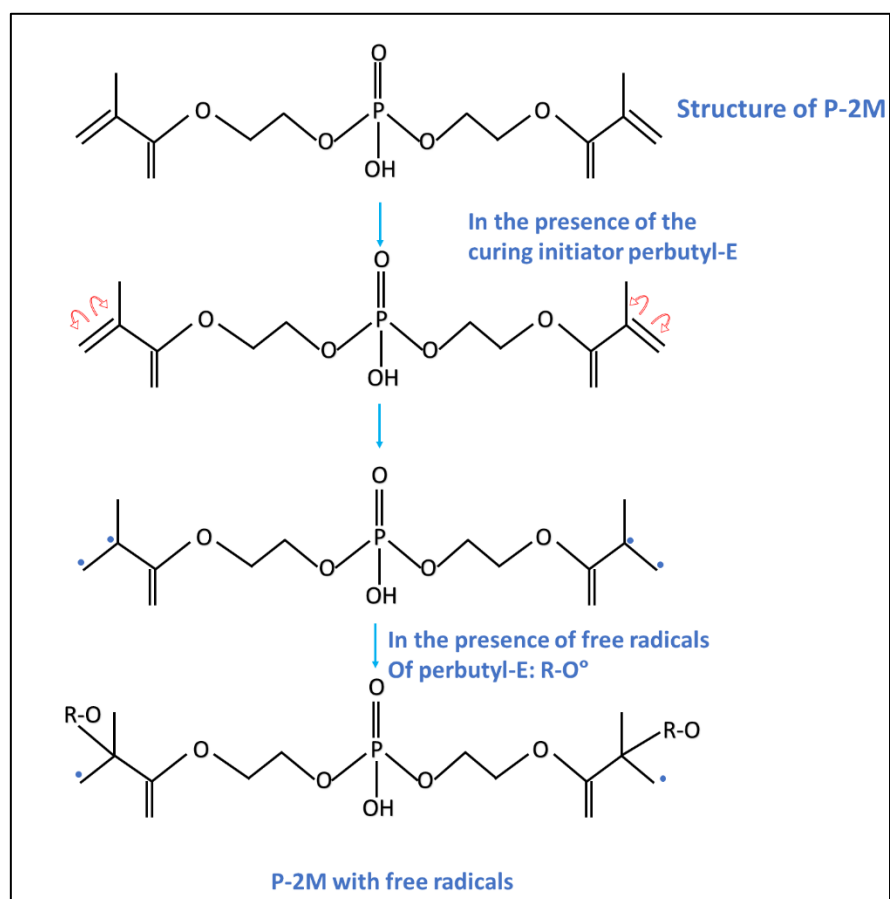


Fig. 4.2. Generation of P-2M based free radicals in the presence of Perbutyl-E [19].

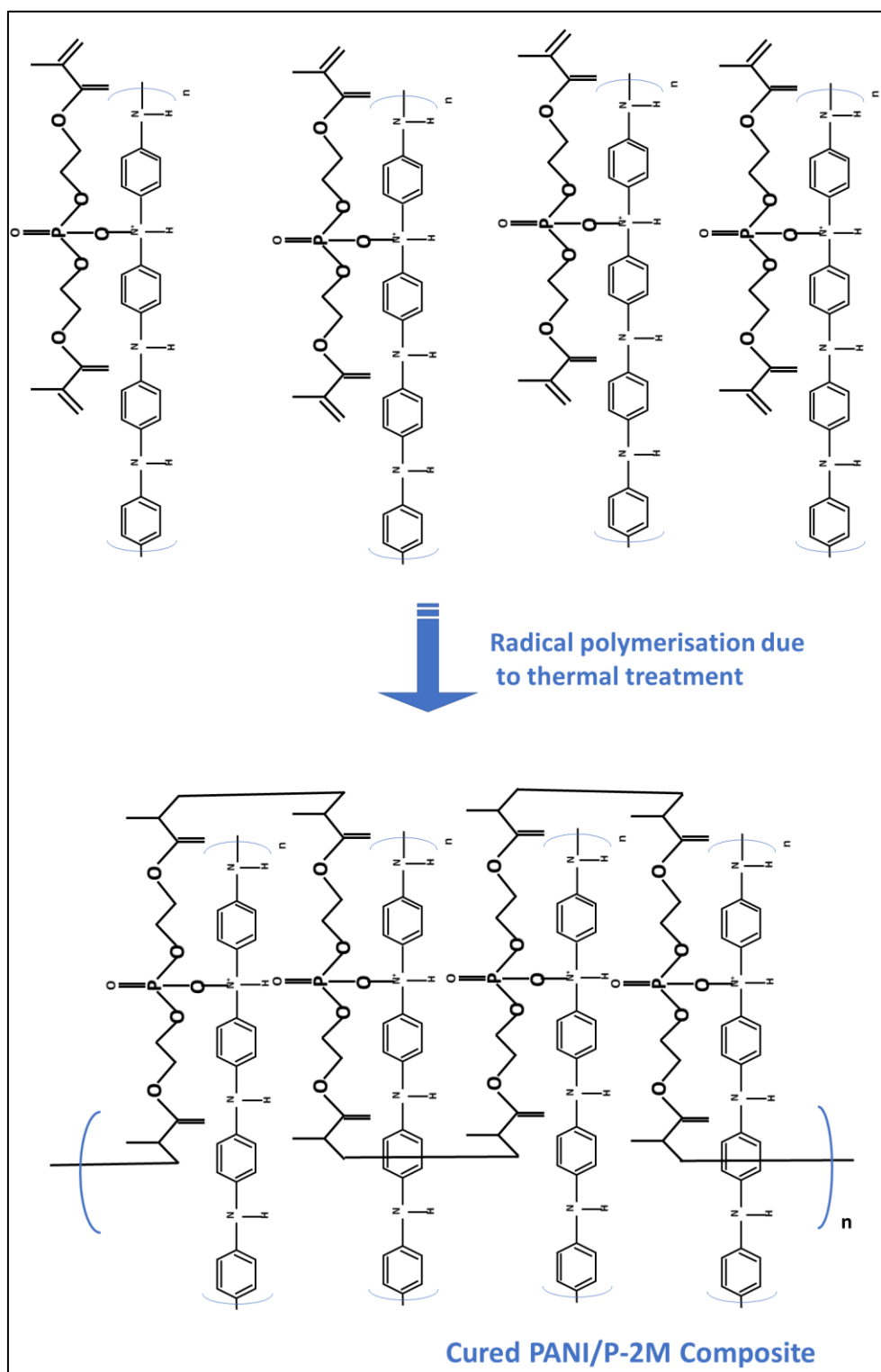


Fig. 4.3. Curing mechanism by radical Polymerisation: Cross-linked network formation of the PANI-P-2M complex due to radical polymerisation upon thermal treatment [19].

4.2. P-2M as a curable dopant:

P-2M is a new material introduced into the arena of composites [19]. Thorough analysis of the material was done in various phases: firstly, the simple mixture of PANI and P-2M was studied using techniques like Thermal microscopy and UV-Vis spectroscopy. These characterisation techniques could confirm the change in the state of PANI from insulating to conducting, in the presence of P-2M and hence, help to confirm that P-2M acts as a dopant for PANI. FTIR was used as an overall analysis tool, which helped us verify all the structural changes in the chemical due to doping and curing. Secondly, we used differential scanning calorimetry to quantify the extent of doping and estimate how much duration of time was required to dope and cure the PANI-P-2M samples [19].

4.2.1. Thermal Microscopy:

The thermal microscope was used to analyze the morphological changes in the material with temperature. The Fig. 4.4 shows the morphology at 25°C (room temperature), 50°C and 100°C. The sample used for this analysis is the simple mixture of PANI (15 wt. %) and P-2M (85 wt. %) [19]. In this analysis temperature is varied from 25°C to 120°C. As seen in the Fig. 4.4, the sample changes colour from transparent to green when the temperature is increased. The PANI, which is in insulating emeraldine base form, takes H^+ ion from the Phosphoric acid group of P-2M and heat from the environment for the process of doping. The change in the colour at around 70°C confirms the functionality of P-2M as a dopant for PANI.

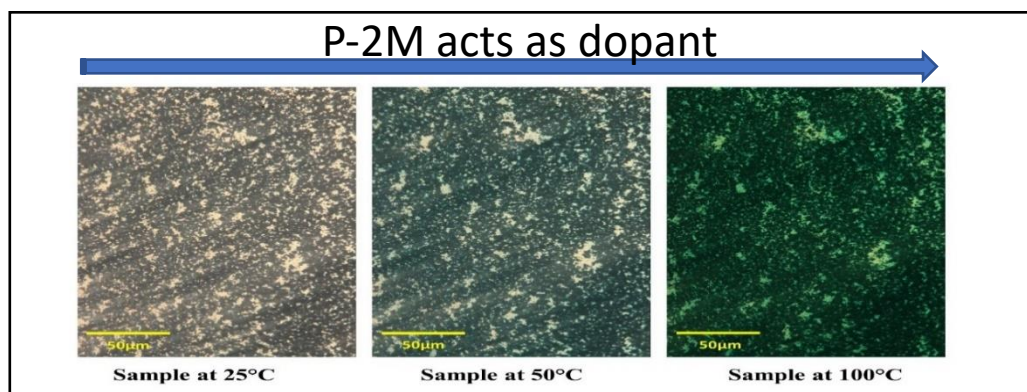


Fig.4.4: Thermal microscopy image of PANI-P-2M sample at various temperature and the onset of green colour due to doping at elevated temperature [19]

4.2.2 UV-Vis spectroscopy:

Fig. 4.5 shows the results from the UV-Vis spectroscopy of the PANI (15 wt. %)-P-2M (85 wt. %) sample. The plot displays the UV-Vis's absorbance for two different stages of the same sample: one at room temperature, shown as un-doped PANI, and the other, thermally treated, denoted as doped PANI. The thermal treatment is provided by heating the sample for 15 minutes at 120°C. Literature suggests that UV-Vis is a strong tool to determine the doping levels [31,36]. The thermal energy contributes to the doping of the PANI in the presence of P-2M thereby changing the state from insulating base to a conducting salt. The change in the absorbance level is seen in the longer wavelength range (1000 cm^{-1} - 2500 cm^{-1}). The absorbance is improved significantly even after thermal treatment of just 15 minutes. The increased absorbance indicates the change of the state of PANI from insulating base to conducting salt form. Hence this plot helps us confirm the doping of PANI with P-2M and hereafter confirms doping property of the bifunctional P-2M.

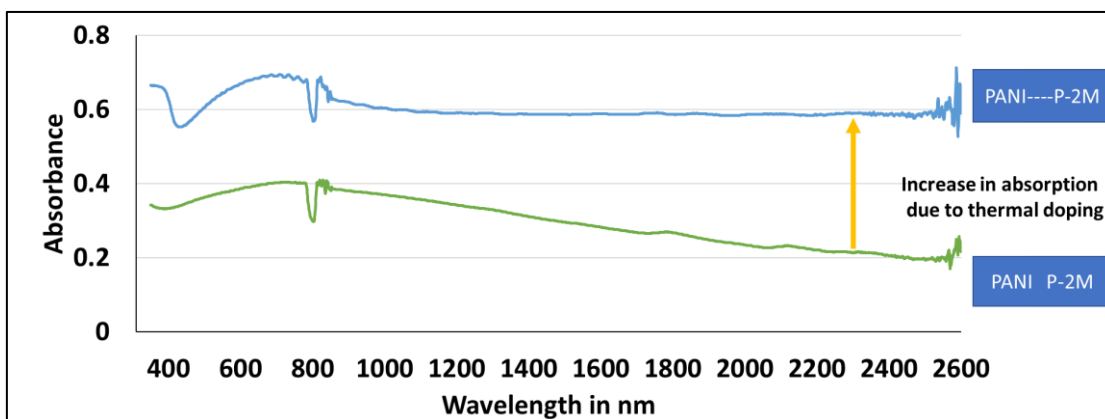


Fig. 4.5. UV-Vis plot of PANI-P-2M sample [19].

4.2.3 FTIR analysis:

Fourier transform infrared spectroscopy (FTIR) is the technique which is used to analyse the chemical structure using IR rays and examining the various levels of

absorbance. The exact mechanism is already explained in the chapter 3. The FTIR spectra were measured with an average of 20 scans and a resolution of 4 cm^{-1} . The FTIR absorbance values were normalized to obtain the comparative analysis chart so that the value shifted accordingly to get a clear view of the peaks [19]. The structural changes corresponding to doping and to curing are distinctly visible in the spectra. In order to identify and confirm that the peaks in IR spectra corresponded to each of the structural transformations in the material, a comparative FTIR breakdown was done involving the analysis at five different stages, which are listed in the Table. 4.1.

Table. 4.1. Different stages of the sample for FTIR analysis

Serial number	Stages	Description/Material	Explanation
1.	A.	PANI	-
2.	B.	P-2M	-
3.	C.	PANI and P-2M mixed	PANI is mixed with P-2M in the weight ratio of 30 wt. % PANI, at 2000rpm for 5 minutes.
4.	D.	Doped PANI and P-2M	The sample C is heated at 80°C for 2.5hours. This results in the doping of the PANI by the H^+ ions of P-2M.
5.	E.	Cured P-2M and PANI	10 wt. % of Perbutyl-E is added to the sample C and heated at 120°C for 2hours using a hot press. Thereby a fully cured composite is obtained when P-2M is cured by radical polymerisation.

All five different stages of the process were deeply analysed to study the structural changes in PANI and P-2M due to doping and curing. Fig. 4.6 shows the comparative FTIR plot of all five different samples. Now if we examine the spectra, we can see that PANI shows its distinctive benzenoid and quinoid ring peaks at around 1495 and 1582 cm^{-1} among other peaks [19]. The heated mixture of PANI and P-2M does not exhibit the peak at 1582 cm^{-1} which rather shifts towards the lower wavenumber with a much lower relative intensity [37]. In the case of doped PANI, the quinoid rings change into benzenoid rings, therefore the intensity of the peak is reduced in the doped structure. Another distinctive structural change in the process of doping is the formation of a polar covalent bond between Nitrogen atoms of PANI chain and the Oxygen atom from the acidic functional group attached to Phosphorous in P-2M. The N-O bond shows a peak at 1345-1385 cm^{-1} [38]. This newly formed peak can be seen in the Fig. 4.7 and 4.8 at same range in the doped PANI-P-2M (sample D). Another small yet noticeable peak is from the -OH group of P-2M that is seen distinctly at 2700-3000 cm^{-1} [39–41] which is not visible in the final composite when all of the OH is used up for the doping mechanism (sample C and E in the Fig. 4.6.). Hence, these confirm the structural changes appearing due to the doping of PANI.

Next, we analyse the structural changes owing to the curing of the sample through radical polymerisation. The FTIR spectrum of the final cured composite shows there is no peak at 1638 cm^{-1} as indicated in the Fig. 4.7. This peak corresponds to C=C bond which is present in P-2M and breaks during the curing procedure (as illustrated in the Fig. 4.8) [42]. Consequently, the comparative FTIR of sample C and E shows that the peaks of the C=C bonds are not present in the cured sample. The comparative detailed analysis of the process shows and confirms the various structural changes due to doping and curing and supports the reaction mechanism as explained in the chapter 3.

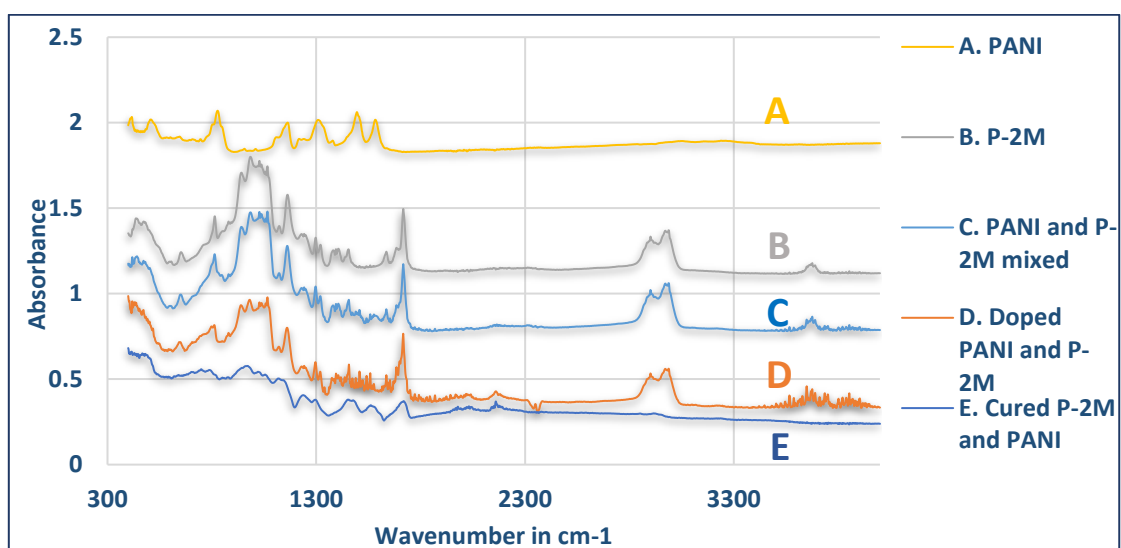


Fig. 4.6. Comparative FTIR analysis of the various stages in the process of synthesis of PANI-P-2M composite [19]

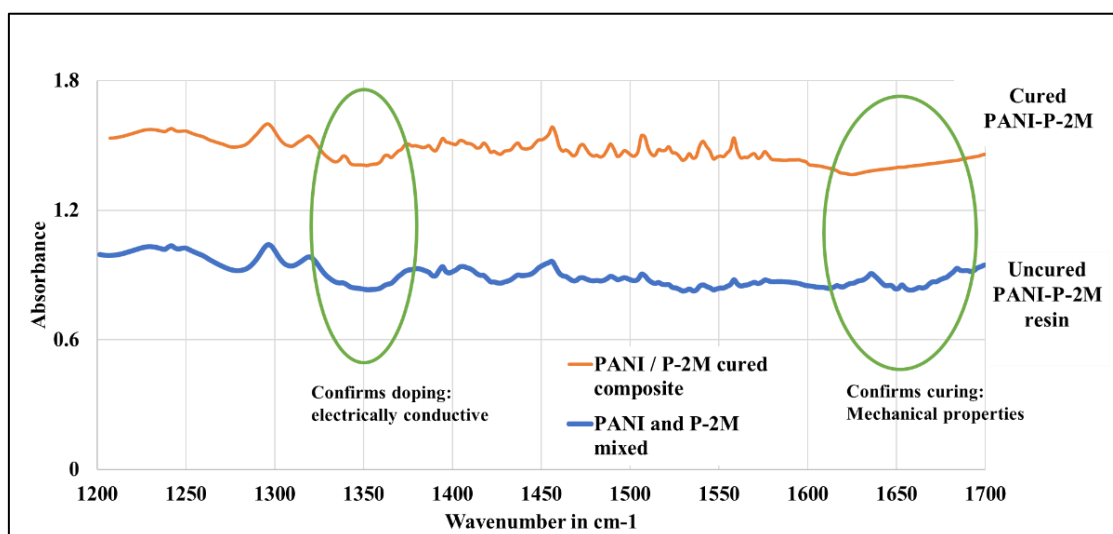


Fig. 4.7. Comparison between cured and uncured resin FTIR

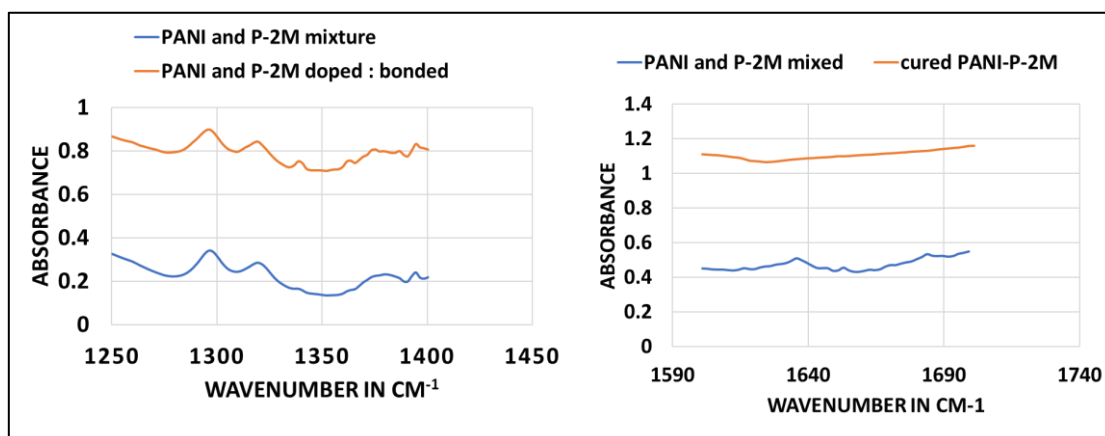


Fig.4.8. Comparison between doping peaks and curing peaks of FTIR [19]

4.2.4. Differential Scanning Calorimetry:

Differential scanning calorimetry (DSC) is a very powerful technique to analyse the thermal properties of a material. It helps examine the various exothermic reactions taking place at different temperatures when PANI and P-2M are mixed. The exact doping and curing reactions qualitatively and quantitatively were investigated using the DSC. The PANI (15 wt. %)-P-2M (85 wt. %) samples was prepared [19]. The doping peak was confirmed using periodic thermal treatment of the sample at 80°C and it was analysed after each period of thermal treatment. The sample was heated from room temperature to a high temperature of 300°C. The heat of the reaction obtained from the software was plotted against temperature. Fig. 4.9 displays four different plots of the sample thermally treated for 0 h, 1 h, 2 h and 2.5 h respectively and the peak of doping is visibly gradually diminishing with the increased heat treatment duration. From the plot and the heat of reaction obtained, we calculated the exact amount of time for doping for the constitution of the sample and the further experiments were performed accordingly.

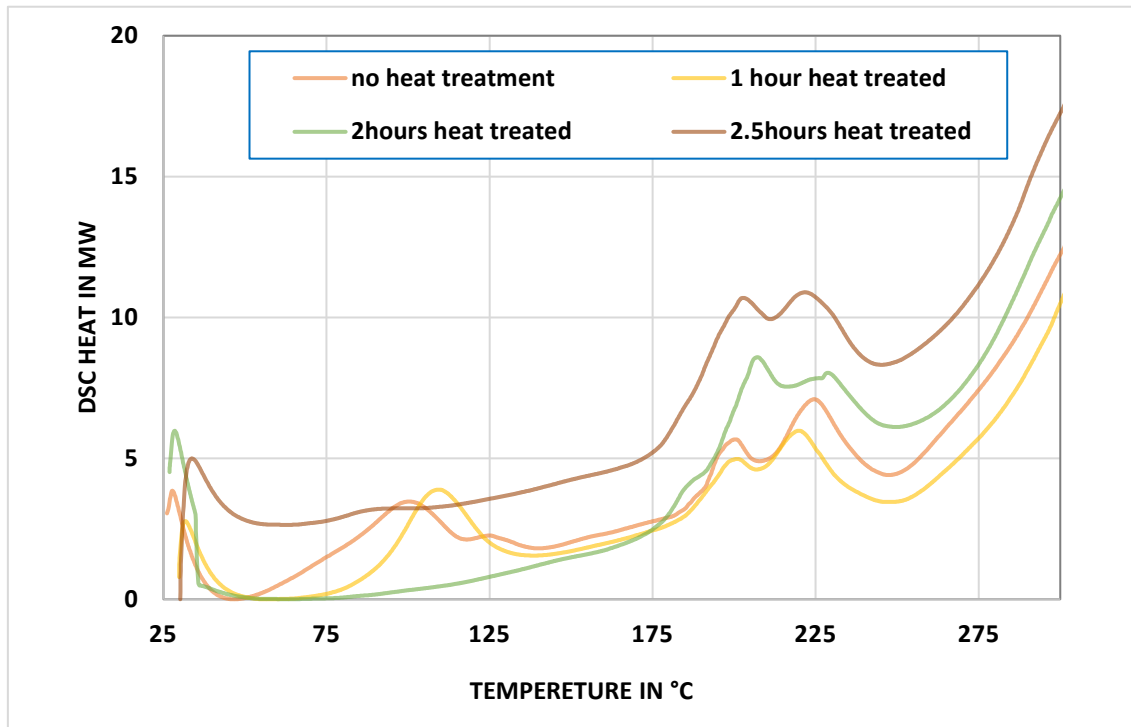


Fig. 4.9. DSC analysis of PANI-P-2M samples in periodic thermal treatment for doping estimation [19]

4.3. Optimization of the PANI/P-2M:

The amount of P-2M required for doping PANI and successfully synthesize the composite was determined after a series of experiments. The theoretical evaluation is shown below to estimate the exact weight ratio of PANI:P-2M that gives the maximum conductivity.

Maximum conductivity is achieved when the doping level is the highest i.e. 100%. The doping level can be denoted by the following formula:

$$\% \text{ Doping} = \frac{[OH]}{[N_{total}]} \times 100 \%$$

Therefore, in order to obtain the maximum doping level the number of OH groups in P-2M should be equal to the total number of N atoms in the PANI. Now, from the

chemical structure of PANI and P-2M as shown in Fig. 4.10. the number of N atoms in a PANI molecule is 2 for doping and each P-2M has one OH group. Therefore 1 PANI molecule required 2 P-2M molecules in order to dope completely. Consequently, the molar ratio for maximum doping is

$$\frac{[PANI]}{[P-2M]} = 2$$

Corresponding weight ratio is estimated by the following formula

$$\begin{aligned} & (PANI/P-2M)_{weight} \\ &= (PANI/P-2M)_{molar} \times \left(\frac{Mol. wt. of PANI}{Mol. wt. of P-2M} \right) \end{aligned}$$

The weight ratio estimated corresponding to the molar ratio of 2 is 0.58. Uncured PANI-P-2M samples were prepared in the following molar ratios: 1:1, 1:0.9, 1:0.8 and 1:0.7 and the electrical conductivity were measured as shown in the Fig. 4.11. The maximum feasible conductivity was obtained in the sample with the molar ratio 1:0.7 of 30 S/m. However, we tried to obtain the 1:0.6 and 1:0.5, but the matrix was not feasible. Therefore, the ideal molar ratio couldn't be synthesized. Nevertheless, the next nearest molar ratio 1: 0.7, which is practically feasible , gave 30 S/m as the conductivity. Fig. 4.11. shows the other molar ratios and their conductivities obtained.

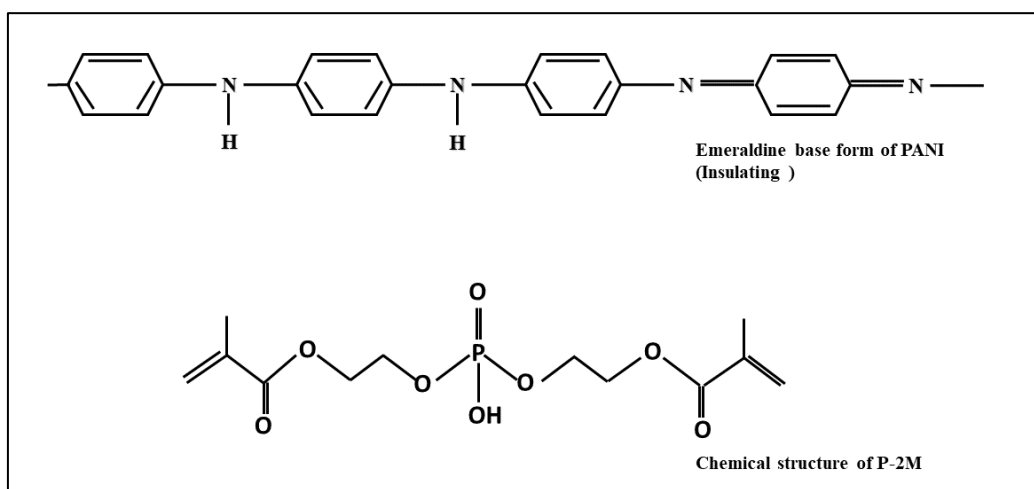


Fig. 4.10. Chemical structure of PANI and P-2M

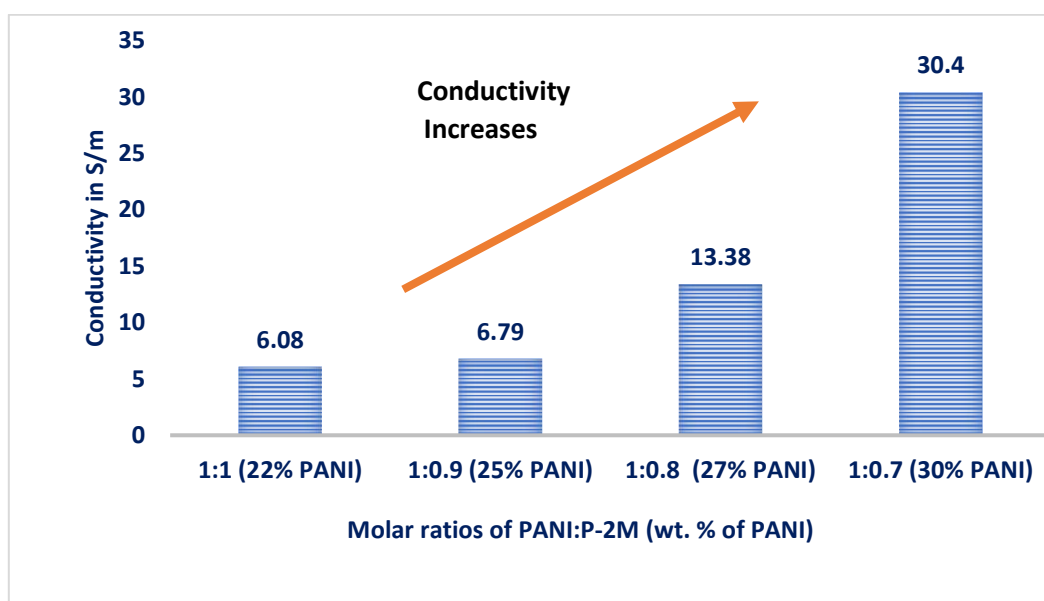


Fig. 4.11. Electrical conductivity of uncured PANI-P-2M samples mixed in various molar ratios [19]

4.4. Discussions:

This chapter introduces P-2M as a curable dopant. Curable dopant is a novel concept introduced in this thesis and P-2M is found to be one of the first materials to show such properties. All these techniques were used to characterize and confirm the functionality of P-2M as a curable dopant. The doping was qualitatively confirmed by Thermal microscopy, UV-Vis spectroscopy and FTIR spectroscopy. The curing was confirmed by the structural changes shown in the FTIR analysis. Further using DSC, we estimated the exact amount of time for doping the complex of PANI-P-2M. Further the amount of PANI and P-2M was optimized to get the maximum conductivity. This chapter summarizes the results and discussions of PANI/P-2M complex. Further, we discuss the properties of the composite of PANI/P-2M resin in the further chapter.

Chapter -5

Development of the PANI/P-2M composite

The P-2M functionality as a curable dopant has been well explained in the previous chapter. This chapter focusses on the resin of PANI/P-2M. The resin characterisation begins with thermal analysis to estimate the activation energy, curing energy. Next, the resin viscosity is studied with various wt. % of PANI and shear rate and time duration. Viscosity is an inevitable property for a CFRP resin. Finally, the chapter discusses the properties of the cured composite obtained from the resin.

5.1. Samples preparation

The exact procedure for the sample preparation is explained in the section 3.3 of the chapter 3. In order to study optimisation of the resin with various wt. % of PANI , different batches of the resin were prepared. In the following sections the thermal analysis of the resin is conducted, then rheological analysis using the liquid resin. Finally in order to check the mechanical and electrical properties, the resin is cured at 120 °C for 2 hours with the necessary post curing applied. Subsequent analysis is elaborated in the following sections .

5.2. DSC analysis for chemical kinetics study

DSC is the most essential technique for composites study conducted in this thesis. The preliminary study was done to estimate the activation energy for the reaction to start doping and curing. Further the exact amount of energy required for doping and curing was estimated for various wt. % of PANI.

5.2.1 Estimation of the activation energy

The objective of this study is to determine the kinetics of the curing reaction PANI/P-2M with the crosslinking agent Perbutyl by Dynamic DSC. There have been many reports on the study of the curing of the thermoset polymers and estimation of the activation energy (E_a) using the DSC [7,43–47]. The E_a has been estimated for the epoxy resin curing with various curing agents and is well documented [24,25]. Rosu et al. estimated the activation energy for the epoxy resin using curing kinetics with various kinds of curing agents [50,51]. However, there is no such study on the curing of the polyaniline-based conducting resins yet. We have used the differential scanning calorimetry to carry out the characterization and thermal analysis. 20mg of the uniformly mixed resin was poured into an aluminium sample holder and closed tightly under pressure. The

internal picture of the DSC with the sample holders is illustrated in the Fig. 3.7 and explained in the chapter 3. The dynamic DSC was performed from room temperature till 200 °C at 5 different heating rates: 2.5, 5, 10, 15, 20 °C/min. The Fig. 5.1 shows the dynamic DSC plots and the inset shows the various heating rates in °C/min .

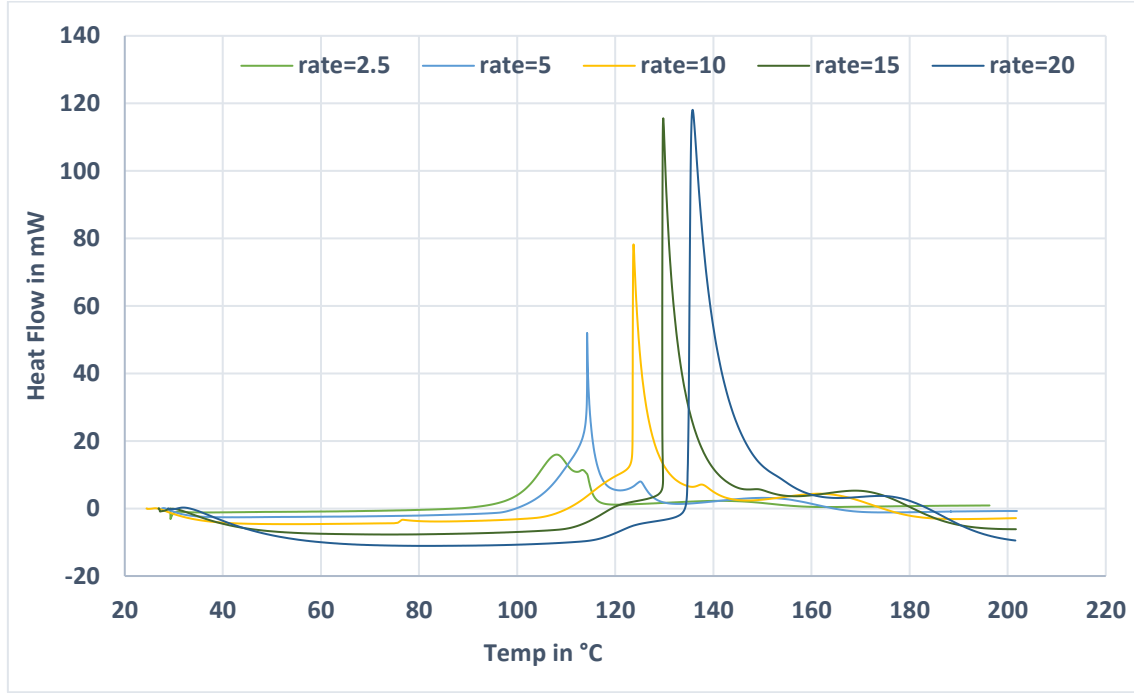


Fig. 5.1. Dynamic DSC thermographs from Room Temp until 200 °C at different heating rates[7].

As expected, the DSC plot shows a broad exothermic peak corresponding to the heat released during the crosslinking. As the heating rate increases, the exothermic peak becomes wider and the peak temperature shifts towards the higher range. Therefore the E_a can be calculated applying the Kissinger method [52]. We also calculated using the Barrett's method [53] and got approximately similar value of E_a . The extent of reaction or the degree of cure (α) is given by $\Delta H_t / \Delta H$, where ΔH_t refers to the heat of the exothermic peak and ΔH refers to the total heat of the reaction.

$$\alpha = \frac{\Delta H_t}{\Delta H} \quad (1)$$

since the peak temperature T_p increases with the increase in the heating rate k , therefore we applied the Kissinger method to derive the E_a through the following equation [54]:

$$\ln \left(\frac{k}{T_p^2} \right) = \ln \left(\frac{AR}{E_a} \right) - \frac{E_a}{RT_p} \quad (2)$$

The plot of the LHS , $\ln (k/T_p^2)$ vs $1/T_p$ gives a straight line of the form $y=mx + c$, where the slope of the plot is $-E_a/R$. Fig. 5.2. shows the plot of $\ln (k/T_p^2)$ vs $1/T_p$ and the slope is -10903 which corresponds to the E_a to be 90.648 kJ /mol.

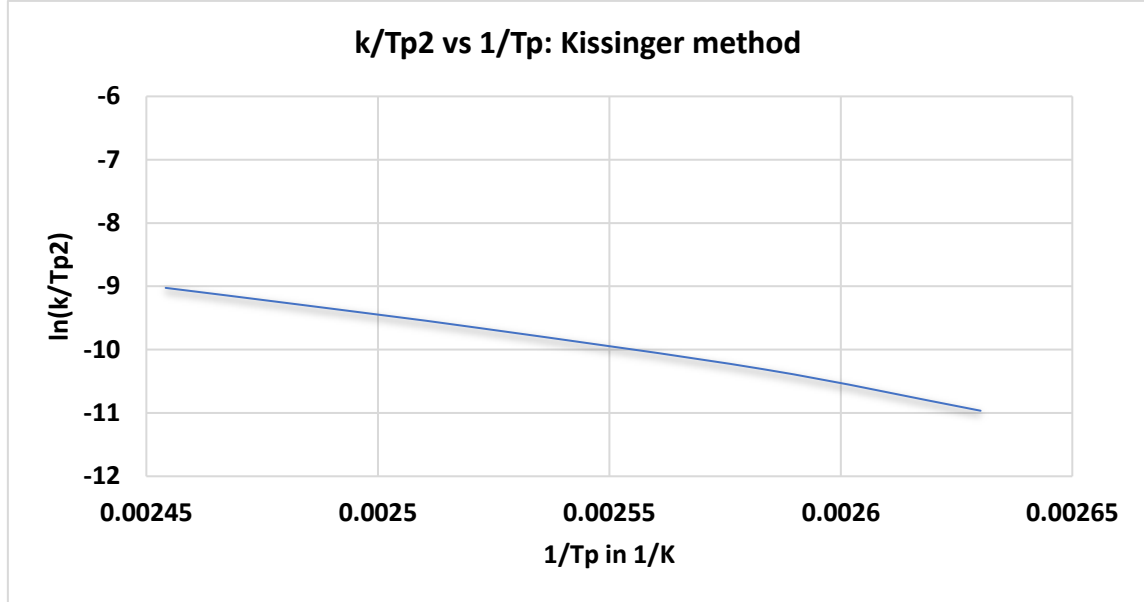


Fig. 5.2 : Kissinger plot to determine the activation energy [7]

Next, we use the classic Barrett's method to calculate the activation energy. For this calculation we followed the work by Ghaemy et al.[48] on the cure kinetics study on epoxy using the Barrett's method. Continuing from equation (1), the reaction rate ($\frac{d\alpha}{dt}$) is directly proportional to the rate of heat generation as given by the equation (3) below.

$$\frac{d\alpha}{dt} = \frac{1}{\Delta H_t} \frac{dH}{dt} \quad (3)$$

The reaction rate is also expressed in terms of Arrhenius equations as :

$$\frac{d\alpha}{dt} = kf(\alpha) \quad (4)$$

Where k is the rate constant and the $f(\alpha)$ is a function of the extent of cure and this depends on the mechanism of the curing reaction.

The rate constant is expressed as:

$$k = A \exp\left(-\frac{E_a}{RT}\right) \quad (5)$$

Where, A is the frequency factor, E_a is the activation energy , R is the universal Gas constant and T is the temperature in kelvin.

Hence, if we substitute value of k from equation (5) to equation (4), we obtain

$$\frac{d\alpha}{dt} = A \exp\left(-\frac{E_a}{RT}\right) f(\alpha) \quad (6)$$

On integrating both sides , we get

$$\ln k = \ln A - \frac{E_a}{RT} \quad (7)$$

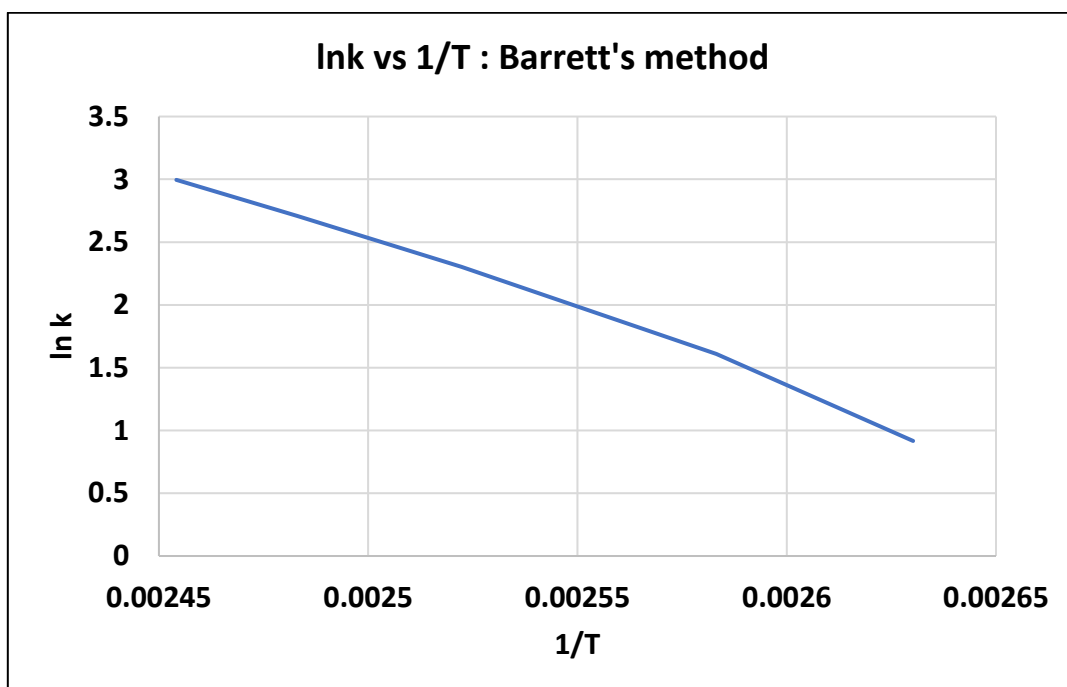


Fig. 5.3 : Plot of $\ln k$ vs $1/T$ for the Barrett's method [7]

The plot of $\ln k$ vs $1/T$ was obtained by getting values from the plot of Fig. 5.1 to obtain the Fig. 5.3. The slope of the plot determines the activation energy to be 97.19 kJ/mol. Hence, the cure kinetics analysis by both the methods provide similar values of the activation energy (97.19 kJ/mol and 90.648 kJ/mol). Similarly , we also estimated the E_a for the control cure resin (P-2M (90 wt. %) and Perbutyl (10 wt. %)) by non isothermal DSC analysis at various rates of heating. The E_a was estimated to be 138.44 kJ/mol (Barrets method) and 132.02 kJ/mol(Kissinger method)

5.2.2 Estimation of the curing and doping energy

We studied the doping mechanism of the PANI-P-2M resin. The doping phenomenon is completely about the doping of polyaniline therefore the study was carried out by preparing resins with various amount of polyaniline. DSC analysis was done using the doping complex (preparation explained in the chapter 3) and estimated the amount of energy required per g of P-2M for the doping phenomenon. Before undergoing thermal treatment, the doping complex was first heated in the DSC test and we estimated the total amount of energy required to fully dope it. And after the thermal treatment of 2hrs at 80 °C , the complex was again heated in the DSC to check the residual exothermic reactions after the Semidoping procedure. The initial total energy that is designated as the ΔH_{doping} is estimated to be 232.8 J/g, the residual energy, designated as ΔH_{res} is estimated to be 72.8J/g as shown in the Fig. 5.4. So the doping energy used up at the semi doping stage is 160J/g.

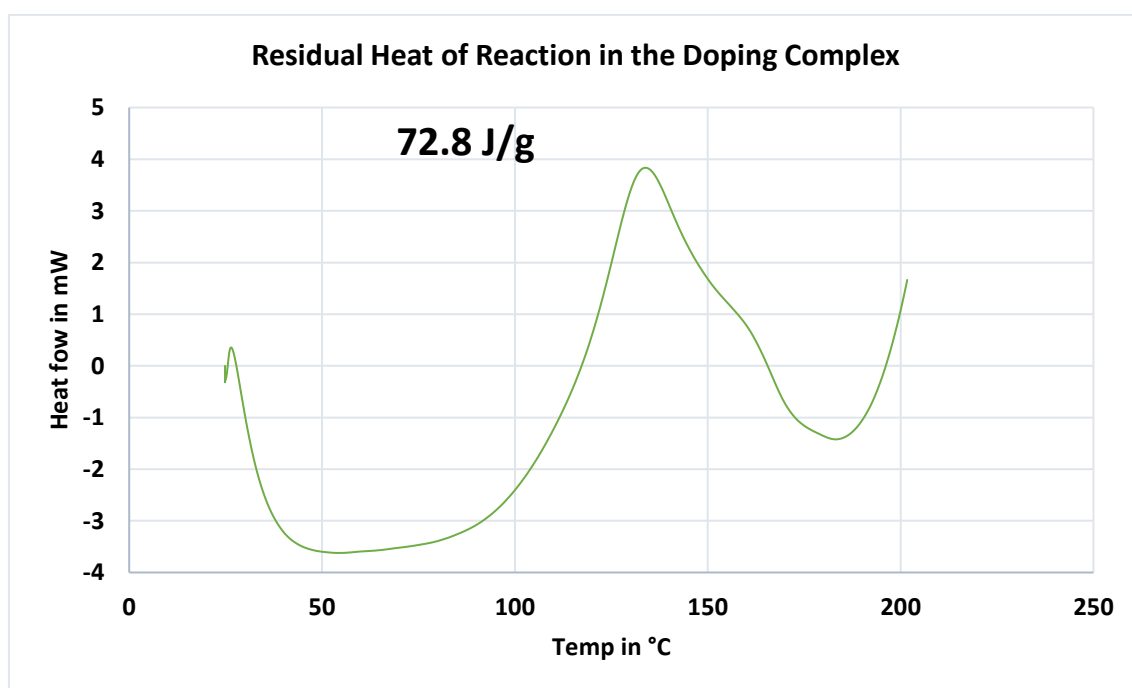


Fig. 5.4. DSC thermograph for the analysis of doping complex [7]

Next, this doping complex was used to prepare the final resin which was ultimately cured. For the sample calculation, following wt. % ratios for the constituents of the resin is prepared: PANI (20 wt. %), P-2M (70 wt. %) and the crosslinking agent Perbutyl as (10 wt. %). Now, this resin sample undergoes non isothermal DSC , and is heated from room temperature till 300 ° C. The exothermic heat of the reaction at around 120°C is the curing reaction, which hardens the resin to form the composite. This exothermic peak must also include the residual of the doping

reaction left to be finished. Hence the heat of reaction here is ΔH_{total} is given by the following equation:

$$\Delta H_{total} = \Delta H_{res} + \Delta H_{cure} \quad (8)$$

Now, in order to estimate the amount of energy required for the curing of the resin material, we need to estimate the ΔH_{total} and ΔH_{res} . ΔH_{total} is the one estimated from the DSC of the resin material (243 J/g) as shown in the Fig. 5.5 and the ΔH_{res} was obtained as 72.8J/g from the DSC of the doping complex as shown in the Fig. 5.4. However, that was per g of the doping complex, so by estimating it per g of the resin, ΔH_{res} is 48.6 J/g. therefore, the ΔH_{cure} is calculated as

$$243 - 48.6 = 194.4 \text{ J/g.}$$

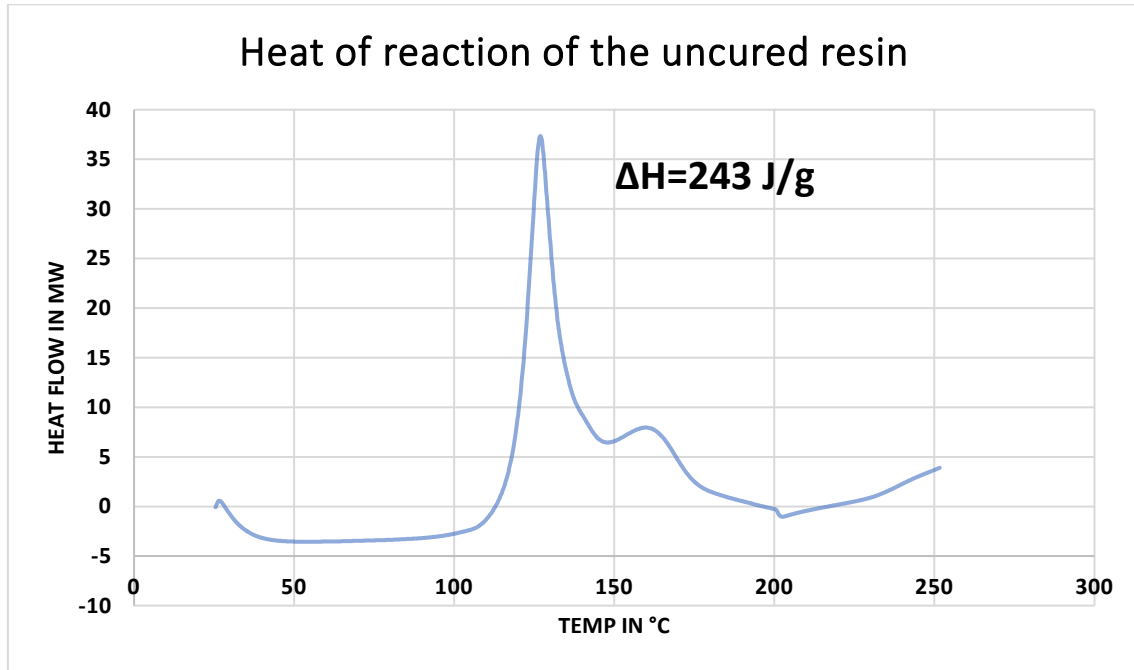


Fig. 5.5 : DSC of the uncured resin with 20 wt. % PANI [7]

Consequently, we estimated the amount of energy per unit gram of the resin used; 155.51 J/g for the doping of the PANI and 194.4 J/g for curing the composite. Now the resin can be prepared in various compositions of PANI and P-2M to vary the electrical and mechanical properties of the resin. Therefore, we calculated the amount of curing and doping energy per unit g of P-2M to be ; 222.2 J/g for doping and 277.7 J/g for curing the composite. This amount of energy was estimated for 4 different compositions of the resin with various wt. % of PANI in them: 5, 10, 15 and 20 wt. %. The various curing energy which estimated is shown in the Fig.

5.6, which explains how the curing energy per unit weight of P-2M decreases with the increasing wt. % of PANI in the resin. This is clearly due to the analogy that as the amount of PANI increases in the resin, the amount of P-2M required for doping increases. Since P-2M is the bifunctional material, responsible for both doping and curing, when higher % of P-2M is used up in the doping, lesser amount is left for curing reaction. Hence with less amount of P-2M, the amount of energy required to cure the resin also decreases. Accordingly, the amount of energy, experimentally required to cure the resin was applied by various duration of the temperature applied. Therefore, when we fabricated the cured composite for characterization as explained in the chapter 3, the resin with 5 wt. % of PANI required more time for post curing whereas the one with 20 wt. % of PANI required less time to obtain a fully cured sample.

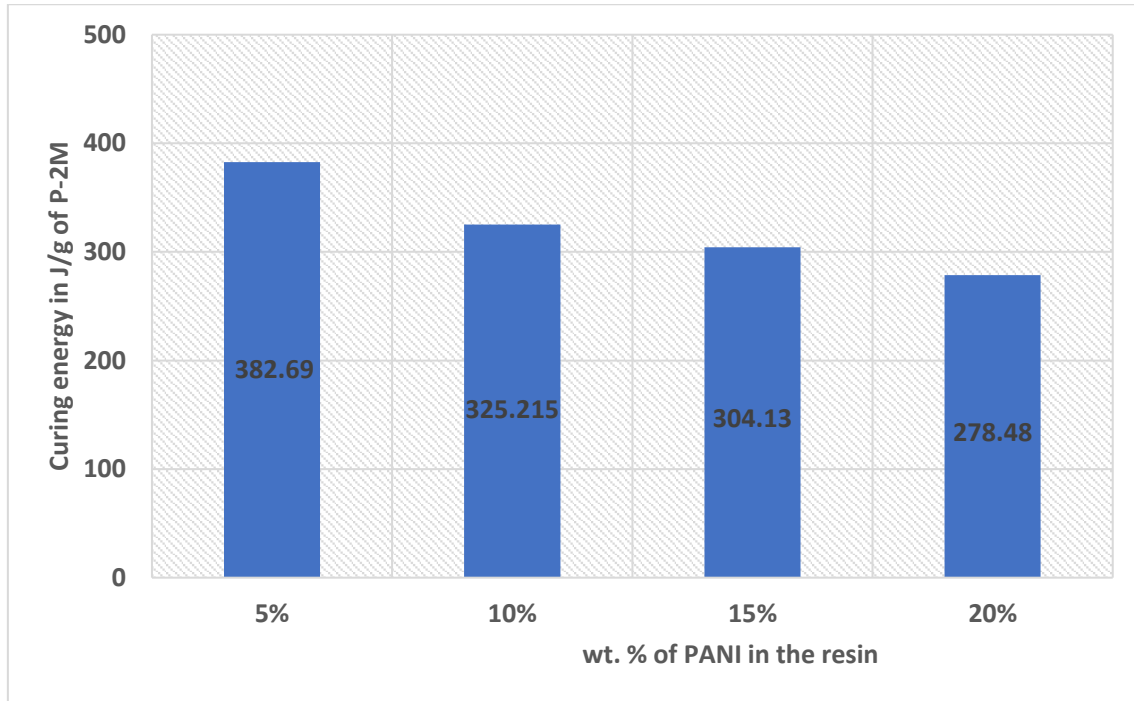


Fig. 5.6. Estimated curing energy for each constitution of the resin [7]

5.3 Rheological analysis of the resin

The viscosity of the resin is a key factor for CFRP structures manufacturing. It determines how well you can make the dry fabric impregnated with the resin. The viscosity in the range of 1.5-2.4 Pa.s is good for processability and good impregnation of the carbon fibers [5]. Fig. 5.7 shows the variation of the viscosity of the resin with increasing shear rate for neat resin (0 wt. % PANI) and 5, 10, 15, 20 wt. % PANI. The neat resin doesn't show any change in the viscosity

with shear rate as expected for a Newtonian fluid behavior. But gradually with the addition of PANI, the resin shows shear-thinning (Non –Newtonian fluid) properties with viscosity decreasing with increase in the shear rate. This is the preliminary study, but it conforms the expected behaviour with the addition of PANI into the P-2M resin. Similar studies have been done extensively on epoxy resin [55] and can be also done elaborately for the PANI based resins using complex viscometer analysis.

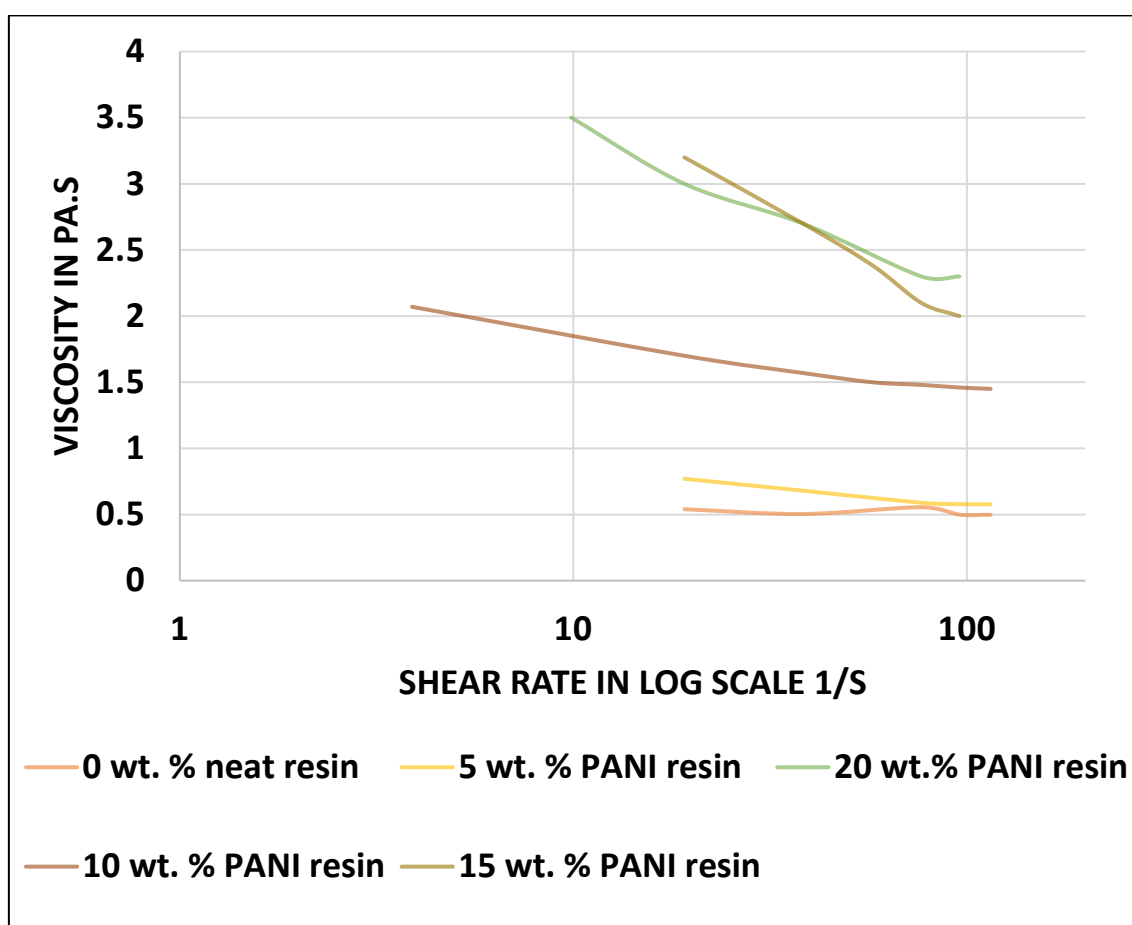


Fig. 5.7. Change in viscosity of the resin with shear rate.

Further we studied the steady state viscosity of the uncured resin. Fig. 5.8 shows the steady state viscosity of the resin with 20 wt. % of PANI . The viscosity was measured using a small amount of the uncured resin and the test was run for 120minutes at 10rpm. The viscosity doesn't increase at room temperature with time unlike our previous resin system of PANI/DBSA [56] . This shows that the resin is quite stable at room temperature and hence quite appropriate to

be used for industrial purpose. One of the most important reasons for the commercial widespread use of epoxy is because the resin can be impregnated into the fabrics to make prepregs and these prepregs can be stored well for long time and cured when required. Further studies show how this factor contributes in the easy fabrication of the CFRP.

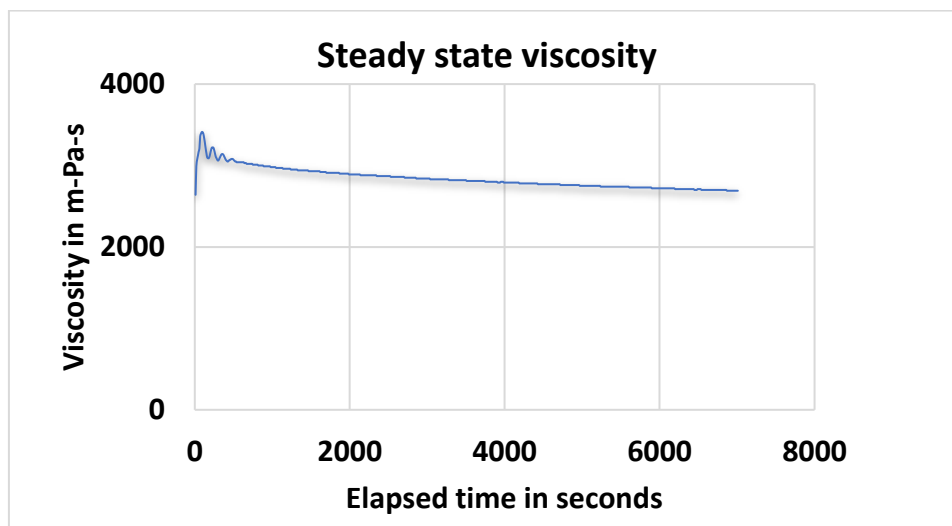


Fig. 5.8. Steady state viscosity for 20 wt. % PANI resin

Similarly, the steady state viscosity was obtained for various kinds of resin including the 0 wt. % PANI resin (neat resin). The following is the constitution of the uncured resin under characterization: 0, 5, 10, 15, 20 wt.% of PANI. The steady state viscosity increases with increases in the amount of PANI in the resin. PANI is in powder form and hence the miscibility is lower and therefore it makes the resin more viscous. The Fig. 5.9 shows the plot of viscosity change with various wt. % of PANI added in the resin. The one with 0 wt. % PANI is quite watery and the one with 20 wt. % PANI has the maximum viscosity. However, the values are constant with time as the P-2M doesn't react at room temperature.

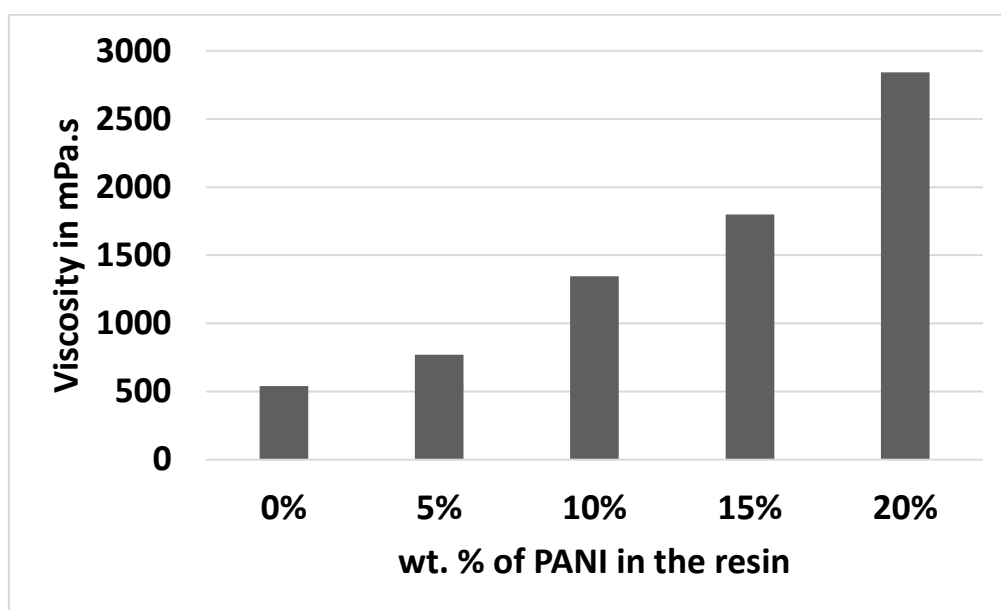


Fig. 5.9. Variation of the viscosity with increasing wt. % of PANI in the resin

5.4 Cured Composite characterisation

The main objective of our study is to use PANI based resin for fabrication of conductive CFRPs for structural applications. Our previous research was based on applying DBSA as the dopant for PANI which has been proven to provide much higher conductivity than epoxy resin system, however the mechanical properties are yet to be enhanced. With this new bifunctional dopant P-2M, we prepared the resin and cured them. By this means we measured their mechanical and electrical properties. The parametric study was done by varying the amount of PANI in the resin.

The mechanical properties were measured using the 3-point bending test which is explained in brief in the chapter 3. The mechanical property is affected by the addition of PANI. The long chains of PANI affect the curing mechanism of the P-2M molecules by radical polymerization. However, the neat resin with 0 wt. % PANI sample resin has extremely low viscosity and therefore we faced many difficulties in successfully curing a composite with this resin in perfect shape for further characterization. Nevertheless, we fabricated some samples under special conditions and obtained the Flexural modulus of 2.83 GPa. Yet, the resin was successfully impregnated into the CFs to fabricate CFRPs, which are reported in the further chapter. The samples show a flexural modulus in the range of 2.5-3.2 GPa. Fig. 5.10 shows the plot of flexural modulus obtained for composites with various wt. % of PANI. Similarly, the maximum stress for all the other variations of wt. % of PANI is also summarized in the fig. 5.12. The mechanical strengthening of the cured resin declines with increase in the wt. % of PANI in

the sample. This is inherently because P-2M provides strength as well as conductivity. Thereby, when PANI is introduced in the system, P-2M's functionality is more active for the doping mechanism. Therefore, the curing process takes time. Hence with the increase in the amount of PANI, the cured resin's mechanical stiffness and modulus decrease. Fig. 5.12 shows a typical load-displacement curve for the PANI/P-2M resin composite with 20 wt. % PANI. The maximum stress is 14.85 MPa.

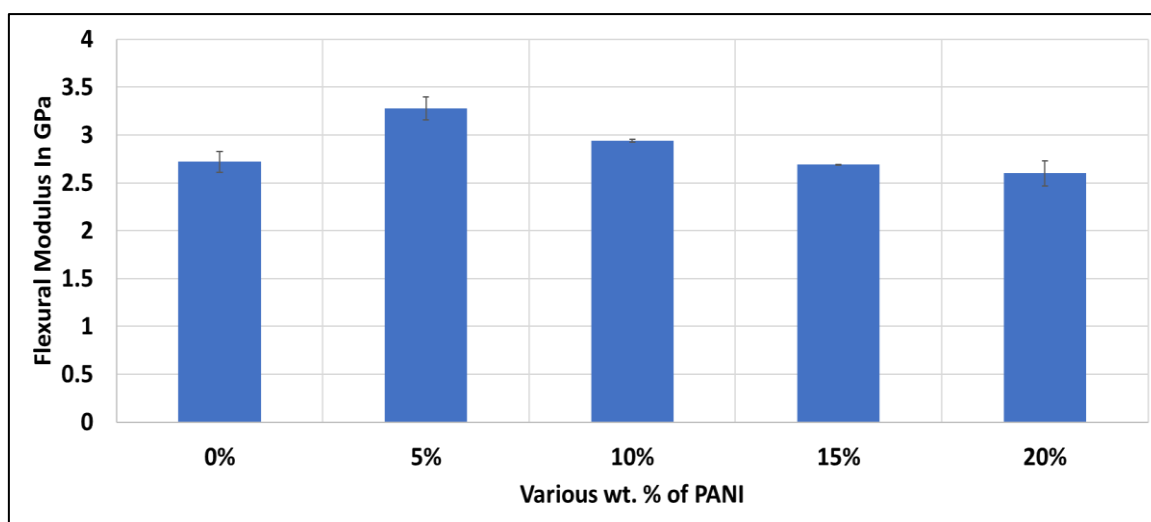


Fig. 5.10. Flexural modulus with various wt. % of PANI in the resin

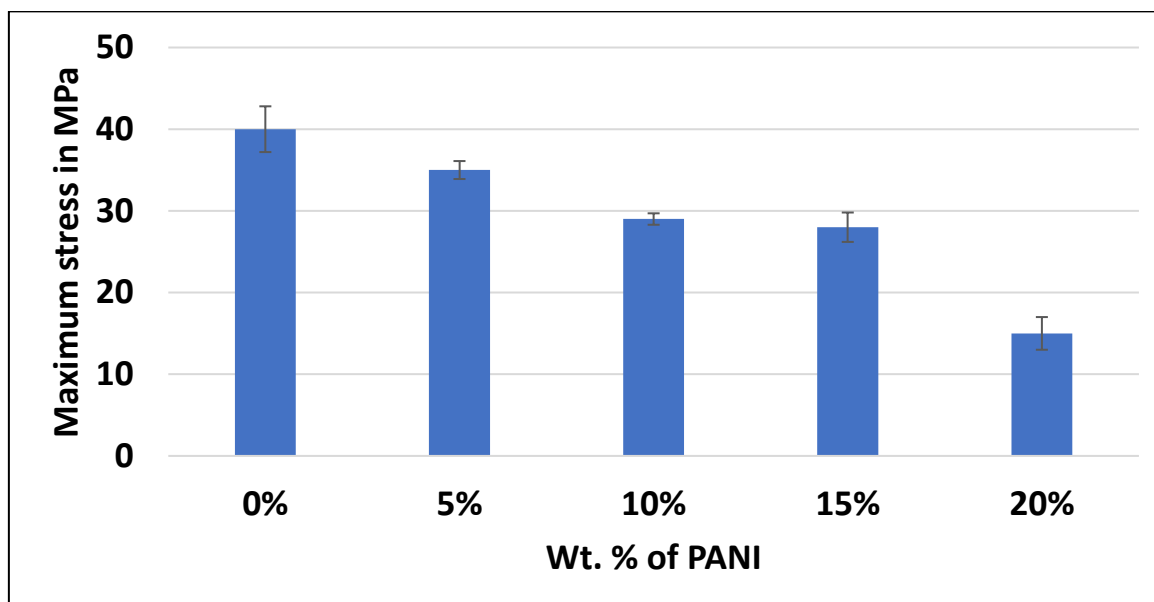


Fig. 5.11. Maximum stress with various wt. % of PANI in the resin

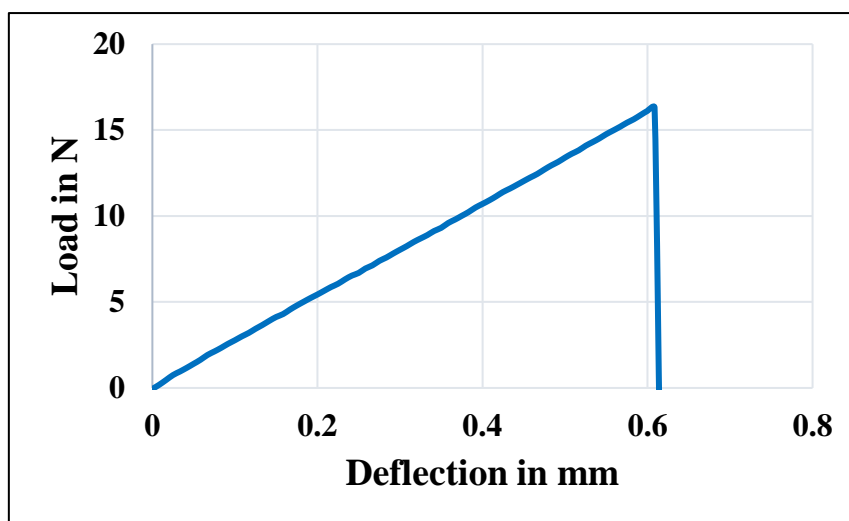


Fig. 5.12. Load displacement curve of a cured composite of PANI-P-2M

The electrical conductivity was measured for the cured composites. The electrical conductivity increased with increasing the amount of PANI. Fig. 5.13 shows the plot of conductivity with wt. % of PANI.

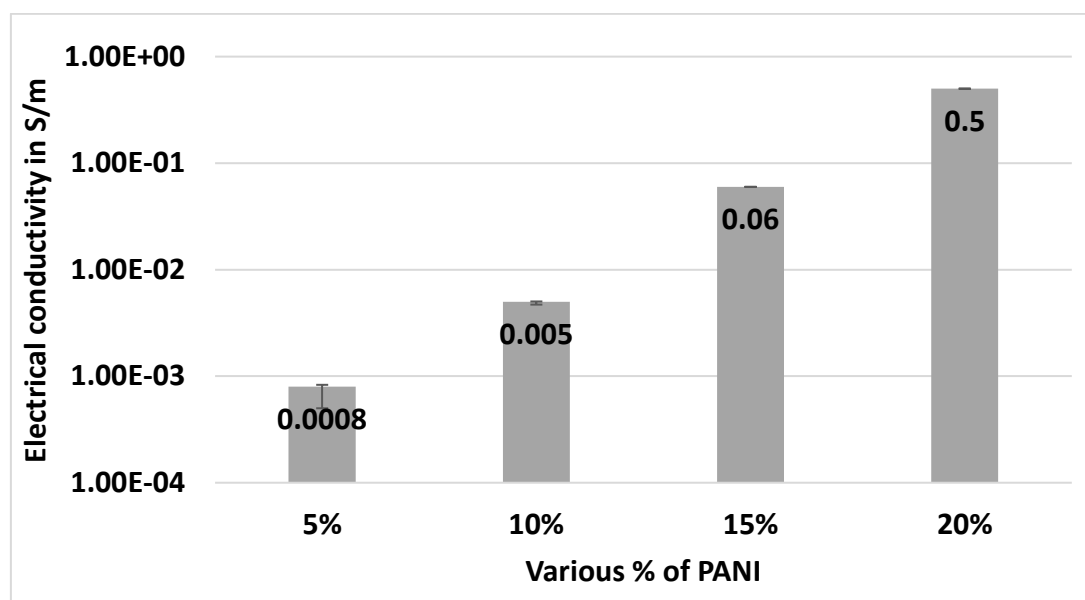


Fig. 5.13. Electrical conductivity for various wt. % of PANI

We also characterized the resin with and without semi-doping procedure and the experiment showed the significantly enhanced electrical conductivity with semi doping treatment especially in the resins with higher constitution of PANI. The 15 wt. % resin showed a 10 times

improvement of the conductivity upon semi doping (0.002 S/m to 0.06 S/m) . Hence, the parametric study with the resin constitution for the optimized conductivity and flexural modulus is the one with 20 wt. % of PANI.

5.5 Discussions

This chapter summarises the complete work on the fabrication of the PANI/P-2M composite [7] . The resin was analysed thoroughly using DSC analysis, Rheological analysis. The parametric study was done with various wt. % of PANI. The viscosity analysis shows that the resin is quite stable at room temperature and at enhanced wt. % of PANI the viscosity shows Non –Newtonian behaviour and further steady state analysis shows that the viscosity for the maximum wt. % PANI is also in the range of the resin for CFRP fabrication. The flexural modulus didn't show much variation (2.5-3.2 GPa). This can be attributed to the fact that P-2M is the bifunctional material being used for both conductivity and strength, however by two quite different mechanisms and hence utilizing two different functional groups. Therefore, the strength of the material is not immensely affected by the addition of PANI or doping complex in the resin. This mechanical property is comparable with epoxy resin. The uncured neat resin showed Newtonian behaviour and for the resin with PANI added we observed shear thinning properties owing to the good dispersion and de-agglomeration of the resin with higher shear rates. Hence, this resin can be used to develop prepreps to fabricate CFRPs using this PANI-P-2M resin.

Chapter-6

Development of CFRPs using the PANI/P-2M resin

There have been numerous studies and reports on PANI based resin system (PANI-DBSA/DVB) developed and CFRP fabricated and proven effective against lightning strike [16,35]. However, the PANI based resin system developed by Kumar et al [26,31] faces certain drawbacks of its own. The resin system is not so stable at room temperature and undergoes rapid curing. The new resin which utilizes a curable dopant P-2M along with PANI shows extended steady state viscosity. P-2M on the other hand introduces a simple bifunctional mechanism based conductive curable dopant for PANI [19]. Therefore P-2M based resin system shows extended stability for the resin material [7]. Therefore, it can be suitable to develop pre-impregnated fabric that can be further developed into laminates. This concept is well known as prepreg technique for CFRP fabrication. Stability aids in the prepreg capability of the resin. Prepregs have immense advantages for industrial applications like: Improved laminate consistency, Reduced matrix making error, Reduced labor cost, Increased production speed. Additionally, prepreg system is fully automated, therefore it can practice the closed mould process which comes under the legislation to control the workshop environment and reduces the general contact with the resin system. Prepregs are used to produce composites faster and with less mess. As per all these advantages, developing a prepreg system for our PANI based resin is of utmost necessity. This is the first study that reports the prepreg system developed using Polyaniline based conductive thermoset resin system. This chapter is subdivided into following sub sections:

1. CFRP fabrication Prepreg technique
2. Prepreg study
3. Cured CFRP characterisation
4. Introducing Trimethylolpropane trimethacrylate (TMP) as a strength enhancer
5. Morphological analysis
6. Lightning strike on the CFRP samples

6.1 CFRP fabrication Prepreg technique

The PANI/P-2M resin was impregnated on the Carbon fibres (TR3110M, TR30-3K fibres, 200 g/m², Mitsubishi Rayon Co., Ltd.) and these impregnated fibres could be stored for a long period of time. The long term prepregs stability study is done intensively and is reported in the further sections. Further, eight plies of the prepreg sheets in the dimension (200 × 200 mm) were stacked and then pressed in the Hot press at 120 °C at 3 MPa pressure for 2 hours. The carbon fibres were 0°/90° cross plies and the laminates were stacked one above the other without any alignment. Therefore, the stacking sequence between the two laminates or prepreg sheets is 0°. The resultant CFRP thickness was 2 ±0.4 mm. Thereafter the CFRPs were cut in the required dimensions for characterisation of the electrical and mechanical properties. Fig. 6.1. shows the sequence of the CFRP development and further Fig. 6.2. shows an image of the prepreg and a fabricated CFRP panel with the PANI/P-2M resin.

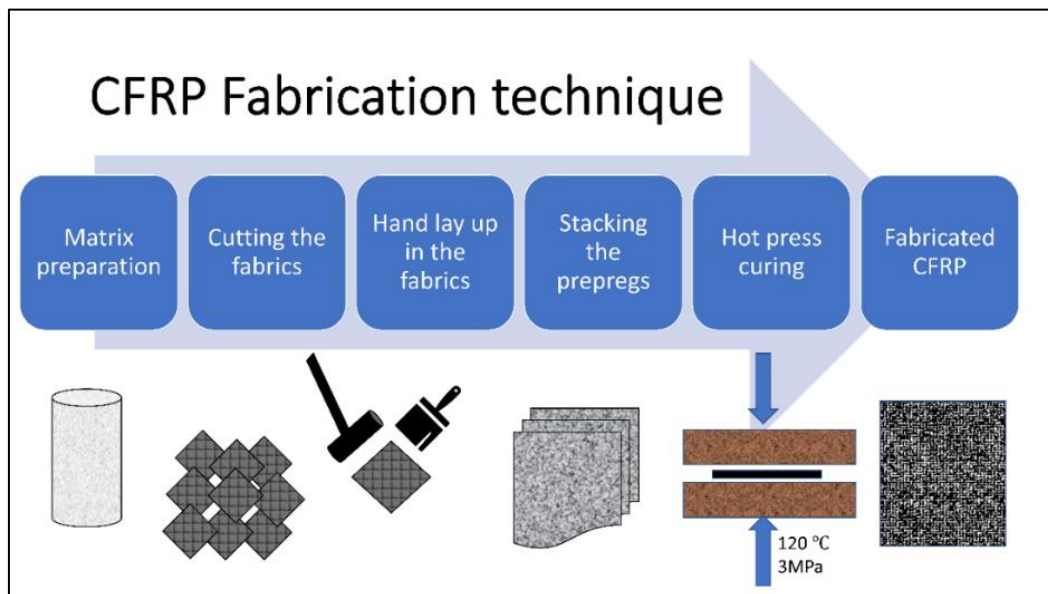


Fig. 6.1. Sequence of the process for the fabrication of CFRP

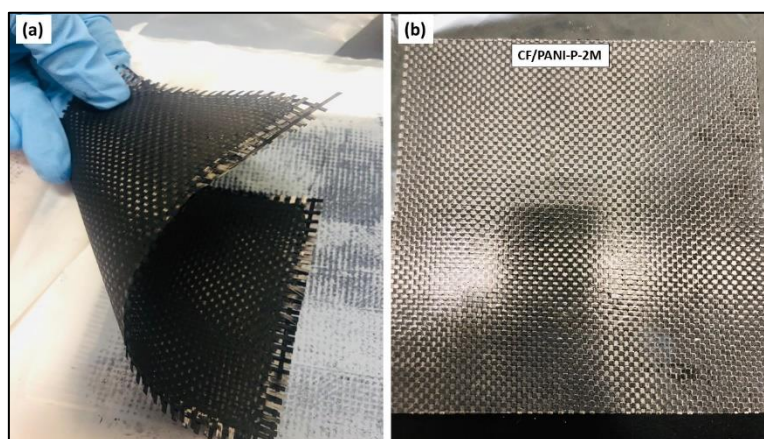


Fig. 6.2. (a) Prepreg of Carbon fibre impregnated with PANI/P-2M resin (b) Fabricated CFRP using the PANI/P-2M resin

6.2 Prepreg study

The prepreg study was conducted for the storage life analysis. The 10 wt.% resin was implemented for this study. The resin shows extremely good steady state viscosity . Therefore, for storage life analysis the resin and the prepregs were kept under study for a span of 80 days. Thereafter in small durations the viscosity of the resin was measured. Additionally the morphology of the prepreg was also analysed from time to time. The resin DSC was conducted.

Fig. 6.3. shows the steady state viscosity of the resin on day 0, 15, 45, 60, 80. The PANI/P-2M resin shows extremely stable viscosity. This is the most reliable property for the fabrication of prepregs.

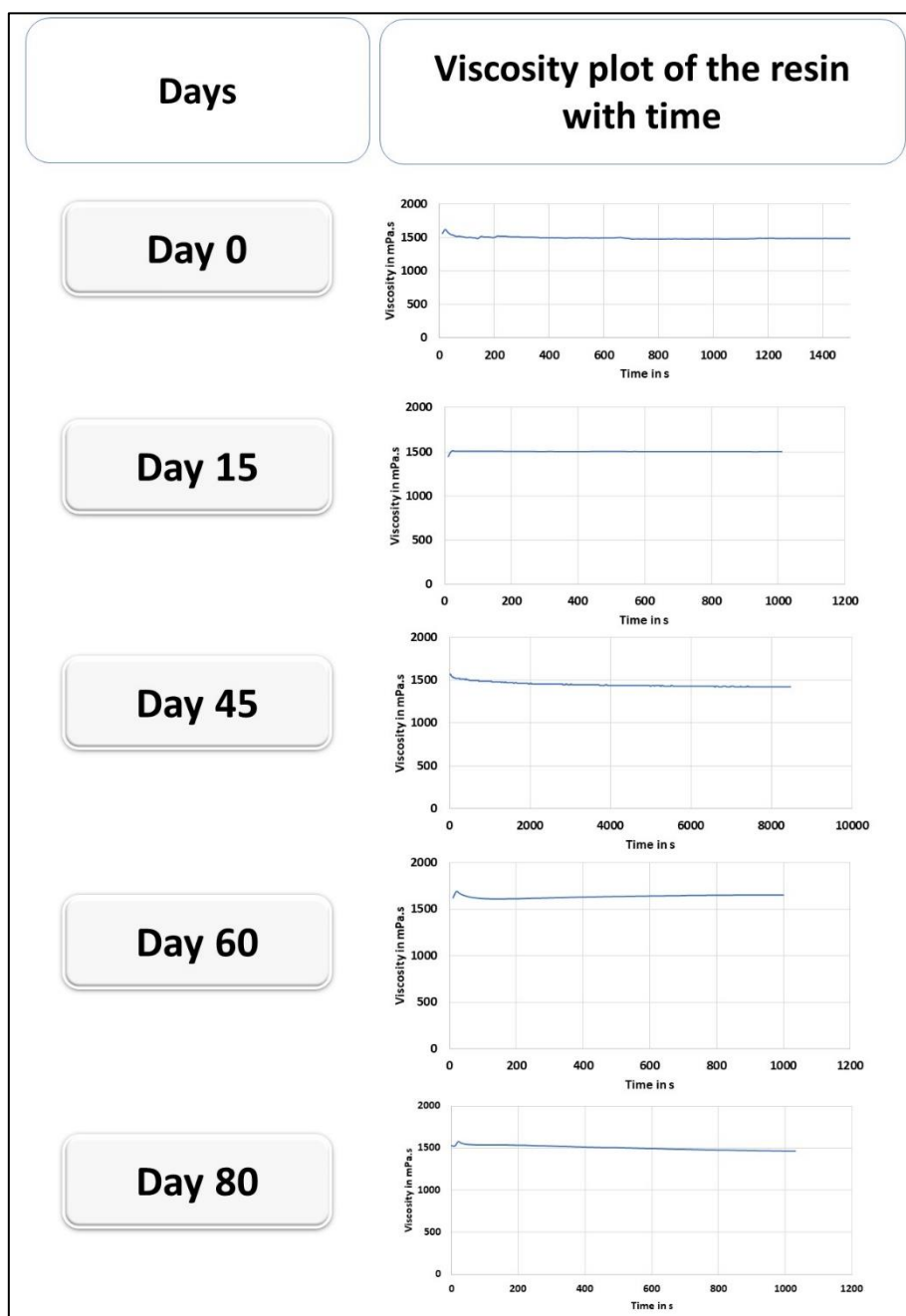


Fig. 6.3. Steady-state viscosity of the resin over a period of 80 days and calculated at regular intervals

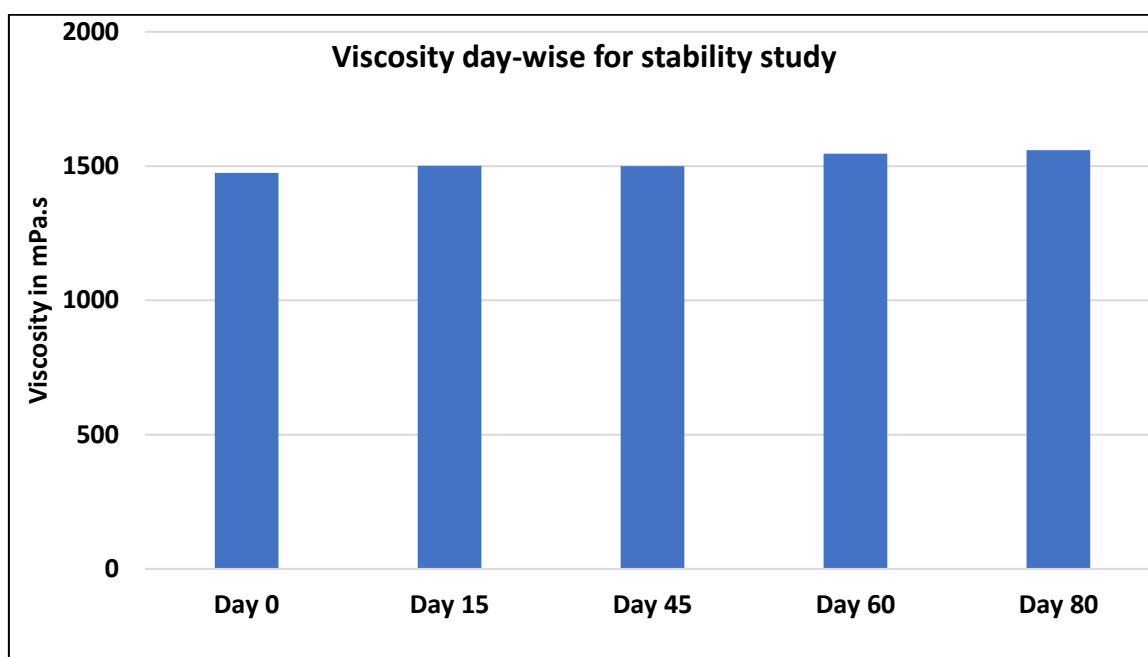


Fig. 6.4. Steady state viscosity day-wise for a span of 80 days

Next, we discuss the physical appearance of the resin and the prepregs. The morphology of the prepregs and the resin doesn't change with time when stored at low temperature. the Fig. 6.5 shows a comparative picture of the new resin with the former resin of PANI/DBSA. The new resin shows promising scope for the fabrication of the CFRP with prepregs technique.

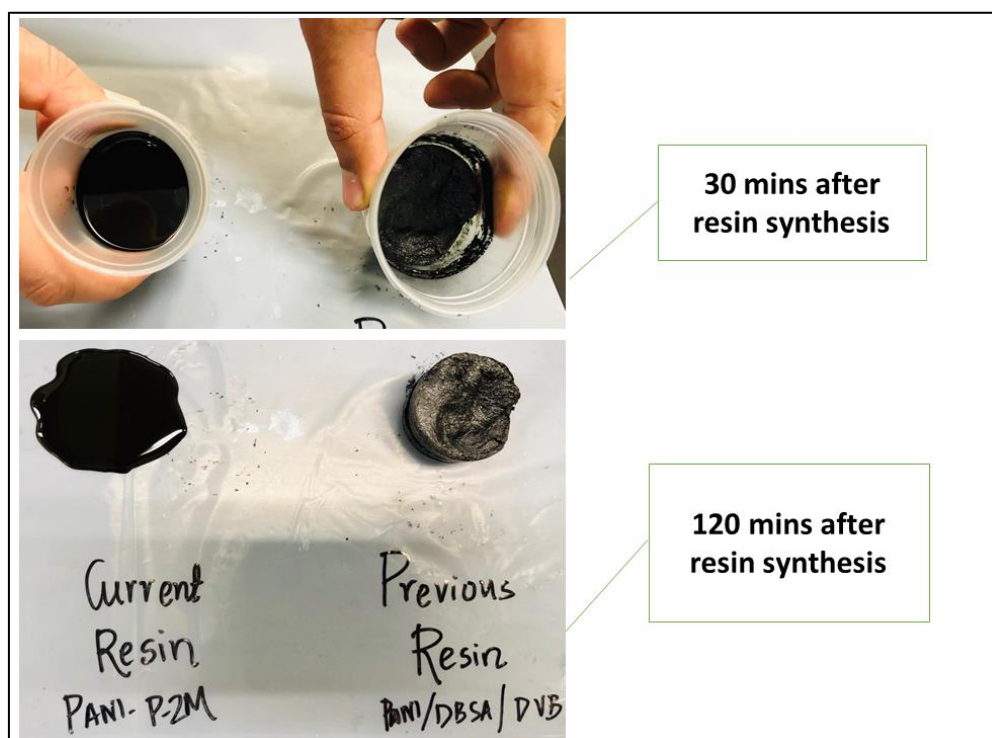


Fig. 6.5. The comparative picture showing resin physical appearance for PANI/P-2M and PANI/DBSA.

The PANI/P-2M resin remains shining and maintains its phase and state for a very long period even at room temperature. As compared to the previous resin of PANI/DBSA, which hardened within hours of synthesis, this new resin remains completely in the state of liquid. This ability aids in the prepregs synthesis, industrial storage, transportation of the resin. Further, the DSC of the resin was also monitored from time to time and the heat of reaction was estimated. Table 6.1 below summarises the heat of reactions of the resin at different time durations.

Table-6.1. Different heats of reaction for the resin on various days

Sl. No.	Resin under study	Day	Heat of reaction ΔH in J/g
1.	PANI/P-2M with 10 wt. % PANI	Day 0	249
2.		Day 15	239
3.		Day 45	240
4.		Day 60	236
5.		Day 80	280

The heat of reaction is almost same for the resin even at the stretch of 80 days. Although the slight variation is owed to the points of calculation of the heat of reaction. This shows that the resin doesn't react until it achieves the required temperature. In order to see the pattern of the resin reaction change with temperature, we also conducted a viscosity with temperature study for the resin (both neat and with PANI) as shown I Fig. 6.6. The resins used in this study are : 0 wt. % PANI resin termed as the neat resin and the 10 wt. % PANI resin .The viscosity of these resins was varied from room temperature (25 °C) to higher temperature (55 °C). epoxy resin also shows similar response with temperature , the viscosity initially decreases with increasing temperature and then it starts increasing as the resin approaches towards curing.

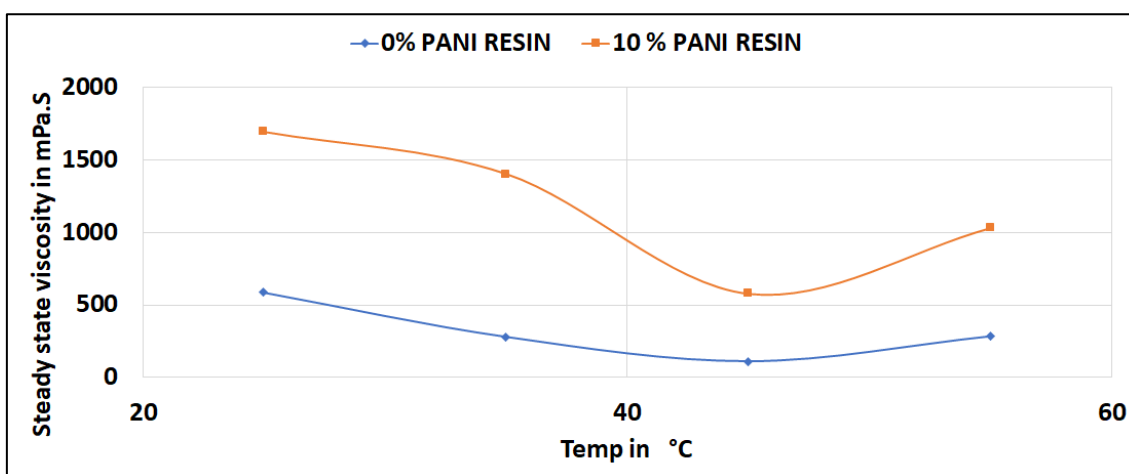


Fig. 6.6. Plot of viscosity with increasing temperature for both neat resin as well as 10 wt. % resin

Therefore, this section discusses the preregs of PANI and their stability study. The resin shows steady state viscosity in a favourable range , thereby successful CFRP fabrication is achieved through prepreg stacking technique. The preregs were studied for a span of 80 days. The resin viscosity remained almost same at ~1500 mPa.s. the morphology also showed how the resin shows a shiny texture even after hours of synthesis, whereas the previous resin hardens sooner. In order to understand the resin reactivity, we also studied the resin viscosity with temperature and like epoxy resin, the PANI/P-2M resin shows initial drop in the viscosity and subsequently hardening of the resin as it goes towards curing. The preregs stacked for 80 days also showed similar texture as day 0. Thus, the attempt to apply prepreg technique with long storage time to PANI based conductive resin is achieved successfully.

6.3 Characterisation of the CFRPs:

The cured CFRPs were characterized for their mechanical and electrical properties. The electrical conductivity increased with the addition of PANI. The CFRPs were characterized with the following resin composition: 0, 5, 10, 15, 20 wt. % of PANI. The flexural modulus of the samples obtained from the three-point bending test is plotted in the Fig. 6.7. The samples curing was immensely affected by the resin composition especially with the amount of PANI.

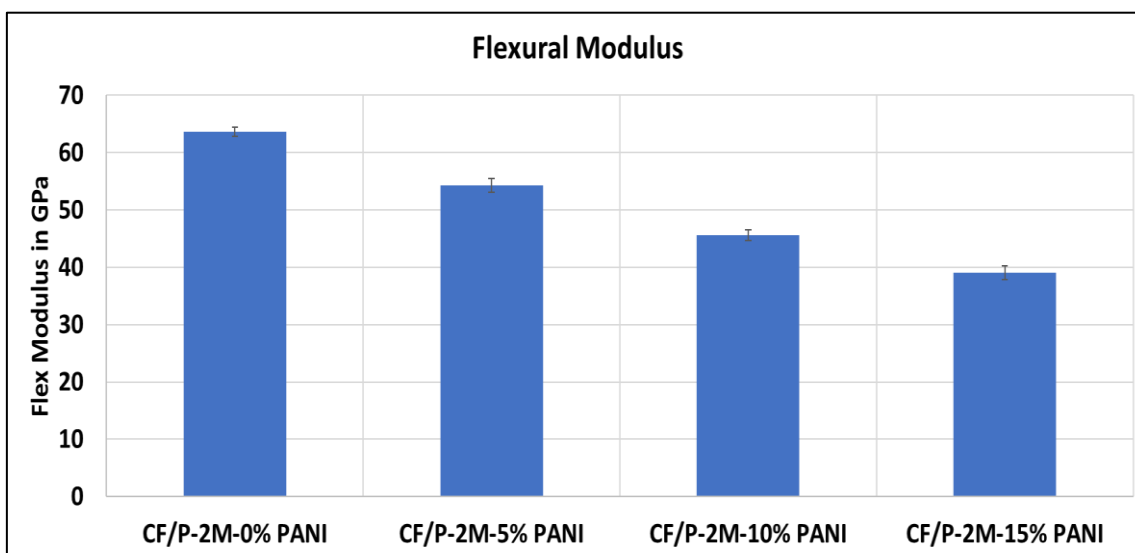


Fig. 6.7. Flexural modulus of the CF/P-2M samples with various wt. % of PANI

The modulus decreases with the increase in the amount of PANI. With the same curing profile, the resin with more amount of PANI is less cured as it required more curing energy. The volume fraction estimated for the samples also shows that the flexural modulus obtained has to be resituated applying the compensated volume fraction concept.

$$E = v_f \times E_f \dots \dots \dots (1)$$

now the v_f is 60 % as we kept this constant for experiments. E_f is calculated from the experimental value

$$E_{f \text{ exp}} = v_{f \text{ exp}} \times E_f$$

$$E_f = E_{f \text{ exp}} / v_{f \text{ exp}}$$

Now putting this value of the E_f in the main equation 1, we get

$$E = v_f \times E_{f \text{ exp}} / v_{f \text{ exp}} \dots \dots \dots (2)$$

The volume fraction of each CFRP is calculated using the image processing method by implementing the GIMP software. The samples are cut into size of 15 × 20 mm and put inside clear plastic rings. CLEARPOXY resin (Sankei, co. ltd) is mixed with CLEARPOXY hardener (Sankei, co. ltd) in weight ratio 100:13 and vacuumed to bleed air out of the resin. The epoxy resin is then poured into the clear plastic ring with specimens inside. The liquid epoxy was let to harden for 24 hours. The ring with hardened epoxy and specimens are polished using grinder-polisher machine (Buehler EcoMet® 250, Buehler AG) with 5 steps of polishing plates. The high resolution cross-sectional images are captured using the LEICA MC170HD. Fig. 6.8. shows the instrument used for preparation of the samples and the samples prepared.



Fig. 6.8. The polisher used for the sample preparation and the samples prepared using clear rings and clear epoxy.

The volume fraction obtained from the above process are summarised in the table 6.2. The compensated flexural modulus, as calculated using the formulas is almost the same for every sample. A sample calculation is shown below:

Sample set-3

$$E = V_f \times E_{f \exp} / v_{f \exp}$$

Where ,

$$V_f = 0.6 \text{ (from fabrication)}$$

$$E_{f \exp} = 45 \text{ GPa (from experimental results)}$$

$$v_{f \exp} = 0.47 \text{ (from morphological studies)}$$

Therefore , the compensated E calculated is ,

$$E = 60 \text{ GPa}$$

Similarly , the modulus calculated for all the samples is obtained to be in the range of 59-65.1 GPa. This is because the fibre contributes the most, in the modulus of the material and as the fibre flexural properties affect the overall properties, they are all in a narrow range.

Table-6.2. : Summary of the volume fraction obtained

Sl. No.	Sample details	Volume fraction
1.	CF/P-2M-0wt.%PANI	0.58
2.	CF/P-2M-5 wt. % PANI	0.52
3.	CF/P-2M-10 wt. % PANI	0.47
4.	CF/P-2M-15 wt. % PANI	0.40

The load -displacement curve in Fig. 6.9 encompasses all the samples. As the amount of PANI increases, the slope of the curve decreases. The breakage is not one shot but gradual. The flexural modulus summarised in the fig. 6.7. is obtained from the linear portion of the load-displacement curve. The nonlinear extended portion after the first breakage is quite unique for PANI based resin and is not shown by epoxy resin. The morphological study presented in the next section elaborates this discussion.

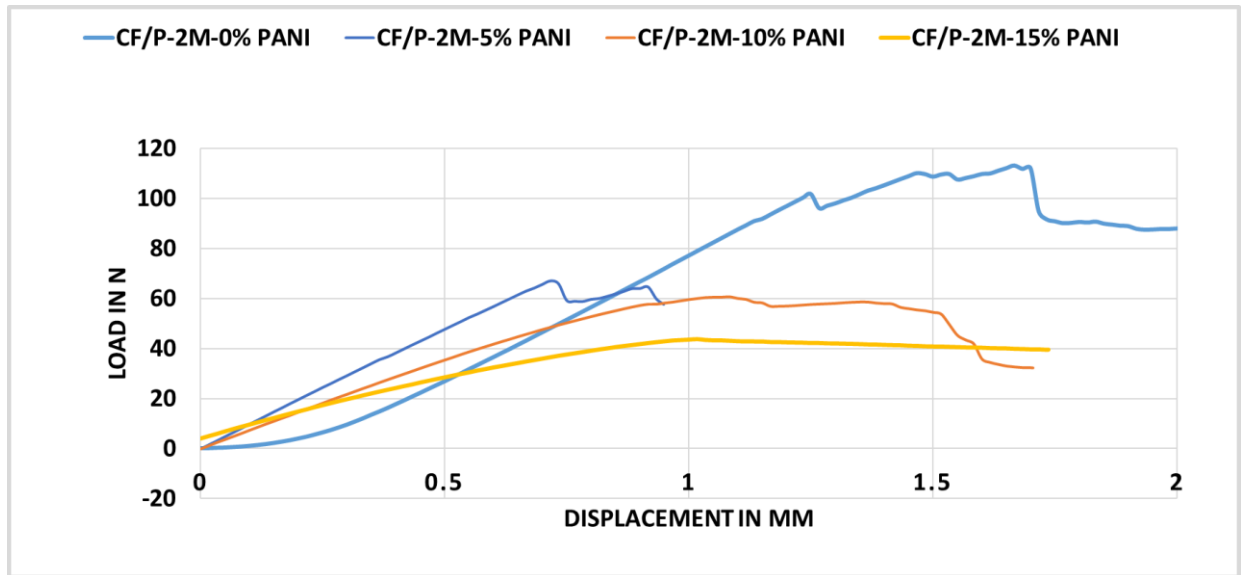


Fig. 6.9. Load -Displacement Curves for the CFRP samples with various wt. % of PANI in the resin

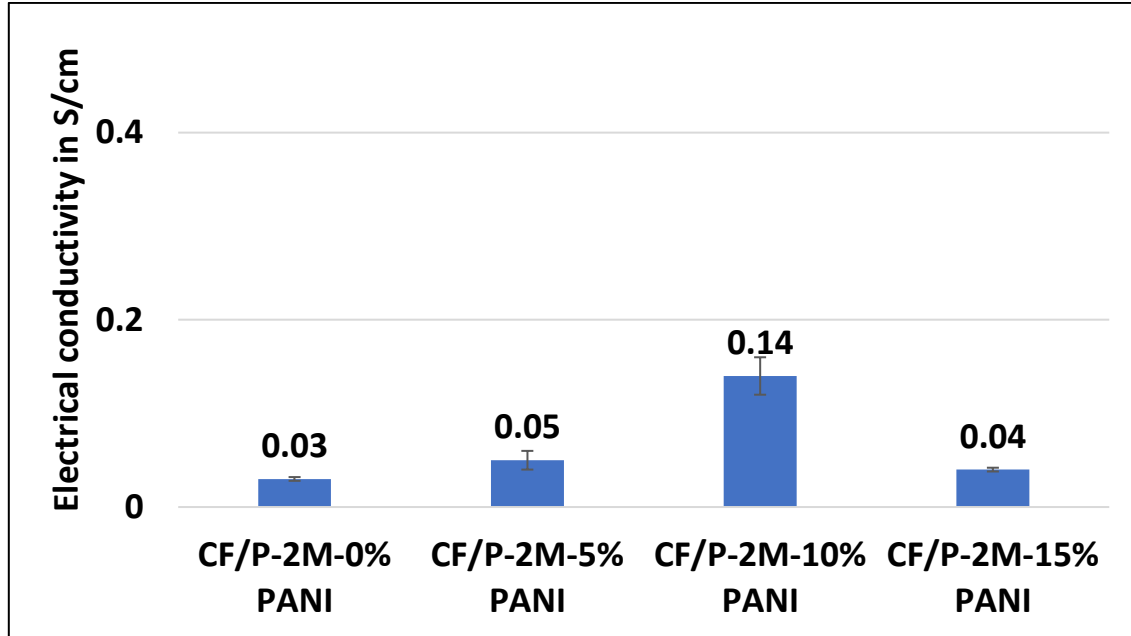


Fig. 6.10. Electrical conductivity in S/cm of the samples with various wt. % of PANI

Electrical conductivity is the critical factor for the CFRP characterisation especially for conducting resin study. The exact evaluation of the panels is done with electrical conductivity and mechanical properties. Fig. 6.10 shows the conductivity plot for all the samples as the amount of PANI is changed in the constitution of the resin. PANI provides conductivity owing to its long chain of alternate double bonds. The trend shows increase in conductivity with PANI amount. However, the sample with 15 wt. % PANI couldn't be fully cured. The mechanical properties also show a significant drop in the modulus. This is because the amount of curing energy and doping energy required to completely fabricate the 15 wt. % PANI CFRP sample is not provided by the uniform curing profile followed for all the samples. Therefore, at this curing profile, 10 wt. % PANI sample is the optimised constitution for the CFRPs. Further this sample was used and tested for lightning strike test. Previous studies show that epoxy has negligible conductivity as compared to PANI based samples. Thereby, P-2M based samples demonstrated a more efficient sample with higher conductivity than epoxy (0.01 S/cm) and comparable mechanical modulus. Although the conductivity (0.14 S/cm with 10

wt. % PANI) is not as high as the previous PANI based systems like CF- PANI/DBSA (1.1 S/cm with 33 wt. % PANI [56]), but the easy fabrication procedure and prolonged prepreg stability acts as a positive strength for this resin system.

6.4.Morphological studies

A brief analysis of the CFRP samples was conducted to verify the surface and the cross section by using the optical microscope. The samples under study were

1. CF/P-2M-0 wt. % PANI
2. CF/P-2M-10 wt. % PANI
3. CF/P-2M-15 wt. % PANI

The comparative pictures showing the cross-sectional view of both healthy and after test samples were conducted. The sample cross sections were thoroughly cleaned before observation. Fig. 6.11 illustrates the comparative pictures of healthy sample and damaged sample. The damage is shown in the diagram and visibly it is more significant as the amount of PANI increases. The orientation of the sample is also mentioned in the figures. The damages are due to resin failure as the modulus of the resin is much lower than that of fibres. The failures are caused due to fibre-matrix debonding at the vicinity of the load. This results in gradual failure and no catastrophic damage as expected in epoxy. In this case the load gradually drops rather than sudden failure (as in fibre failure). Therefore, the damage is mostly dominated by debonding and cracks. As the amount of PANI increases, the damages become more towards the matrix failure. The sample with 0 wt. % PANI has clear fibre -matrix debonding. Therefore, the load-deflection curves experience long and gradual failure rather than sudden drop in the load.

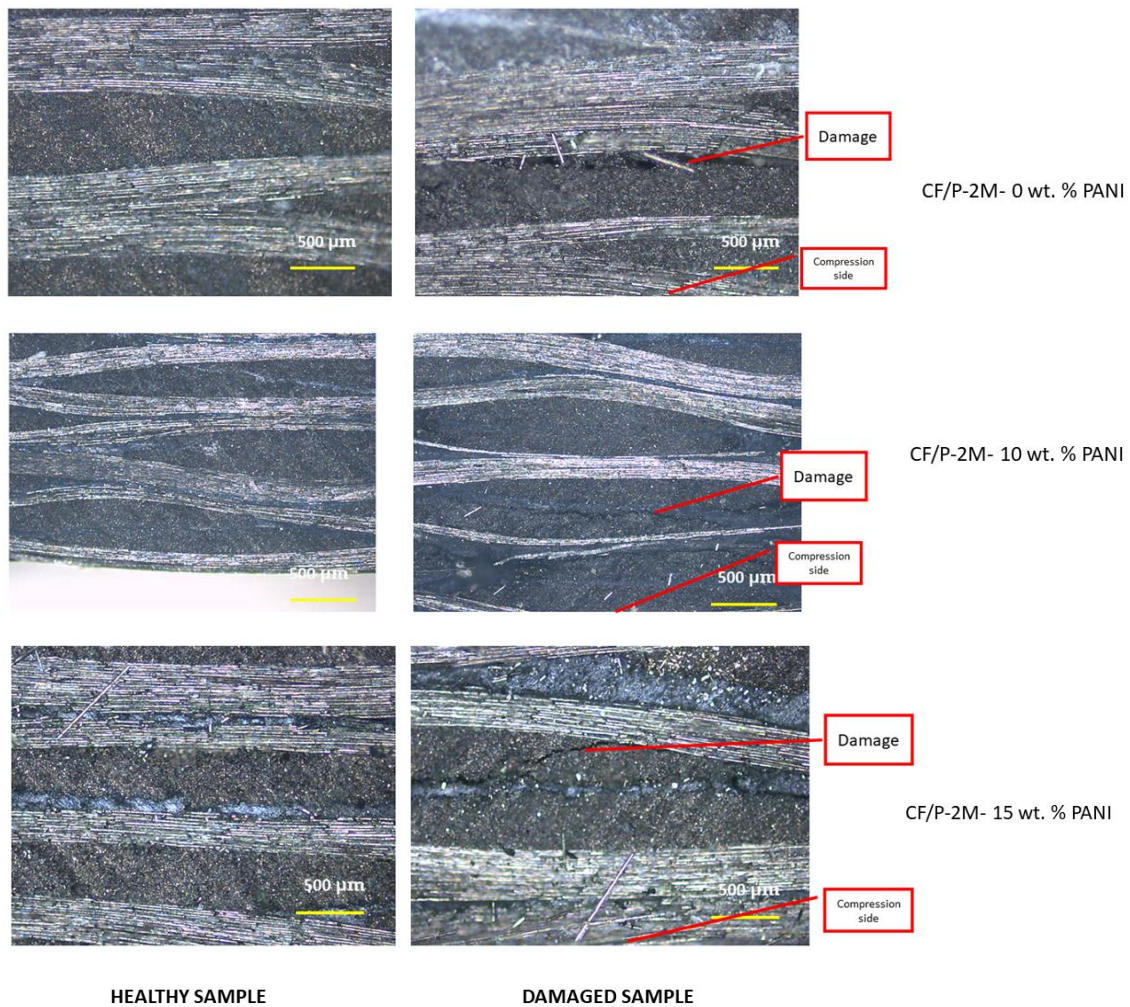


Fig. 6.11. Optical microscope images of the CFRP samples showing the damage sites.

Fig. 6.12 shows a magnified view of the sample with the orientation of the breakage with the edge of the sample. As we can see, the breakage is more towards the end of the sample towards the compression side. This shows that the failure is more of a compression failure than interlaminar failure. Interlaminar failure happens when the resin load bearing is very high. But in this case the resin load bearing is lower, thereby the failure occurs in vicinity of the compression side within few layers rather than in the middle of the sample.

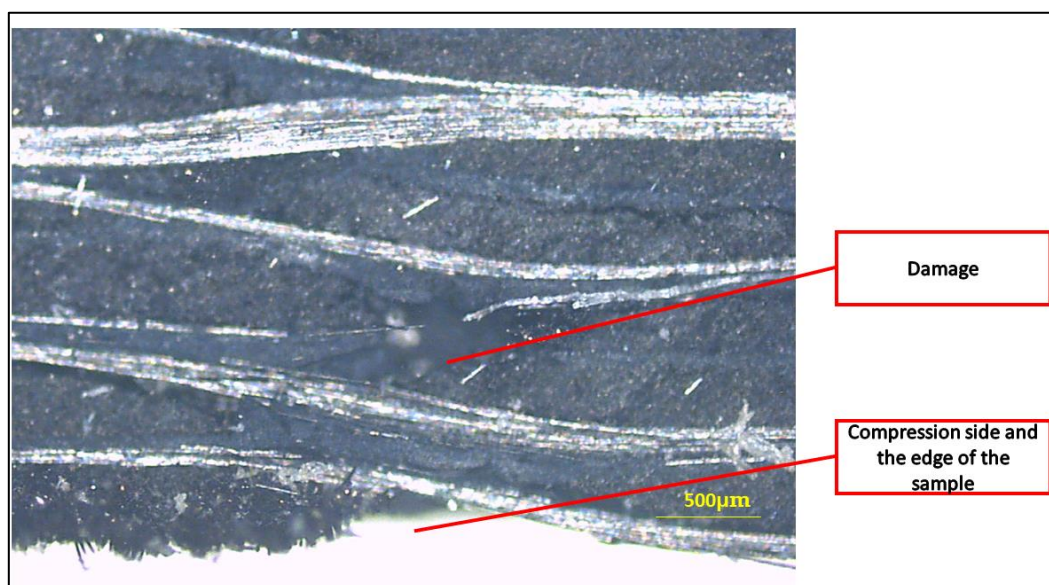


Fig. 6.12. Magnified view of the sample showing the spot of breakage from the edge.

6.5. Introducing Trimethylolpropane trimethacrylate (TMP) as a strength enhancer

The mechanism of the curing by using P-2M is discussed elaborately in the chapter 3 of this thesis. The main functional group that aids in the curing is the methacrylate group, which is also present in PMMA. Therefore, in order to achieve better mechanical properties, we are introducing another material named Trimethylolpropane trimethacrylate (TMP). The structure of TMP is shown in the Fig. 6.13 and the methacrylate functional groups which aids in curing are illustrated in the same figure. TMP only has methacrylate groups and no acidic groups in its chemical structure, therefore, unlike P-2M it won't be able to act as a dopant to PANI. Significant outcome was expected by introducing TMP in a little amount to the PANI/P-2M resin. The brief characterisation of TMP in the resin is presented in this section. Further, the effect of TMP on the mechanical properties is discussed.

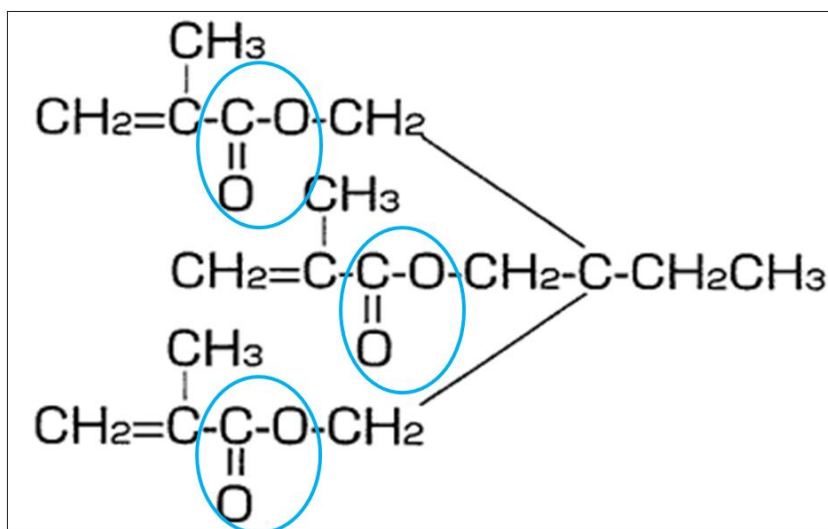


Fig. 6.13. Chemical structure of TMP with illustration on the methacrylate functional groups

The resin preparation was done by adding 15 wt. % of TMP in the resin and as it is extremely easy to mix and lesser viscous liquid, the resin was easier to prepare. The effect of TMP was first studied by using DSC technique so that the curing profile can be applied accordingly. Fig. 6.14. shows the comparative DSC analysis of the resin with and without TMP.

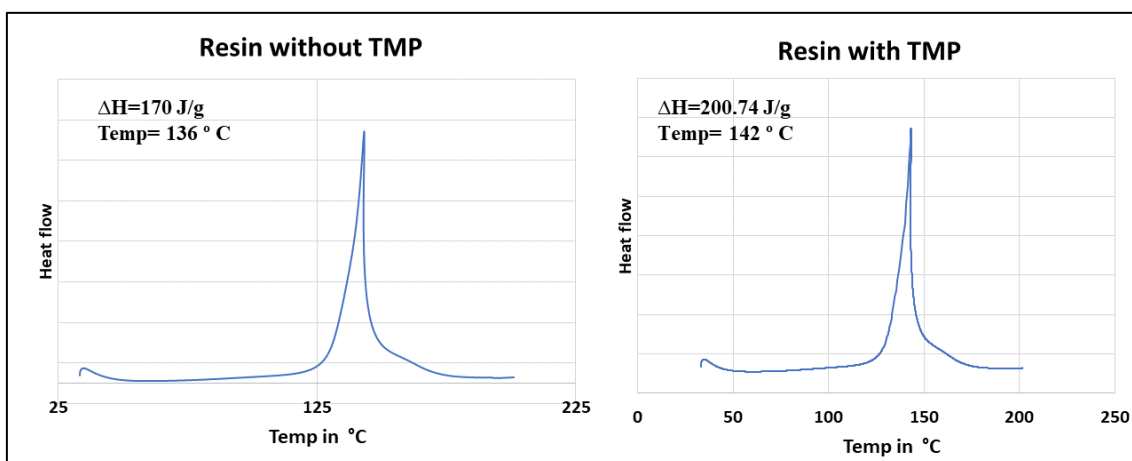


Fig. 6.14. Comparative DSC of the resin with and without TMP

Further the viscosity of the resin was also verified after the addition of TMP. Fig. 6.15 shows the steady-state viscosity of the resin containing 15 wt. % TMP . The brief results show that TMP shows a similar resin profile like P-2M and similar steady state viscosity. Therefore the ease of CFRP fabrication was predicted. Further this resin was utilized to prepare CFRP panels with 9 layers . The resulting samples showed an enhanced maximum stress by almost 40 % as demonstrated in Fig. 6.15. The load displacement curve in Fig.6.16 elaborates the difference when TMP is included in the resin. The sample stiffness increases, the load bearing of the resin increases, thereby the maximum load increases. These results show that TMP is effectively proven to be a mechanical properties enhancer.

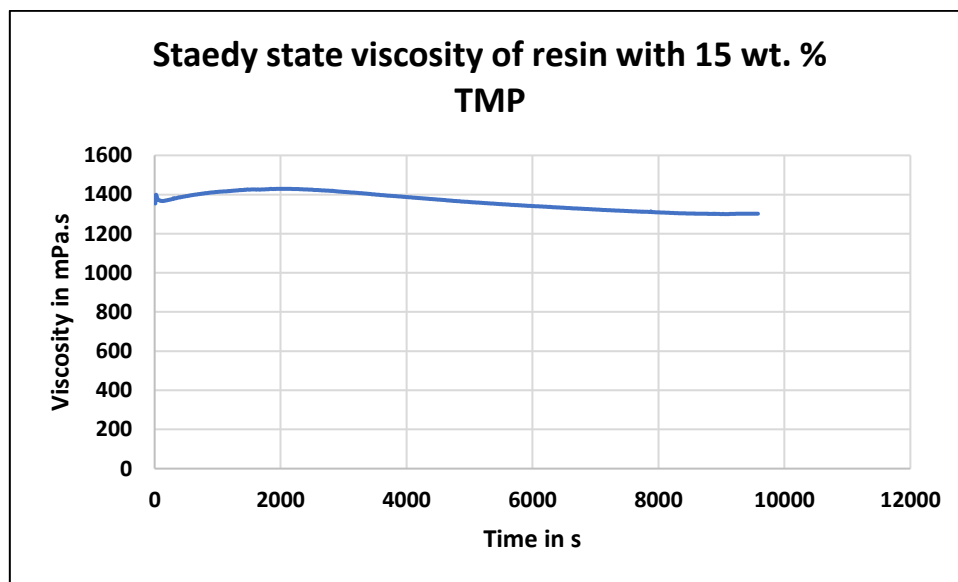


Fig. 6.15. Steady state viscosity of the resin with 15 wt. % TMP added

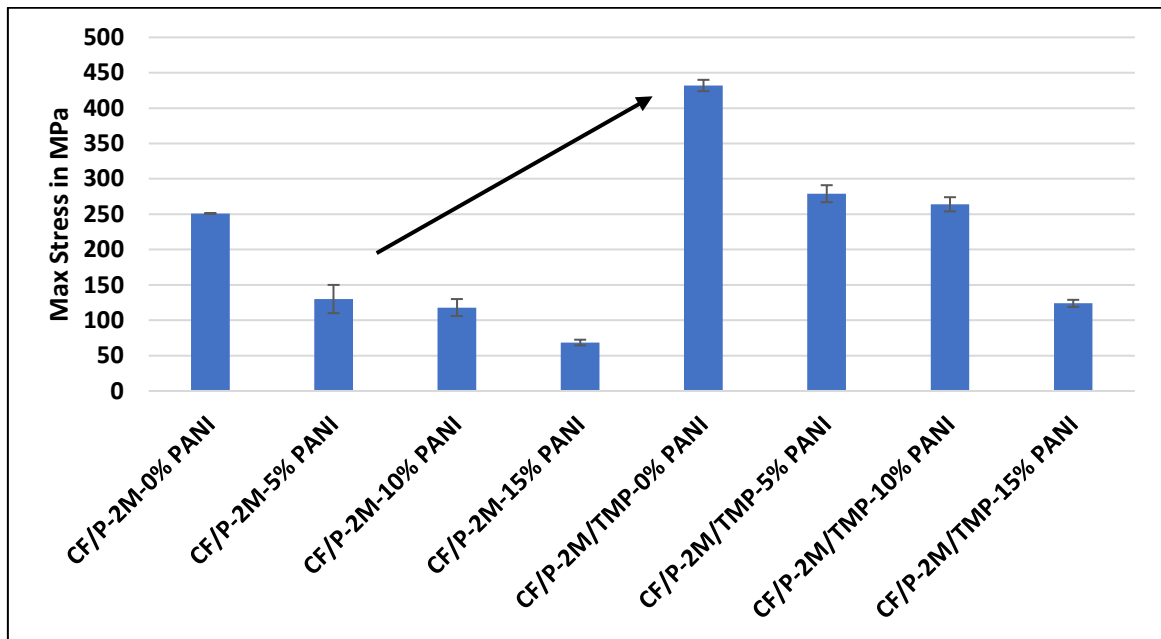


Fig. 6.16. Effect of TMP on the maximum stress of the CFRP samples

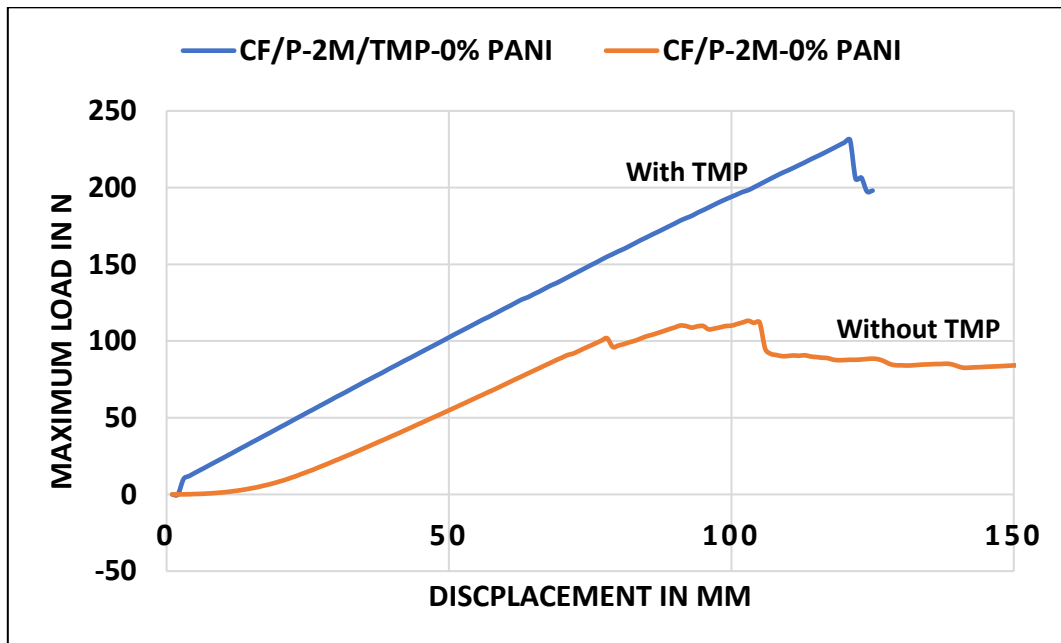


Fig. 6.17. Load displacement curve showing the effect of adding TMP into the resin

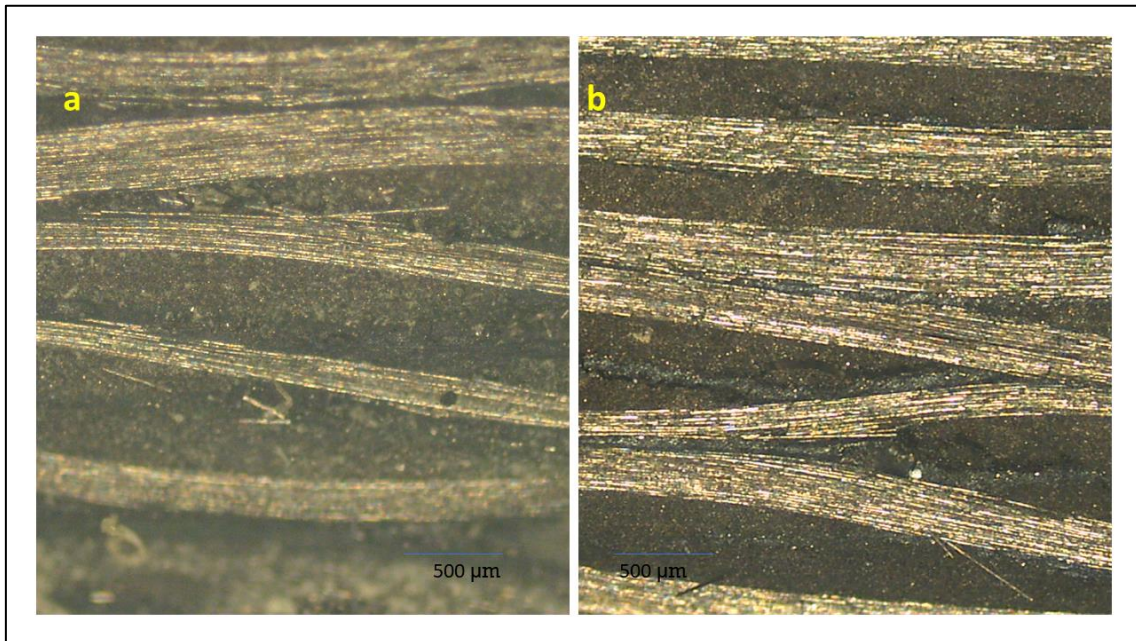


Fig. 6.18. The optical microscope images for 10 wt. % PANI with (a) and without (b) TMP.

The optical microscope image in Fig. 6.18 illustrates the difference in the morphology of the CFRP sample owing to the addition of the TMP and its role as a mechanical strength enhancer. The Fig. 6.18 (b) shows more resin rich areas and less toughened portions as compared to Fig. 6.18 (a). This is owing to the presence of TMP in the resin.

6.6. Lightning strike test on the CFRP samples

As part of a very basic analysis, the CFRP samples were tested under simulated lightning strike conditions to verify the resin effectiveness against lightning strikes. This is a preliminary study and the further optimisation of the CFRP based on the lightning strike effectiveness is under future scope. Simulated lightning strike was applied to the specimens using an impulse current generator (developed by Otowa electric Co., Ltd., owned by National Composite Centre Japan at Nagoya University). The specimen was fixed to the copper frame-type jig. Only the edges of the specimens were connected to the copper jig and cover frame clamped by screws. Fig. 6.19 shows the setup of the lightning strike test and the right hand side illustrates the specimen set up. The technical

details of the lightning strike test is the same as our previous tests conducted in collaboration with JAXA [57].

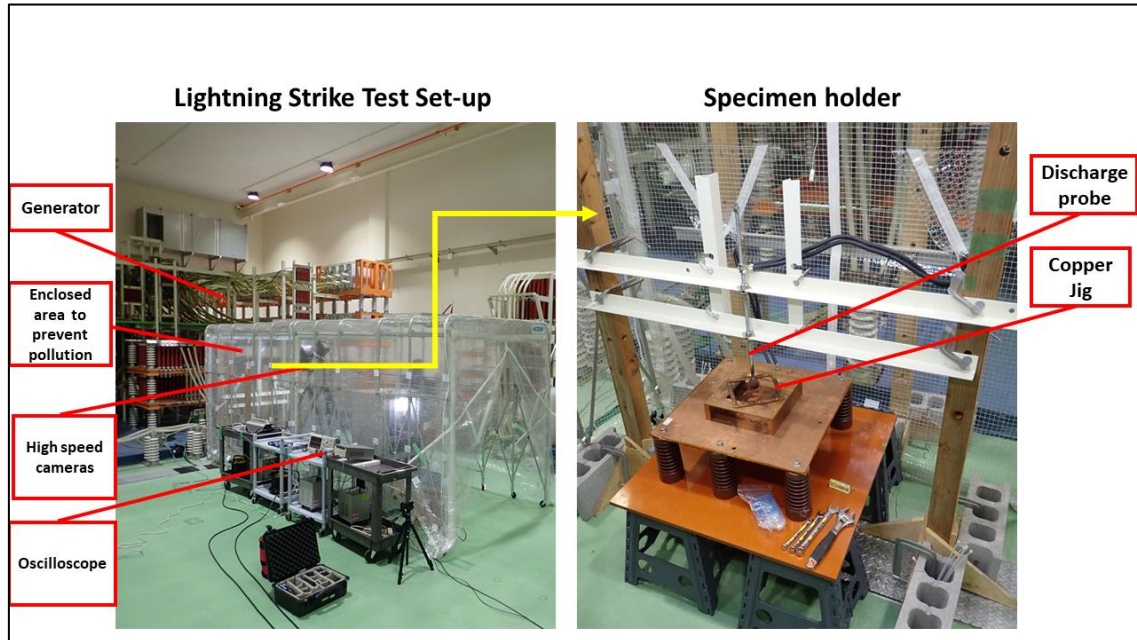


Fig. 6.19. Set up for the lightning strike test. Right hand side shows the enlarged view of the specimen holding set up.

The sample under study is CF/P-2M-10 wt. % PANI with a thickness of 2 mm, electrical conductivity of 0.14 S/cm and flexural modulus of 46 GPa. Fig. 6.20. shows the sample before and after the lightning strike of 40 kA was applied on the samples. Physical examination shows that unlike epoxy there was no burning of the sample. However, owing to the high impact the panel suffered from delamination . The NDI results shown in the Fig. 6.21. demonstrate that the impact is only in the first layer and the internal layers seem intact. The yellow portions even before strike imply the voids and irregularities in the CFRP fabrication as this is by hand lay up process. The images confirmed that the damages were only confined to the top layer. Therefore the sample shows much better results than CF/epoxy samples conducted previously [16] .

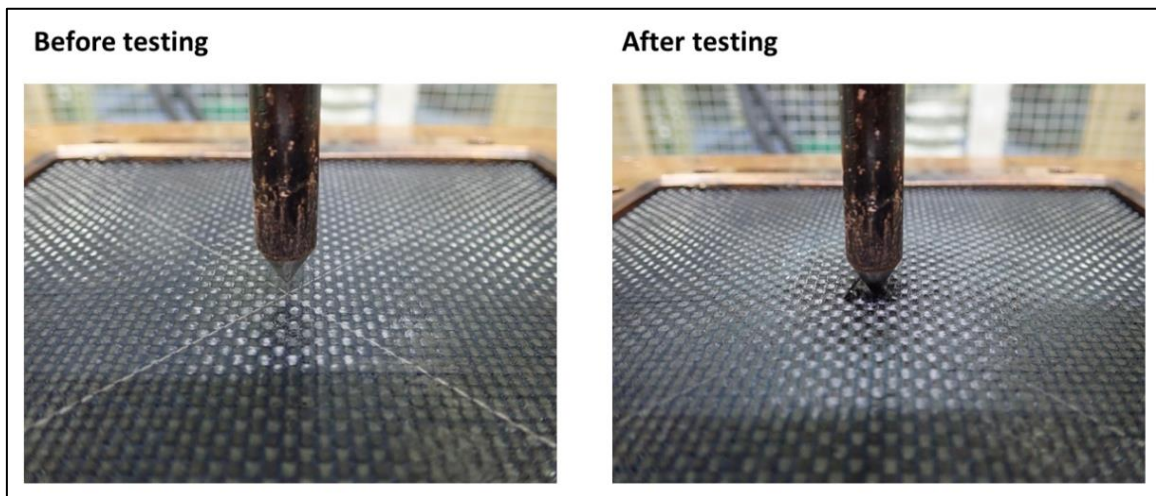


Fig. 6.20. Sample on the specimen holder before and after the strike.

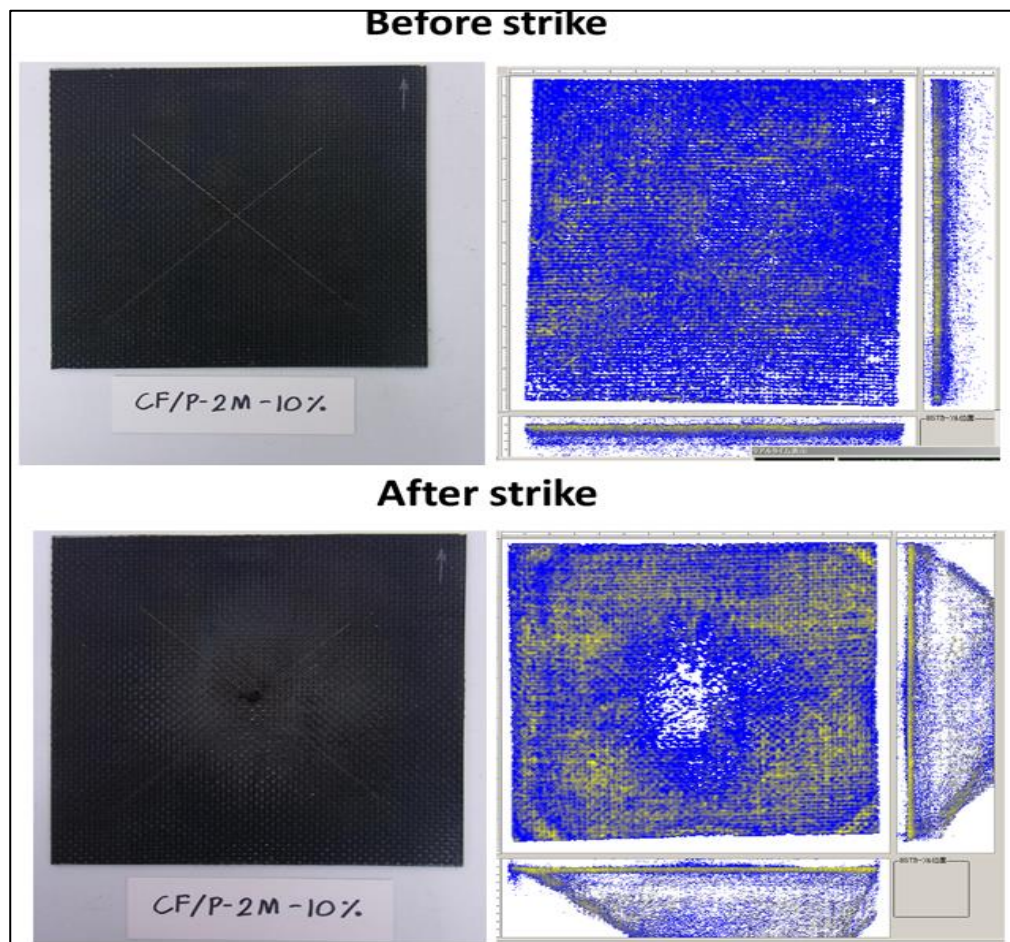


Fig. 6.21. The sample physical study and the NDI before and after the lightning strike.

6.7.Discussion

This chapter is the most elaborated experimental part of this thesis. The new resin formulated was utilized to fabricate CFRPs. The new technique of prolonged stored prepreg was used which is unique for a PANI based resin. Further the resin and prepreg was studied for 80 days for stability. The CFRPs showed flexural modulus 45 ± 1 GPa and the conductivity of 0.14 ± 0.02 S/cm for the sample with 10 wt. % PANI. The samples were morphologically analysed to study the damage development and the effect of the amount of PANI.

A new methacrylate material named TMP was introduced into the resin and the TMP incorporated CFRPs showed a 40 % improvement in mechanical properties. At the end the fabricated CFRP sample was tested against a lightning strike of 40 kA where the physical examination and the NDI results confirmed lower damage as compared to CF/Epoxy samples .

Chapter -7

MD simulation on the resin

Polyaniline has been very well studied as a component of the conductive resin material for the CFRPs [58]. This thesis also introduces a new concept of curable dopants for PANI. All these researches are focussed to synthesize conducting CFRPs for aircrafts [59]. However, no work has been reported yet about the theoretical analysis on the PANI based resin. There are many reports on the MD simulations to estimate the material properties of the epoxy resin compounds [60–62]. Fan and Yuen have studied MD simulations on epoxy [60]. Further Wu and Xu have reported estimation of the elastic constants and density of epoxy by using MD simulations [63]. Li and Strachan [64,65] have conducted the theoretical study by using MD to simulate the cure of 2 epoxy thermosets and study their network topology and hence how it affects the stiffness, yield stress and Tg. Apart from epoxy, researchers have also done similar studies on other polymers. Bermejo and Ugarte [66] reported MD simulation studies on PVA (Polyvinyl alcohol) to estimate the Young's modulus and Tg.

This chapter is an attempt to predict the material properties of the PANI based resin using molecular dynamics simulations. The main components under study are PANI and P-2M which have been the principal focus of this thesis. P-2M consists of PMMA like methacrylate groups. Doherty et al reported in 1998 about the radical polymerisation in methacrylate materials studied using the MD simulations [67]. This thesis attempts to predict the mechanical properties of the resin as we change the composition of the resin. Throughout the experimental results reported in the previous chapter of this thesis, various wt. % of PANI have been used to optimise the resin to obtain the desirable properties of the composite and thereby the CFRP. This chapter aims to predict the modulus of the resin as we change the amount of PANI using MD simulations through JOCTA software. The chapter is divided into further sections: Section 1 explains the methodology and steps for the MD simulations utilized to work and also explains the models that have been implemented for the simulation. A brief analysis of the results is presented in the next section 3. This is a basic study attempted to start MD simulations on a PANI resin, therefore the future prospective are also encompassed in the final section.

7.1. Methodology and Models:

JOCTA is an integrated simulation software for polymers provided by JSOL corporation, Japan [68,69]. The MD simulations were done using the COGNAC in JOCTA package.

- Introducing COGNAC

COGNAC is a general purpose molecular dynamics program developed to handle various coarse grained and atomistic models. It can be used to study higher order structure and physical properties of polymeric materials. Here we have used it to study the mechanical properties of the polymeric materials like Youngs modulus and the stress strain curve.

- Potential functions

The potential function used to handle these are derived from the DREIDING [70] which is used to predict structures and dynamics of the molecules by using the force constants and geometry parameters.

The potential energy for the geometry of a molecule is constituted by bonding interactions and non-bonded interactions given by the equation 7.1.

$$E_{total} = E_{bond} + E_{non-bond} \quad 7.1$$

The bonded interactions consists of bond stretch(E_B), bond angle bend (E_A), dihedral angle torsion (E_T) and inversion term (E_I) as capitulated in the equation 7.2 . the non bonded interactions comprises of the Van der Waals (E_{vdw}) , electrostatic (E_Q) and hydrogen bonding (E_{hb}) as described by the equation 7.3.

$$E_{bond} = E_B + E_A + E_T + E_I \quad 7.2$$

$$E_{non-bond} = E_{vdw} + E_Q + E_{hb} \quad 7.3$$

- Equations of motion

In addition to the conventional Newtons equation of motion ($F=ma$), the COGNAC also follows the Langevin dynamics that takes into account the friction force given by the equation 7.4.

$$m \frac{d^2 r}{dt^2} = F - m\mu \frac{dr}{dt} + W(t) \quad 7.4$$

Where m and r are the mass and the position of the particle and F is the force acting on the particle [71].

- Ensembles

NVT ensemble refers to constant number of atoms, volume and temperature and NPT refers to constant number of atoms, pressure and temperature.

- Boundary conditions

Periodic boundary conditions is applied independently in each axis to obtain the full model for simulation.

- Deformation

The simple elongation technique is used in which the unit cell is elongated or compressed by constant deformation speed. The COGNAC model is elongated at a particular speed and then the obtained stress strain curve is analysed using linear regression to obtain the slope in the linear portion. The slope of the stress strain curve indicates the modulus for the resin.

- Total flow of the execution of the MD

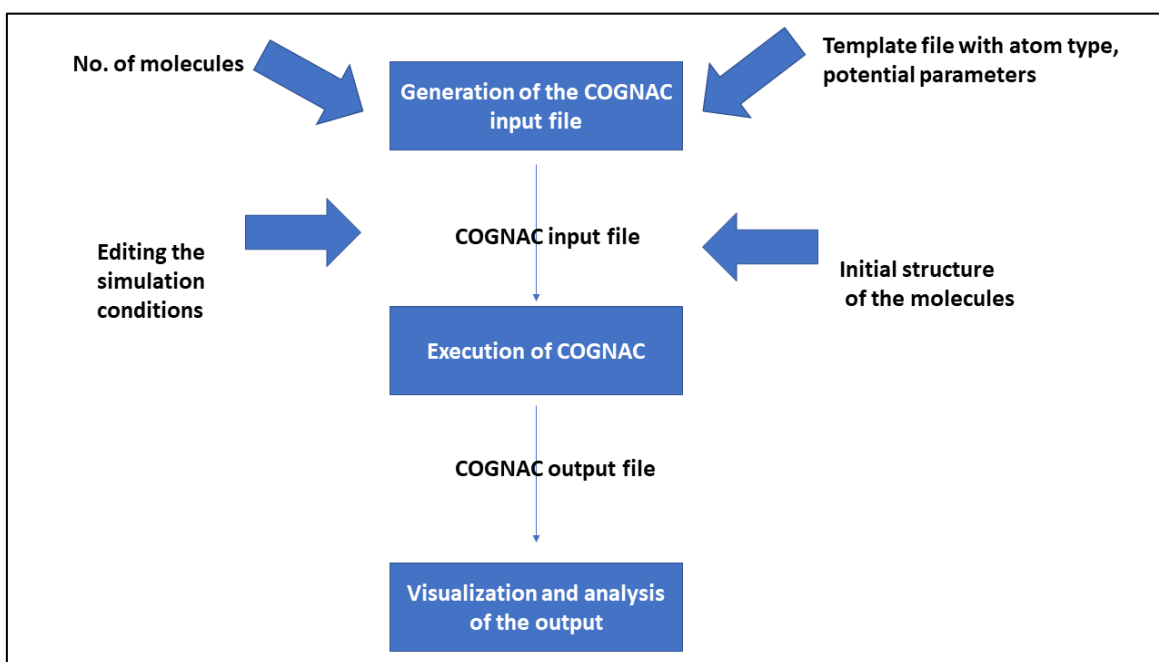


Fig. 7.1. Flow chart showing the execution of the COGNAC [71]

The methodology involved three basic steps: Modelling, Conditioning to the initial settings, Simulation for the deformation.

Models were first built for the monomers. Thereafter the 30 monomers were made into polymers. Finally, 30 polymers were studied inside 3D cell. Monomer models were built by using the exact chemical structure of the PANI and P-2M. Further, the force field parameters for bond interactions like angle, stretch were assigned using the DREIDING force field [70]. The spatial coordinates were provided by molecular mechanics study. Fig. 7.2. illustrates the modelling in a stepwise structure. Next step was to obtain fully relaxed state for the COGNAC models in the 3D cell. In this research, the equilibrium step for all the simulated models were achieved by running simulation in NVT and NPT conditions. NVT ensemble refers to constant number of atoms, volume and temperature and NPT refers to constant number of atoms, pressure and temperature.

Having gone through both NVT and NPT and then again NVT, the system compresses the models to generate the structure with correct density with minimalistic residual stress. The first NVT is to relax the system by eliminating the overlapping of the molecules, subsequently the NPT relaxes the system and finally the NVT is done to eliminate any residual stresses.

Afterwards, the COGNAC models of the 3D cell boxes were subjected uniaxial deformation using NVT (constant number of atoms, volume and temperature) simulation and the constant strain was applied along z-direction. The stress-strain curves of the simulated resin under longitudinal loading direction were also calculated. The elastic modulus was computed from the linear regime of the stress-strain curve.

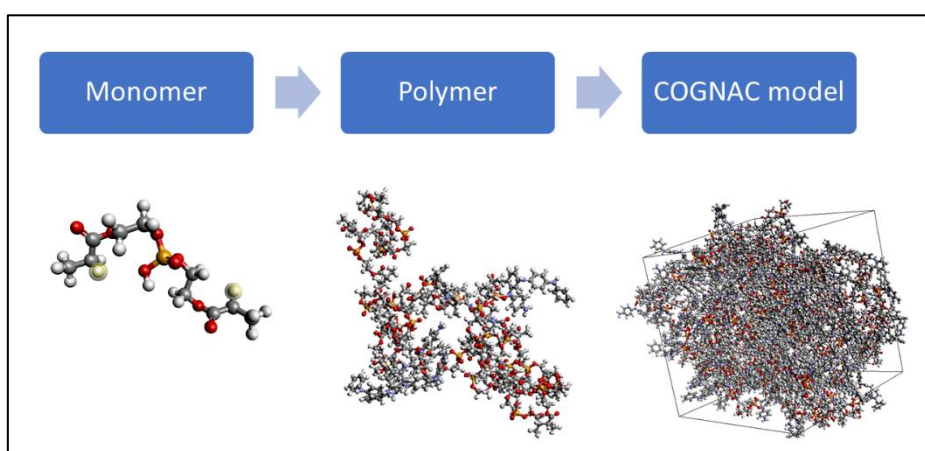


Fig. 7.2. Building the MD model for simulation

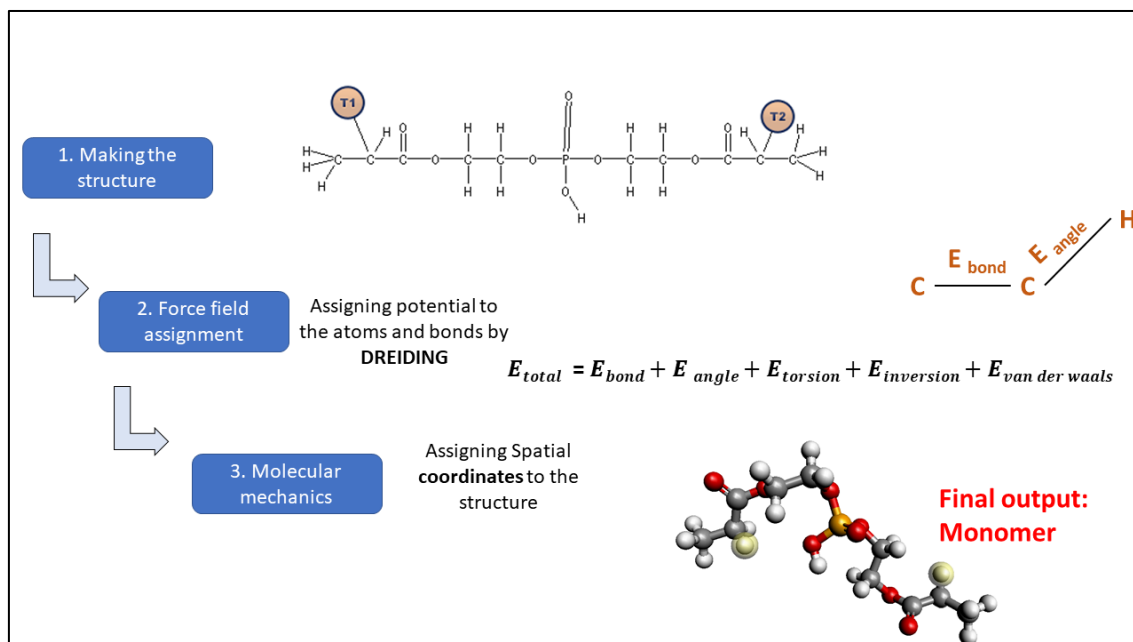


Fig. 7.3. Monomer modelling step wise illustration

Four basic types of models were made for the study. The model resin constitution is shown in the table 7.1. The structure of P-2M and PANI/P-2M is shown in the Fig. 7.4. That constitutes for the model: Neat and Basic. Further the models Combine and First are built based on the models of Neat and Basic.

Table 7.1. Models with the respective PANI constitution

Sl. No.	Model name	Constitution	Amount of PANI
1.	Neat	P-2M	0%
2.	Basic	PANI/P-2M	50 %
3.	Combine	$(\text{P-2M})_{10} + (\text{PANI/P-2M})_{10}$	33 %
4.	First	$(\text{P-2M})_{10} + (\text{PANI/P-2M})_5 + (\text{P-2M})_{10}$	15 %

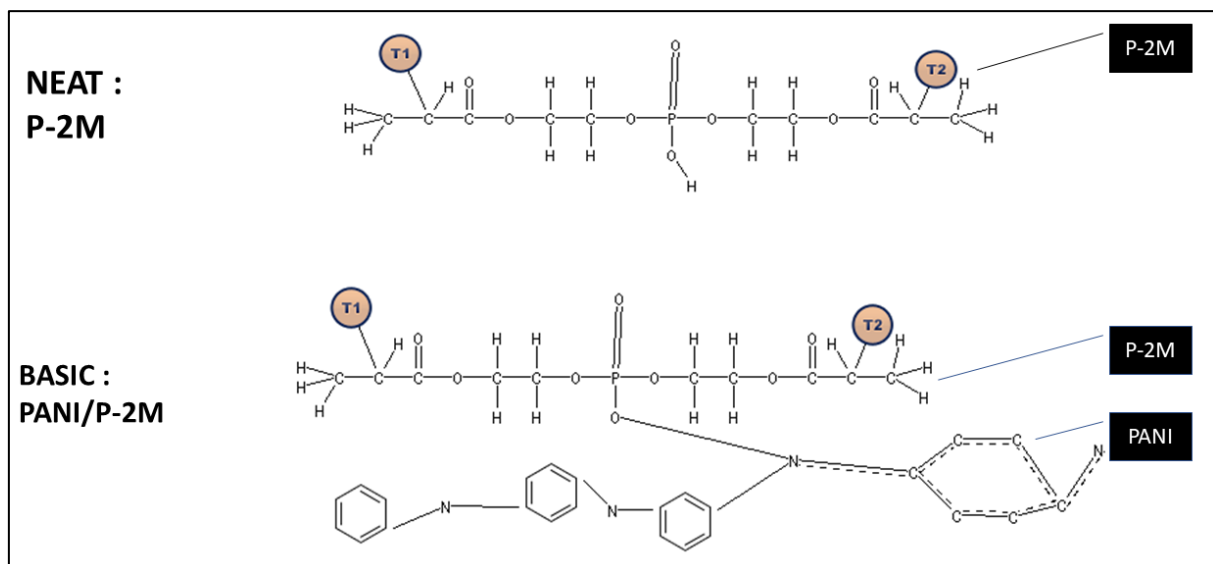


Fig. 7.4. Structure of the fundamental resin constituents: P-2M (neat resin) and PANI/P-2M (basic resin)

7.2. Results and discussion

In this section, the stress strain curve obtained from the simulations are studied to obtain the effect of PANI amount on the mechanical properties of the resin. The stress strain curves obtained are plotted in the Fig. 7.5. for all the four models. In order to study the impact of the PANI amount, the neat resin is also simulated, and its mechanical properties can serve as the basic modulus. As we go from model 2 to model 4 in the table 7.1. the amount of PANI decreases. The expected behaviour from the experimental results show that the modulus also decreases but maximum by 15 %.

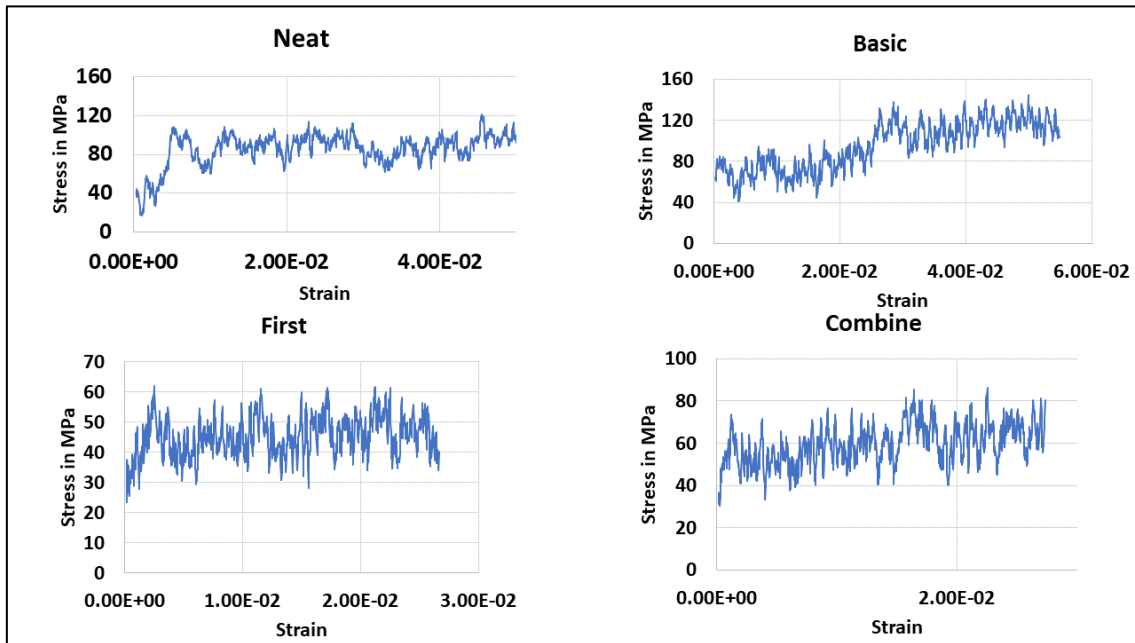


Fig. 7.5. Stress strain curves obtained from the MD simulations

However , the simulations encompassed scope for further improvements . Some of the modifications with the increased output intervals, reduction in the deformation limit making it closer to the experimental results. Further, the Fig. 7.5 only shows the curves with deformation in one direction. In reality, the samples are supposed to be anisotropic ,therefore all three directions can be considered to obtain the average modulus with the not so uniform distribution of the materials inside the ensemble. Therefore the deformation was done in x-axis, y-axis and z-axis and the average modulus from the three deformations is considered.

JOCTA doesn't encompass the technique to do deformation in x-axis and y-axis, therefore the 3D cell was rotated accordingly to deform in all three directions as illustrated in the Fig. 7.6. Upon further work on the simulations, the deformations schedule was changed and the model was elongated in all three directions to obtain better noise free stress strain curves. The stress strain curves in all three directions for the basic model is shown in the Fig. 7.7.

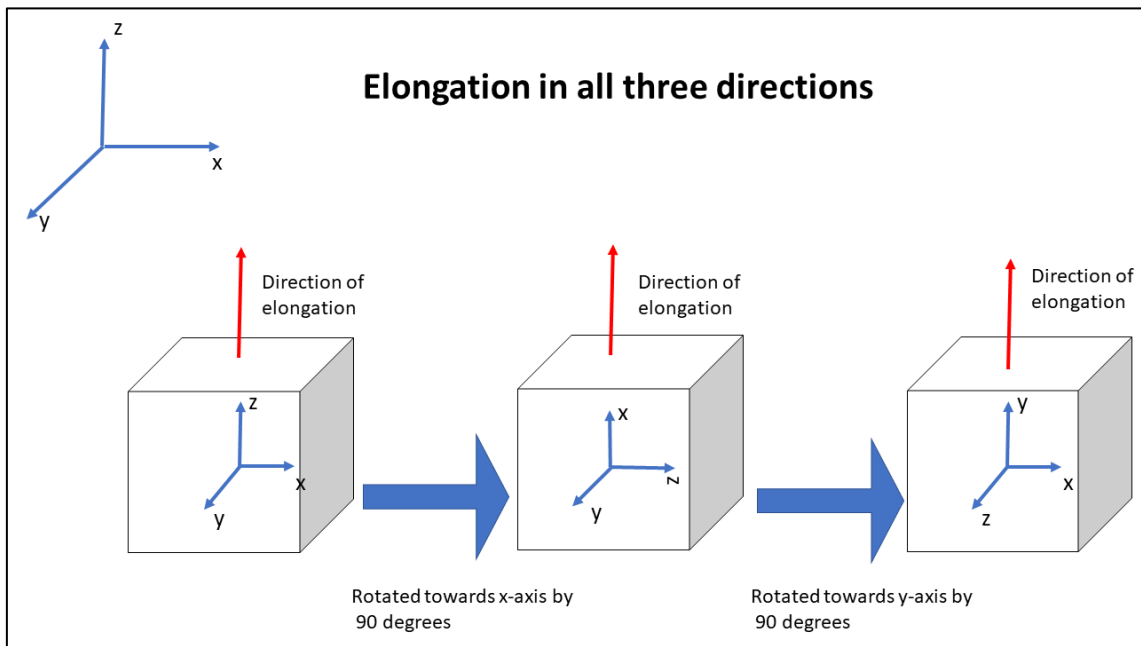


Fig. 7.6. Illustration of achieving 3 axis rotation in the MD elongation.

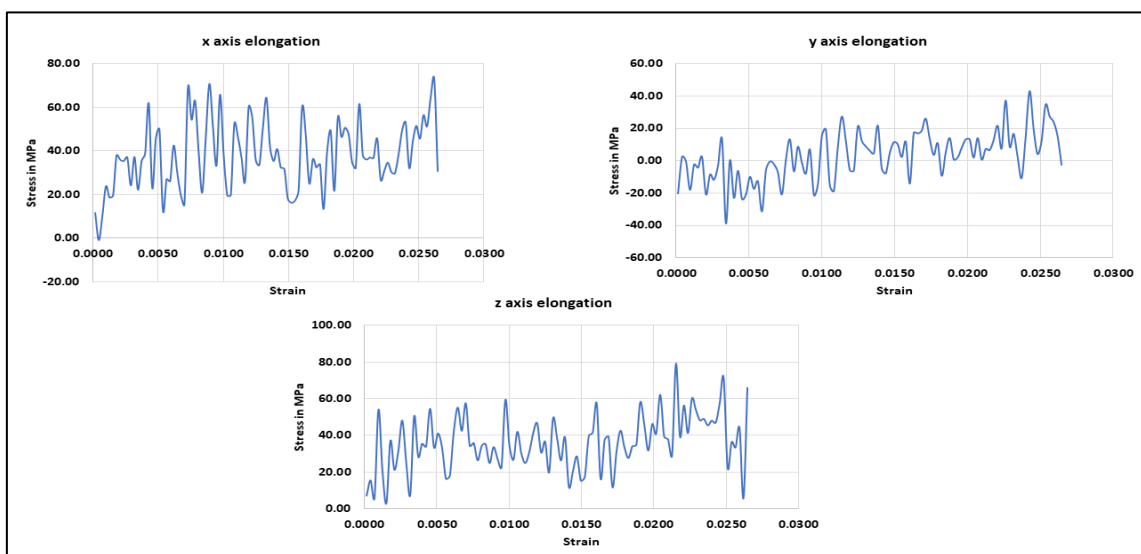


Fig. 7.7. Improved stress strain curve for the basic model

Table 7.2. summarises the modulus derived from the improved stress strain curves obtained from the MD simulations. The modulus decreases as we increase the wt. % of PANI in the resin. This trend is analogous to that obtained from the experimental results (Fig. 7.8). Although the reduction in modulus is almost to 50 % which is quite unlike than the experimental results. The experimental values plotted are taken from the flexural modulus obtained from the 3-point bending test as explained in the chapter 5 of this thesis. The MD simulations results plotted however is not the exact modulus for the material owing to the number of assumptions taken into considerations. However, this disparity can be explained in the following terms :

1. The models are not exactly as expected in the experiments, not only the scale difference but also the charge distribution is not considered
2. The bonding between the PANI and the P-2M is assumed to be covalent , however it is not exactly known yet as to what is the exact kind of bonding in terms of chemistry between PANI and the dopant.

Summarising, this section reports the preliminary work on the MD simulations on a PANI based conductive resin which has not yet been done anywhere. There is a lot of scope for the further development of the model and the exact prediction of the mechanical properties for the conductive resins.

Table 7.2. Summary of the results obtained

Sl. No.	Model name	Constitution	Amount of PANI	Slope from the SS curve
1.	Neat	P-2M	0%	2.45 GPa
2.	Basic	PANI/P-2M	50 %	1.22 GPa
3.	Combine	$(\text{P-2M})_{10} + (\text{PANI/P-2M})_{10}$	33 %	1.47 GPa
4.	First	$(\text{P-2M})_{10} + (\text{PANI/P-2M})_5 + (\text{P-2M})_{10}$	15 %	1.76 GPa

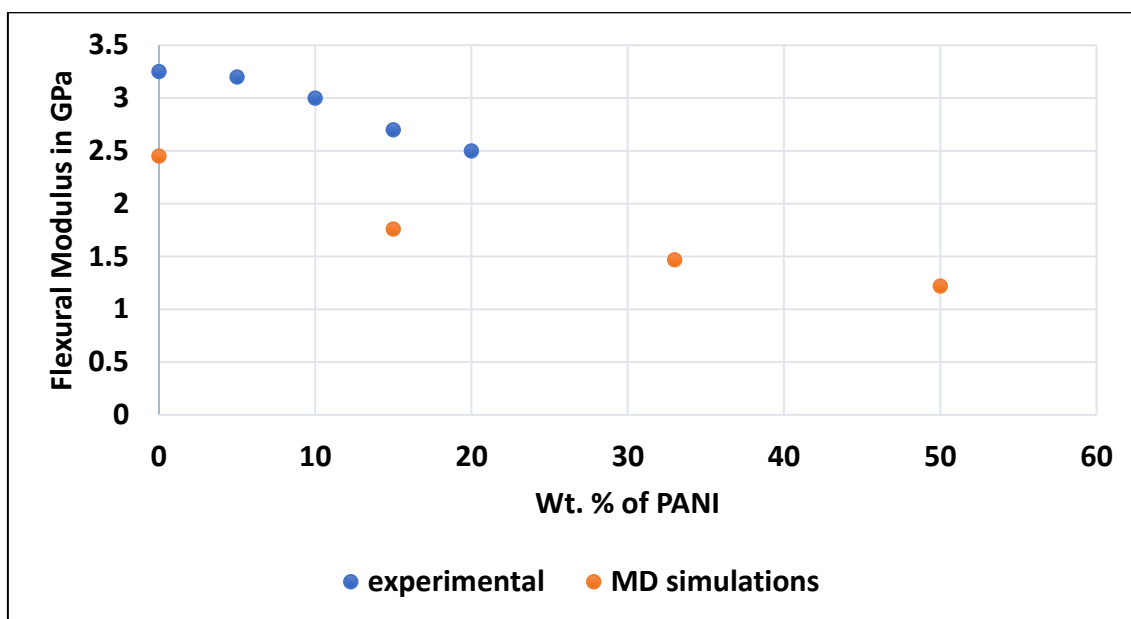


Fig. 7.8. Comparative analysis of the modulus obtained from experiments and MD simulations

7.3. Discussion:

MD simulations are an extremely important and critical tool for the composite's analysis. PANI based resin has been studied now for more than five years. The theoretical prediction of the properties of these conductive resins can be an enormous field of study. This thesis attempts to begin such studies on the resin material. The four basic models under study illustrate how the constitution of the resin plays an significant part in the final properties of the composite. Charge consideration of the chemical structures also makes the final properties of the resin more relatable. So, the future scope also entails the molecular orbital calculations to be done in modelling part. Another separate study can be done by changing the bonding type between PANI and P-2M which is assumed covalent in this study, but in reality it is predicted to be polar covalent. Therefore , many other points of study can be done to expand the MD simulation research on the conductive PANI resin system. However , this thesis gives a qualitative comparison between the results obtained by experimental analysis and MD simulations. The trend is similar in both

of them , however the difference between the exact values can be reduced when the detailed quantitative analysis is done.

Chapter 8

Conclusions

This is the final chapter of this thesis that will summarise the complete work reported in this research. The main goal of this research thesis named : Development of conductive polymer composites using curable dopants, is to demonstrate a new conducting resin using polyaniline by employing a curable dopant that can provide strength and conductivity simultaneously. Further to apply this resin to fabricate CFRPs which can be tested against lightning strike. Thereby providing solution to the composites industries with a conducting and easy to synthesize CFRP with in-built lightning strike protection . The 7 chapters of this thesis have attempted to explain step by step the process and research carried out to achieve this goal.

Chapter 1 is about introduction to the research and explains the necessity of conducting CFRP which can aid as a lightning strike protection for aircrafts . It also explains about conducting polymers and polyaniline and the motivation to choose polyaniline as the focus of this research problem.

Chapter 2 is the summary of the literature survey conducted in the field of the chosen research topic which is another important step to understand how much and in which direction the global research community is working to solve this problem. Further this chapter also explains how we introduced the topic of curable dopants and P-2M.

Chapter 3 encompasses all the techniques used in this research along with their brief working principle. The materials used and methodology applied are also elaborated in this section.

Chapter 4 focusses on the analysis of P-2M as a dopant for PANI. Several dopants have been studied which can impart conductivity to PANI, but P-2M not only provides conductivity but also gets radically cured to impart strength. Various techniques like Thermal microscopy and FTIR were used to verify how P-2M acts as a curable dopant for PANI. Consequently, the optimised weight ratio of PANI:P-2M is determined experimentally and theoretically to obtain the maximum doping of PANI.

Chapter 5 explains the development of the resin of PANI/P-2M and goes on to estimate the activation energy and curing energy using chemical kinetics studies. Further the cured composite of PANI/P-2M is obtained and characterised for its mechanical and electrical properties. The cured composite shows a flexural modulus of Almost 2.8-3.2 GPa and a conductivity of 0.5 S/m for 20 wt % PANI resin. The steady state viscosity also showed a constant viscosity for a long duration.

Chapter 6 demonstrates the CFRP fabrication using the PANI/P-2M resin. Owing to a long term steady state viscosity of the resin, the prepregs could be stored for a long time before making CFRPs. A prepreg and resin stability study for 80days was also conducted. Finally, the cured CFRPs showed maximum conductivity of 0.14 S/cm and the flexural modulus of 45 GPa for 10 wt. % PANI content. Further another methacrylate material called TMP was introduced into the resin which enhanced the maximum stress of CFRPs by almost 40 %. At the end , the CFRP panels were tested against lightning strike of 40 kA. The samples proved to be effective against it after thorough physical examination and NDI results.

Chapter 7 is the theoretical prediction of the mechanical properties of the resin using MD simulations and is the first of its kind study on PANI based resin. Using the JOCTA software, various wt. % of PANI resin was simulated to obtain the stress strain curves. The results obtained from the MD simulations followed the similar trendline as the experimental results. However this is a basic study and these preliminary results show promising scope for deeper MD analysis on the PANI based conducting resin.

Therefore, this thesis has formulated a conducting resin for CFRP fabrication using polyaniline with a curable dopant named P-2M. The CFRPs showed effective lightning strike protection with optimal conductivity and mechanical properties. The unique part of this resin is the highly stable prepreg technology which has been demonstrated to show constant viscosity for 80 days. This makes the PANI/P-2M resin a considerable and appropriate choice for making CFRPs for immediate repair. Additionally, this research also demonstrated preliminary MD simulations to predict the final composite properties from the resin constitution which is a unique attempt in this

field. There are many future perspectives in which the conductive resin can be modified and used for various purposes which require conducting and easy to synthesize CFRPs.

References:

- [1] Shulin L, Junjie Y, Xueling Y, Fei C, Xiaopeng S. Damage analysis for carbon fiber/epoxy composite exposed to simulated lightning current. *J Reinf Plast Compos* 2016;35:1201–13. doi:10.1177/0731684416645202.
- [2] Feraboli P, Miller M. Damage Resistance and Tolerance of Carbon/Epoxy Composite Coupons Subjected to Simulated Lightning Strike. 50th AIAA/ASME/ASCE/AHS/ASC Struct. Struct. Dyn. Mater. Conf., American Institute of Aeronautics and Astronautics; 2009. doi:doi:10.2514/6.2009-2423.
- [3] Hirano Y, Katsumata S, Iwahori Y, Todoroki A. Artificial lightning testing on graphite/epoxy composite laminate. *Compos Part A Appl Sci Manuf* 2010. doi:10.1016/j.compositesa.2010.06.008.
- [4] Abdelal G, Murphy A. Nonlinear numerical modelling of lightning strike effect on composite panels with temperature dependent material properties. *Compos Struct* 2014;109:268–78. doi:https://doi.org/10.1016/j.compstruct.2013.11.007.
- [5] Siddiqui NA, Khan SU, Ma PC, Li CY, Kim J-K. Manufacturing and characterization of carbon fibre/epoxy composite prepregs containing carbon nanotubes. *Compos Part A Appl Sci Manuf* 2011;42:1412–20. doi:10.1016/J.COMPOSITESA.2011.06.005.
- [6] El Sawi I, Olivier PA, Demont P, Bougherara H. Processing and electrical characterization of a unidirectional CFRP composite filled with double walled carbon nanotubes. *Compos Sci Technol* 2012;73:19–26. doi:10.1016/J.COMPSCITECH.2012.08.016.
- [7] Pati S, Kumar V, Goto T, Takahashi T, Yokozeki T. Synthesis and characterization of PANI/P-2M conductive composites: Thermal, rheological, mechanical, and electrical properties. *Polym Compos* 2019;1–8. doi:10.1002/pc.25293.
- [8] Bauhofer W, Kovacs JZ. A review and analysis of electrical percolation in carbon nanotube polymer composites. *Compos Sci Technol* 2009;69:1486–98. doi:10.1016/J.COMPSCITECH.2008.06.018.
- [9] McClory C, McNally T, Baxendale M, Pötschke P, Blau W, Ruether M. Electrical and rheological percolation of PMMA/MWCNT nanocomposites as a function of CNT geometry and functionality. *Eur Polym J* 2010;46:854–68. doi:10.1016/J.EURPOLYMJ.2010.02.009.

- [10] Song YS, Youn JR. Influence of dispersion states of carbon nanotubes on physical properties of epoxy nanocomposites. *Carbon* N Y 2005;43:1378–85. doi:<https://doi.org/10.1016/j.carbon.2005.01.007>.
- [11] Du F, Scogna RC, Zhou W, Brand S, Fischer JE, Winey KI. Nanotube Networks in Polymer Nanocomposites: Rheology and Electrical Conductivity. *Macromolecules* 2004;37:9048–55. doi:10.1021/ma049164g.
- [12] John Macdonald. *Using Thermoplastics in Aerospace Applications* 2018:1–2.
- [13] Alagirusamy R, Das A, editors. Front matter. *Tech. Text. Yarns*, Woodhead Publishing; 2010, p. i–iii. doi:<https://doi.org/10.1533/9781845699475.frontmatter>.
- [14] Gangopadhyay R, De A, Ghosh G. Polyaniline-poly(vinyl alcohol) conducting composite: Material with easy processability and novel application potential. *Synth Met* 2001;123:21–31. doi:10.1016/S0379-6779(00)00573-7.
- [15] Kang ET, Neoh KG, Tan KL. Polyaniline: A polymer with many interesting intrinsic redox states. *Prog Polym Sci* 1998;23:277–324. doi:10.1016/S0079-6700(97)00030-0.
- [16] Hirano Y, Yokozeki T, Ishida Y, Goto T, Takahashi T, Qian D, et al. Lightning damage suppression in a carbon fiber-reinforced polymer with a polyaniline-based conductive thermoset matrix. *Compos Sci Technol* 2016;127:1–7. doi:10.1016/J.COMPSCITECH.2016.02.022.
- [17] Ramakrishnan S. From a laboratory curiosity to the market place. *Resonance* 2011;16:1254–65. doi:10.1007/s12045-011-0141-x.
- [18] Wnek GE. A proposal for the mechanism of conduction in polyaniline. *Synth Met* 1986;15:213–8. doi:10.1016/0379-6779(86)90026-3.
- [19] Pati S, Kumar V, Goto T, Takahashi T, Yokozeki T. Introducing a curable dopant with methacrylate functionality for polyaniline based composites. *Polym Test* 2019;73:171–7. doi:10.1016/J.POLYMERTESTING.2018.11.019.
- [20] Cao Y, Smith P, Heeger AJ. Counter-ion induced processibility of conducting polyaniline and of conducting polyblends of polyaniline in bulk polymers. *Synth Met* 1992;48:91–7. doi:10.1016/0379-6779(92)90053-L.
- [21] Chiang J-C, MacDiarmid AG. ‘Polyaniline’: Protonic acid doping of the emeraldine form to the metallic regime. *Synth Met* 1986;13:193–205. doi:10.1016/0379-6779(86)90070-6.

- [22] Motheo A., Santos J., Venancio E., Mattoso LH. Influence of different types of acidic dopant on the electrodeposition and properties of polyaniline films. *Polymer (Guildf)* 1998;39:6977–82. doi:10.1016/S0032-3861(98)00086-X.
- [23] Chiou NR, Epstein AJ. Polyaniline nanofibers prepared by dilute polymerization. *Adv Mater* 2005;17:1679–83. doi:10.1002/adma.200401000.
- [24] Rajasekharan V, Stalin T, Viswanathan S, Manisankar P. Electrochemical evaluation of anticorrosive performance of organic acid doped polyaniline based coatings. *Int J Electrochem Sci* 2013;8:11327–36.
- [25] Sen T, Mishra S, Shimpi NG. A β -cyclodextrin based binary dopant for polyaniline: Structural, thermal, electrical, and sensing performance. *Mater Sci Eng B* 2017;220:13–21. doi:10.1016/J.MSEB.2017.03.003.
- [26] Kumar V, Yokozeki T, Goto T, Takahashi T. Synthesis and characterization of PANI-DBSA/DVB composite using roll-milled PANI-DBSA complex. *Polymer (Guildf)* 2016;86:129–37. doi:10.1016/J.POLYMER.2016.01.054.
- [27] da Silva AB, Bretas RES. Preparation and characterization of PA6/PAni-TSA nanofibers. *Synth Met* 2012;162:1537–45. doi:10.1016/J.SYNTHMET.2012.07.018.
- [28] Geethalakshmi D, Muthukumarasamy N, Balasundaraprabhu R. CSA-doped PANI/TiO₂ hybrid BHJ solar cells – Material synthesis and device fabrication. *Mater Sci Semicond Process* 2016;51:71–80. doi:10.1016/J.MSSP.2016.05.006.
- [29] Paul RK, Vijayanathan V, Pillai CKS. Melt/solution processable conducting polyaniline: doping studies with a novel phosphoric acid ester. *Synth Met* 1999;104:189–95. doi:10.1016/S0379-6779(99)00063-6.
- [30] Laska J, Proń A, Lefrant S. Phosphoric acid diesters protonated polyaniline: Preparation, spectroscopic properties, and processability. *J Polym Sci Part A Polym Chem* 1995;33:1437–45. doi:10.1002/pola.1995.080330904.
- [31] Kumar V, Yokozeki T, Goto T, Takahashi T. Mechanical and electrical properties of PANI-based conductive thermosetting composites. *J Reinf Plast Compos* 2015;34:1298–305. doi:10.1177/0731684415588551.
- [32] Yokozeki T, Goto T, Takahashi T, Qian D, Itou S, Hirano Y, et al. Development and characterization of CFRP using a polyaniline-based conductive thermoset matrix. *Compos*

- Sci Technol 2015;117:277–81. doi:10.1016/J.COMPSCITECH.2015.06.016.
- [33] Yang S, Ruckenstein E. Processable conductive composites of polyaniline/poly(alkyl methacrylate) prepared via an emulsion method. *Synth Met* 1993;59:1–12. doi:10.1016/0379-6779(93)91152-R.
 - [34] Choi YK, Kim HJ, Kim SR, Cho YM, Ahn DJ. Enhanced Thermal Stability of Polyaniline with Polymerizable Dopants. *Macromolecules* 2017;50:3164–70. doi:10.1021/acs.macromol.6b02586.
 - [35] Pati S, Yokozeki T, Kumar V, Goto T, Takahashi T. Synthesis of advanced PANI based conductive composites using methacrylate group based materials. *Conf. ECCM18 - 18th Eur. Conf. Compos. Mater., Athens, Greece: 2018.*
 - [36] Yin W, Ruckenstein E. Soluble polyaniline co-doped with dodecyl benzene sulfonic acid and hydrochloric acid. *Synth Met* 2000;108:39–46. doi:10.1016/S0379-6779(99)00179-4.
 - [37] Tang J, Jing X, Wang B, Wang F. Infrared spectra of soluble polyaniline. *Synth Met* 1988;24:231–8. doi:10.1016/0379-6779(88)90261-5.
 - [38] list of FTIR peaks n.d.
 - [39] FTIR peaks n.d.
 - [40] Carrillo F, Colom X, Suñol J., Saurina J. Structural FTIR analysis and thermal characterisation of lyocell and viscose-type fibres. *Eur Polym J* 2004;40:2229–34. doi:10.1016/J.EURPOLYMJ.2004.05.003.
 - [41] Mansur HS, Oréfice RL, Mansur AAP. Characterization of poly(vinyl alcohol)/poly(ethylene glycol) hydrogels and PVA-derived hybrids by small-angle X-ray scattering and FTIR spectroscopy. *Polymer (Guildf)* 2004;45:7193–202. doi:10.1016/J.POLYMER.2004.08.036.
 - [42] Dzulkurnain NA, Hanifah SA, Ahmad A, Mohamed NS. Characterization of random methacrylate copolymers synthesized using free-radical bulk polymerization method. *Int J Electrochem Sci* 2015;10:84–92.
 - [43] Ramis X, Salla JM. Time-temperature transformation (TTT) cure diagram of an unsaturated polyester resin. *J Polym Sci Part B Polym Phys* 1997;35:371–88.
 - [44] Ozawa T, Koto T. A simple method for estimating activation energy from derivative

- thermoanalytical curves and its application to thermal shrinkage of polycarbonate. *J Therm Anal* 1991;37:1299–307. doi:10.1007/BF01913863.
- [45] Jeffrey Gotro. *Epoxy Cure Chemistry Part 4: Nucleophiles in Action* 2014.
- [46] Montserrat S, Málek J. A kinetic analysis of the curing reaction of an epoxy resin. *Thermochim Acta* 1993;228:47–60.
- [47] Dupuy J, Leroy E, Maazouz A. Determination of activation energy and preexponential factor of thermoset reaction kinetics using differential scanning calorimetry in scanning mode: Influence of baseline shape on different calculation methods. *J Appl Polym Sci* 2000;78:2262–71.
- [48] Ghaemy M, Sadjady S. Study the curing kinetics of DGEBA with imidazoles and property-structure relationships. *Iran Polym J* 2006;15:103.
- [49] Vyazovkin S, Sbirrazzuoli N. Mechanism and Kinetics of Epoxy–Amine Cure Studied by Differential Scanning Calorimetry. *Macromolecules* 1996;29:1867–73. doi:10.1021/ma951162w.
- [50] Roşu D, Caşcaval CN, Mustaă F, Ciobanu C. Cure kinetics of epoxy resins studied by non-isothermal DSC data. *Thermochim Acta* 2002;383:119–27. doi:https://doi.org/10.1016/S0040-6031(01)00672-4.
- [51] Caşcaval CN, Roşu D, Stoleriu A. Curing of some epoxy-acrylate glycidyl ethers based on para-alkyl substituted phenols. *Polym Degrad Stab* 1997;55:281–5.
- [52] Kissinger HE. Reaction kinetics in differential thermal analysis. *Anal Chem* 1957;29:1702–6.
- [53] Barrett KEJ. Determination of rates of thermal decomposition of polymerization initiators with a differential scanning calorimeter. *J Appl Polym Sci* 1967;11:1617–26.
- [54] Hardis R, Jessop JLP, Peters FE, Kessler MR. Cure kinetics characterization and monitoring of an epoxy resin using DSC, Raman spectroscopy, and DEA. *Compos Part A Appl Sci Manuf* 2013;49:100–8.
- [55] Abdalla M, Dean D, Adibempe D, Nyairo E, Robinson P, Thompson G. The effect of interfacial chemistry on molecular mobility and morphology of multiwalled carbon nanotubes epoxy nanocomposite. *Polymer (Guildf)* 2007. doi:10.1016/j.polymer.2007.06.073.

- [56] Kumar V, Yokozeki T, Goto T, Takahashi T, Dhakate SR, Singh BP. Irreversible tunability of through-thickness electrical conductivity of polyaniline-based CFRP by de-doping. *Compos Sci Technol* 2017;152:20–6. doi:10.1016/J.COMPSCITECH.2017.09.005.
- [57] Kumar V, Yokozeki T, Okada T, Hirano Y, Goto T, Takahashi T, et al. Effect of through-thickness electrical conductivity of CFRPs on lightning strike damages. *Compos Part A Appl Sci Manuf* 2018. doi:10.1016/j.compositesa.2018.09.007.
- [58] Katunin A, Krukiewicz K, Turczyn R, Sul P, Dragan K. Lightning strike resistance of an electrically conductive CFRP with a CSA-doped PANI/epoxy matrix. *Compos Struct* 2017. doi:10.1016/j.compstruct.2017.08.091.
- [59] Katunin A, Krukiewicz K, Turczyn R, Sul P, Łasica A, Bilewicz M. Synthesis and characterization of the electrically conductive polymeric composite for lightning strike protection of aircraft structures. *Compos Struct* 2017. doi:10.1016/j.compstruct.2016.10.028.
- [60] Fan HB, Yuen MMF. Material properties of the cross-linked epoxy resin compound predicted by molecular dynamics simulation. *Polymer (Guildf)* 2007;48:2174–8. doi:https://doi.org/10.1016/j.polymer.2007.02.007.
- [61] Yarovsky I, Evans E. Computer simulation of structure and properties of crosslinked polymers: Application to epoxy resins. *Polymer (Guildf)* 2001. doi:10.1016/S0032-3861(01)00634-6.
- [62] Wu C, Xu W. Atomistic molecular modelling of crosslinked epoxy resin. *Polymer (Guildf)* 2006. doi:10.1016/j.polymer.2006.06.025.
- [63] Wu C, Xu W. Atomistic molecular simulations of structure and dynamics of crosslinked epoxy resin. *Polymer (Guildf)* 2007. doi:10.1016/j.polymer.2007.07.019.
- [64] Li C, Strachan A. Evolution of network topology of bifunctional epoxy thermosets during cure and its relationship to thermo-mechanical properties: A molecular dynamics study. *Polymer (Guildf)* 2015. doi:10.1016/j.polymer.2015.08.037.
- [65] Li C, Strachan A. Molecular simulations of crosslinking process of thermosetting polymers. *Polymer (Guildf)* 2010. doi:10.1016/j.polymer.2010.10.033.
- [66] Bermejo JS, Ugarte CM. Chemical crosslinking of PVA and prediction of material

- properties by means of fully atomistic MD simulations. *Macromol Theory Simulations* 2009. doi:10.1002/mats.200800099.
- [67] Doherty DC. Polymerization molecular dynamics simulations. I. Cross-linked atomistic models for poly(methacrylate) networks. *Comput Theor Polym Sci* 1998. doi:10.1016/S1089-3156(98)00030-0.
- [68] JSOL Corporation. *IEEE Ind Appl Mag* 2010. doi:10.1109/mias.2010.936006.
- [69] JSOL. JOCTA by JSOL Corp. n.d.
- [70] Mayo SL, Olafson BD, Goddard WA. DREIDING: A generic force field for molecular simulations. *J Phys Chem* 1990. doi:10.1021/j100389a010.
- [71] *Computer Simulation of Polymeric Materials*. 2016. doi:10.1007/978-981-10-0815-3.

Achievements

• Journal publications

1. Introducing a curable dopant with methacrylate functionality for polyaniline based composites. Pati.S, Kumar.V, Goto.T., Takahashi, T., and Yokozeki, T. (2019) Polym. Test., 73, 171–177.
2. Synthesis and Characterization of PANI/P-2M Conductive Composites: Thermal, Rheological, Mechanical and Electrical Properties. Pati, S., Kumar, V., Goto, T., Takahashi, T., and Yokozeki, T. (2019) Polymer Composites; 1– 8
3. Development of CFRP with polyaniline-based resin using curable dopants employing storage stable prepregs Santwana Pati, S. Manomaisantiphap, T. Goto, T. Takahashi, T. Yokozeki . Under Review in Polymer composites Journal by Wiley Publications
4. Introducing Trimethylolpropane trimethacrylate into PANI based prepreg system for enhanced strength of the CFRP Santwana Pati, , T. Goto, T. Takahashi, T. Yokozeki . To be submitted for Composites Part B journal.
5. Microwave shielding properties of Co/Ni attached to single walled carbon nanotubes. B.P.Singh, D.K.Saket, A.P.Singh, Santwana Pati, T.K.Gupta, V.N.Singh, S.R.Dhakate, S.K.Dhawan, R.K.Kotnala, R.B.Mathur , published in Journal of materials chemistry A : (2015), 3,1 3203-13209.
6. Economic growth of vertically aligned multiwalled carbon nanotubes in nitrogen atmosphere Abhishek Kumar Arya, Bhanu Pratap Singh*, Jeevan Jyoti, Santwana Pati, S.R. Dhakate, published in Advanced Materials Letters ,2015, doi: 10.5185/amlett.2015.6082
7. In-situ growth of silicon carbide- carbon nanotube composites Santwana Pati, BP Singh, DK Saket, BK Gupta, VN Singh - New Journal of Chemistry, 2016, Volume 40, 4,pages:3863-3868

• International conferences

1. Synthesis of advanced PANI based conductive composites using methacrylate group based materials. Pati, S., Yokozeki, T., Kumar, V., Goto, T., and Takahashi, T. (2018) Conf. ECCM18 - 18th Eur. Conf. Compos. Mater.

2. Synthesis Of Advanced PANI Based Conductive Composites Using Methacrylate Groups Based Materials , Santwana Pati, Tomohiro Yokozeki, V.Kumar, T.Goto and T. Takahashi, 3rd Joint Turkey-Japan Workshop on Polymeric Composite Materials Kyoto Institute of Technology, Kyoto, Japan
3. Variation in through-plane electrical conductivity of CFRP for thunder lightning protection . Presented at International conference on lightning and static electricity 2017 At: Nagoya, Japan

- **International workshops**

1. Presented research on Development of Advanced Composites for Aerospace Applications at workshop on Global Research Challenges In Africa Compared To Japan in Tanzania and Benin , Africa from 16th-25th Feb 2018. And awarded for the Best Innovative Idea.
2. Presented research on Synthesis of Advanced PANI Based Conductive Composites Using Methacrylate Groups Based Materials for Aerospace Applications at the workshop on Advanced Materials for Future from 20th -27th august, 2017 in Melbourne, Australia.

- **Book chapters**

1. Book chapter titled: Self healing polymer composites based on graphene and carbon nanotubes in the book "Smart Polymer Nanocomposites-Energy harvesting, Self-healing and Shape memory" by Springer publishers

